

Modification of Recycled Poly(ethylene terephthalate) for FDM 3D-Printing Applications

by

Mohammed Alzahrani

A thesis

presented to the University of Waterloo

in fulfillment of the

thesis requirement for the degree of

Master of Applied Science

in

Chemical Engineering

Waterloo, Ontario, Canada, 2017

© Mohammed Alzahrani 2017

Author's Declaration

I hereby declare that I am the sole author of this thesis. This is a true copy of the thesis, including any required final revisions, as accepted by my examiners. I understand that my thesis may be made electronically available to the public.

Abstract

In this work, we have studied the suitability of recycled Poly(ethylene terephthalate) (R-PET) for 3D-printing applications by studying the melt flow characteristics of the polymer. R-PET is known to experience a significant deterioration in its mechanical properties when recycled due to molecular weight loss that results from reprocessing. Lower molecular weight affects the polymer's viscosity which hinders R-PET from being 3D-printable from two aspects. First, due to this low viscosity the melt has a low melt strength not sufficient for the filament-making process which involves pulling the melt at certain force to achieve the desired filament diameter size. Second, the polymer would have a significantly higher melt flow when extruded in the 3D-printer and that is likely to result in a very poor printing quality if not a failure for the printing task.

The hypothesis was that R-PET can be modified with a reasonable effort and resources to overcome the low viscosity problem which should enhance both the melt strength and the melt flow of the polymer to become 3D-printable. Since the filament-making process involves extrusion, it was decided that reactive extrusion is the most suitable modification method to be followed. Moreover, the melt flow index test was chosen to be an indicator of suitability of a thermoplastic for 3D-printing applications.

Before attempting modifying the polymer's properties, the effect of moisture content and the reprocessing of R-PET on the melt flow index (MFI) value was studied. Results showed that for unprocessed R-PET, the MFI value was 400% higher when the polymer was not dried compared to the value obtained after 1 hour of drying. This quantified the impact that the hydrolytic degradation makes on the polymer's melt flow characteristics. Moreover, results showed a vast difference of around 3.5-fold in the MFI value between R-PET versus reprocessed R-PET which is attributed to the thermal and thermo-oxidative degradation that occur during reprocessing. Furthermore, the MFI values of 6 commercial filaments, that include 5 different kinds of thermoplastics, were all found to be within the range of 5 ~ 38 g/10min when the MFI test for each filament was performed at the recommended 3D-printing temperature. R-PET, on the other hand, had an MFI value of around 90.56 g/10min (mean value) when tested at 260 °C. This proved that there is a significant difference in the melt flow characteristics between R-PET and 3D-printable thermoplastics.

Modifying R-PET for the purpose of enhancing its melt flow characteristics was done by reactive extrusion with the chain extender PMDA (pyromellitic dianhydride) at 3 concentration levels 0.25, 0.5 and 0.75 wt%.

Furthermore, single-screw and twin-screw extruders were used for compounding and the MFI results of final products were compared. MFI results revealed that PMDA has successfully increased the viscosity of our polymer when used as the chain extender. A decrease of around 72fold in the MFI was recorded when PMDA was added at 0.75 wt% which lowered the MFI of our modified R-PET to a comparable value to commercial 3D-printing filaments. Moreover, the comparison between the products processed by single-screw and twin-screw extruders showed that lower MFI was obtained when the single-screw extruder was used at PMDA concentrations of 0.25 wt% and 0.5 wt%. At 0.75 wt%, however, the product of the twin-screw extruder had slightly lower MFI. It was proposed that when 0.75 wt% PMDA was added, an excess PMDA has helped in recovering the molecular weight loss caused by several degradation routes that are anticipated to take place more severely in the twin-screw extruder. Having said that, it is worth noting that the difference between MFI obtained by single-screw and twin screw extruders at 0.75 wt% is not vary large. Moreover, the effect of copolymer SEBS-g-MA (Styrene-Ethylene-Butylene-Styrene grafted Maleic Anhydride) on melt rheology when added along with PMDA was briefly studied. SEBS-g-MA has been used as a toughening agent but it was also reported that it acts as a thermal stabilizer when processed with polymers. Our results showed that MFI was higher when the copolymer was added and, therefore, it was eliminated as an additive from our final product.

Furthermore, FT-IR analysis was performed to investigate the chemical composition of our product and compared it with unmodified R-PET. Three cases were investigated including: the composition change resulted from not drying the polymer prior extrusion, the change resulted from PMDA addition, and the change resulted from addition of SEBS-g-MA. First, when the polymer was not dried prior to extrusion it is expected that hydrolytic degradation will occur and, as a result, an increase in the hydroxyl end-group content should be seen as was confirmed by the FT-IR results. Moreover, the sample that contained SEBS-g-MA in the blend showed clear signals that are associated with SEBS-g-MA. This indicates that SEBS copolymer was effectively dispersed in our polymer. Furthermore, a very mild indication was seen in the IR spectrum that suggests a lower carboxyl end-group content when PMDA was added at the highest level (0.75

wt%). This was attributed to the chain extension reaction which is known to reduce the -COOH end-group content.

Finally, making a 3D-printing filament from our modified R-PET was done by mimicking the main processing stations that exist in a filament making process which are: extrusion stage, water bath cooling stage and spooling stage. After setting certain important operational parameters, including extrusion temperature and cooling water bath temperature, we were able to obtain segments of on-spec filament shape. This result was much harder to achieved when PMDA concentration was lowered to 0.5 wt% and it was impossible to be done with PMDA concentration of 0.35 wt%. With 0.75 wt% PMDA, the melt strength was satisfactory for pulling the filament by the spooler which is needed to control the filament's diameter. Then, produced filaments were tried in a 3D-printer.

A small shape was successfully 3D-printed using our filament product. It was found that the minimum recommended 3D-printing temperature is 275 °C which required, in our case, a mild hardware and software modification on the 3D-printer. Furthermore, recommendations were made to promote a smooth printing task and to enhance the quality of the print.

Acknowledgment

First and foremost, I would like to express my deep gratitude to my supervisors Prof. Ali Elkamel and Prof. Leonardo Simon for their tremendous support. They inspired me in every step of the way and they dedicated their time and resources to support this project. This work would have never been completed without their guidance and encouragement.

Additionally, I am grateful to my thesis committee members Prof. Ting Tsui and Prof. Mazda Biglari for dedicating their time to read and discuss my thesis.

Moreover, I would like to thank and acknowledge Alaa Alalawi (co-op student), Priscila Vitor (co-op student) and Lika Chowdhury (volunteering student) for their participation in some of the experiments that were performed in this project.

I also would like to thank Christina Dalziel-Mallet from Post Plastics Inc. and Sharman McGilbert from Kraton Polymers for donating some resources that were used in the project.

Furthermore, I would like to thank my beloved wife who was a true supporter to me throughout my study. I also would like to thank my family back home in Saudi Arabia who were always a source of comfort during difficult times.

Last but not least, I would like to thank the government of Saudi Arabia for awarding me the scholarship and for funding my research costs.

Dedication

I dedicate this work to my mother, Dr. Fauzia Alabdulkader, who sacrificed a lot to provide me with decent education and an opportunity in life. She did not have an easy life and she died young.

Table of Contents

List of Figures	x
List of Tables	xii
List of Abbreviations	xiii
Chapter 1	1
Introduction	1
Chapter 2	4
Literature review	4
2.1- Additive Manufacturing	4
2.2- History and development.....	6
2.3- Additive Manufacturing technologies	7
2.3.1- Fusion Deposition Modelling (FDM)	9
2.3.2- Liquid photopolymer-based machines	10
2.3.3- Selective Laser Sintering (SLS)	12
2.4- Thermoplastics in Additive Manufacturing	13
- Acrylonitrile Butadiene Styrene (ABS)	13
- Polylactic Acid (PLA)	14
- High Impact Polystyrene (HIPS)	14
- Nylon	14
- Thermoplastic Elastomers	15
- Glycol-modified Poly(ethylene terephthalate) (PETG)	16
2.5- Manufacturing process of thermoplastic filaments	17
2.5.1- Mixing	17
2.5.2- Drying	17
2.5.3- Extrusion.....	18
2.5.4- Quenching	19
2.6- Reactive extrusion, chain extension and degradation routs for reprocessed PET	19
2.6.1- Types of Extruders and their Suitability for Reactive Extrusion	19
2.6.2- Chain extension of PET via reactive extrusion	23
2.6.3- Degradation routs of PET	27
a- Hydrolytic degradation	27

b- Thermal degradation	27
c- Thermo-oxidative degradation	27
Chapter 3	28
Methodology, Materials and Equipment.....	28
3.1- Experiment, Equipment and materials	28
3.2- Methodology.....	30
- Melt Flow Index test	30
- Investigating the chemical composition by FT-IR	31
- Additives mixing and samples preparation	32
- Drying.....	33
- Extrusion	34
- Lab-scale filament production process	36
Chapter 4	39
Results and Discussion.....	39
4.1- Identifying melting point and crystallinity of R-PET by DSC analysis	39
4.2- Quantifying moisture in R-PET and its effect on the MFI value.....	40
4.3- Comparison between MFI values of commercial filaments and R-PET	42
4.4 Effect of chain extender concentration and extruder’s type on decreasing MFI of R-PET	44
4.5 FT-IR test.....	52
4.6 Manufacturing a lab-made 3D-printing filament	58
4.7 3D-printing with lab-made R-PET filament	63
Chapter 5	69
Conclusions and Recommendations	69
Bibliography	73
Appendix	78

List of Figures

Figure 2-1: CAD image of an object at the design stage (Gibson, Rosen, & Stucker, 2015).....	4
Figure 2-2: General setup of a laser-based 3D-printer (Grynol, 2013).....	7
Figure 2-3: Classification of 3D-printing technologies (Pham & Gault, 1998).....	8
Figure 2-4: Illustration of FDM technology	10
Figure 2-5: 3-Dimensional illustration of FDM technology	10
Figure 2-6: Illustration of SLA 3D-printer (source: https://leedsunicareers.wordpress.com).....	11
Figure 2-7: Illustration of DLP 3D-printer (Wallace et al., 2014)	12
Figure 2-8: Illustration of SLS 3D-printer (source: http://www.spilasers.com)	12
Figure 2-9: An object 3D-printed with dried nylon (left) has better quality than non-dried (right)	15
Figure 2-10: Scheme of reactive extrusion process (Tzoganakis, 1989)	20
Figure 2-11: types of screw arrangements: (a) single-screw, (b) co-kneader, (c) nonintermeshing, mixing mode, (d) nonintermeshing, transport mode, (e) counterrotating, closely intermeshing, (f) corotating, closely intermeshing, (g) conical counterrotating, and (h) self-wiping, corotating (Xanthos, 1992).....	21
Figure 3-1: PMDA reactions with PET (Awaja et al, 2004).....	29
Figure 3-2: Filabot wee single-screw extruder	34
Figure 3-3: HAAKE 2 mini compounder (twin-screw extruder by ThermoFisher Scientific)	35
Figure 3-4: 3D-printed cooling water bath used in our project	37
Figure 3-5: Filabot spooler	38
Figure 4-1: DSC results of unmodified R-PET	39
Figure 4-2: Weight loss as a function of drying time in R-PET sample.....	40
Figure 4-3: Drying effect on MFI result on unprocessed R-PET.....	41
Figure 4-4: MFI results of various filaments	43
Figure 4-5: MFI values of reprocessed and unprocessed R-PET (both unmodified)	44
Figure 4-6: MFI values of modified and unmodified R-PET at 260 °C	46
Figure 4-7: MFI values obtained by single-screw vs. twin-screw extruders (MFI at 260 °C).....	46
Figure 4-8: MFI values obtained by single-screw vs. twin-screw extruders (MFI at 275 °C).....	47
Figure 4-9: MFI values obtained by single-screw vs. twin-screw extruders (MFI at 290 °C).....	47
Figure 4-10: MFI as a function of temperature (Single-Screw)	49

Figure 4-11: MFI as a function of temperature (Twin-Screw).....	49
Figure 4-12: MFI values of R-PET modified with PMDA and PMDA / SEBS-g-MA	50
Figure 4-13: MFI values of various filaments and modified R-PET.....	51
Figure 4-14: FT-IR spectrum of reprocessed R-PET dried and undried prior to extrusion.....	53
Figure 4-15: Hydroxyl end-group region shows different intensities between dried and undried R-PET.....	54
Figure 4-16: FT-IR results of modified R-PET (single-screw) and PMDA	55
Figure 4-17: Carboxyl end-group region for modified R-PET	55
Figure 4-18: Carbonyl group region for modified R-PET	56
Figure 4-19: FT-IR results of R-PET modified R-PET with PMDA and PMDA/SEBS-g-MA	57
Figure 4-20: Laboratory filament-making setup.....	59
Figure 4-21: Modified R-PET filament being pulled from the extruder.....	60
Figure 4-22: Cross-sectional view of the filament shows good ovality	61
Figure 4-23: Magnified image of cross-sectional area of lab-made filament from modified R-PET shows good ovality (magnification: X12.6).....	61
Figure 4-24: DSC result of commercial PLA filament.....	64
Figure 4-25: DSC results of Modified R-PET.....	64
Figure 4-26: Modified R-PET filament being extruded in 3D-printer	66
Figure 4-27: Small dog-shape 3D-printed with modified R-PET (right)	67
Figure A-1: DSC results of Nylon 3D-printing filament.....	78
Figure A-2: DSC results of TPE 3D-printing filament.....	78
Figure A-3: Magnified image of the cross-sectional area of ABS commercial filament.....	79
Figure A-4: The barrel design (dimensional) in Filabot Wee extruder	80
Figure A-5: The screw design (dimensional) in Filabot Wee extruder	81

List of Tables

Table 2-1: Various types of reactions were performed in extruders (Xanthos, 1992).....	23
Table 3-1: Materials and Chemicals.....	29
Table 3-2: Equipment and apparatus	30
Table 3-3: Prepared samples.....	33
Table 3-4: Comparison between the two types of extruders used in this project	35
Table 4-1: Weight loss in R-PET due to drying.....	40
Table 4-2: Summary of MFI results of various filaments	42
Table 4-3: MFI results of modified R-PET	45
Table 4-4: Relevant IR assignments in PET, PMDA and SEBS-g-MA	58
Table 4-5: Measurements of the diameter of the lab-made filament from modified R-PET	62

List of Abbreviations

Abbreviations	
\$	U.S. dollar
μ_x	Mean testing temperature
1,3 PBO	2,2'-(1,3-phenylene)bis(2-oxazoline)
1,4 PBO	2,2'-(1,4-phenylene)bis(2-oxazoline)
3D	Three Dimensional
ABS	Acrylonitrile Butadiene Styrene
AM	Additive Manufacturing
ASTM	American Society for Testing and Materials
CAD	Computer-Aided Design
CE	Chain Extender
CSTR	Continuous Stirred Tank Reactor
dL	Deciliters
DLP	Digital Light Processing
DSC	Differential Scanning Calorimetry
FDM	Fused Deposition Modelling
FT-IR	Fourier Transform Infrared
g	Gram
h	Hours
HIPS	High Impact Polystyrene
I.D.	Inner Diameter
IV	Intrinsic Viscosity
KBr	Potassium Bromide
MFI	Melt Flow Index
min	Minutes
mm	Millimeter
MW	Molecular Weight
MWD	Molecular Weight Distribution
°C	Degrees Celsius
PA	Phthalic Anhydride
PET	Poly(ethylene terephthalate)
PETG	Glycol-modified Poly(ethylene terephthalate)
PLA	Poly(lactic Acid)
PMDA	Pyromellitic dianhydride
RE	Reverse Engineering
REX	Reactive Extrusion
R.I.	Relative Intensity
R-PET	Recycled Poly(ethylene terephthalate)
Rpm	Round Per Minute
RTD	residence time distribution

s	Second
SD	Standard deviation
SEBS-g-MA	Styrene-Ethylene-Butylene-Styrene grafted Maleic Anhydride
SL	Stereolithography
SLA	Stereolithography Apparatus
SLS	Selective Laser Sintering
T _{cc}	Cooling Crystallization Temperature
TGDDM	Tetraglycidyl-diaminodiphenyl methane
TPE	Thermoplastic Elastomer
TPU	Thermoplastic Polyurethane
USB	Universal Serial Bus
UV	UltraViolet
wt%	Weight per cent

Chapter 1

Introduction

Additive manufacturing, or 3D-printing, market has been growing fast in recent years as many companies and entrepreneurs see a great potential in the market. Figures shows a massive 29% increase in the market value between 2011 and 2012 in which the market was valued at around \$2.2 billion (“3D Printing”, 2013). Later in 2016, Wohlers Associates Inc.’s 2016 annual report valued the market at around \$5.1 billion (McCue, 2016) and other reports projected the market to value between \$7 billion and to generate \$21 billion in revenue by 2020 (Columbus, 2015). Among several technologies, Fused Deposition Modelling (FDM) is recognized as the most used technology for 3D-printing due to its simplicity and low capital cost (Palermo, 2013). FDM technology serves mainly home users and enthusiasts as well as serving educational purposes.

In FDM 3D-printers, thermoplastic filaments are used as the building material. Hence, many thermoplastic companies have contributed to the 3D-printing market by introducing thermoplastic filaments that has certain advantages either from the mechanical or the economical point of views. Several kinds of thermoplastics, such as PLA, ABS, Nylon, PETG and Polycarbonate, gain popularity in the 3D-printing industry due to their suitability to the application. Each kind of thermoplastic holds unique properties compared to other kinds. Consequently, end-users make their filament choices based on the applications that the printed part is meant to serve. Although the properties of the thermoplastic might be the main factor for marketing it, the price of the thermoplastic is also strongly considered when buying filaments. Hence, a competitive thermoplastic filament has to offer good quality in a reasonable price especially that many home-users do 3D-printing for entertainment purposes. From the economical point of view, recycled plastics are known of being cheaper than virgin plastics since their uses are significantly limited when recycled due to the loss of some mechanical properties. Therefore, one can see a great economical potential in using a recycled thermoplastic that is highly available in the market for 3D-printing.

Poly(ethylene terephthalate), or PET, is the most recycled thermoplastic in Canada and arguably worldwide (“Canadian Plastics”, 2016). Additionally, it has unique desirable properties over other thermoplastics such as heat and chemical resistances, toughness and stiffness. This makes R-PET an interesting candidate for 3D-printing. On the other hand, like any other thermoplastics,

R-PET suffers drastic change in its mechanical properties when is recycled mainly due to the loss in molecular weight. This loss is mainly brought by as a result of degradation that occurs when the recycled PET is reprocessed at high temperatures (melting temperature of PET is around 260 °C) and, in some cases, with presence of contaminations. As a result of that, recycled PET is known to have low viscosity that hinders using it in many plastic processes. For all thermoplastics, the manufacturing of filaments requires the polymer's melt to have certain melt strength, which is a property that is dependent on the molecular weight, in order to withstand a pulling force that is required to draw a filament with consistent dimensions. Furthermore, certain flow characteristics are needed in the polymer so that when extruded in a 3D-printer the melt should flow at a certain rate. Hence, it is expected that making filaments from R-PET and 3D-print with it is challenging due to the deterioration in the polymer's melt flow characteristics that is resulted from molecular weight loss. However, the characteristics of polymers, including molecular weight and melt flow rate, can be modified by several techniques; and among the popular ones is "Reactive Extrusion" (REX).

Reactive extrusion is an approach that involves mixing polymers, and sometimes along with additives, and processing them in extruders to carry out various types of reactions. This technique became a popular method of modifying properties of polymers since it offers several advantages over conventional polymerization processes. For instance, it is a continuous process, massively reduces processing time and provide precise thermal control throughout the process as, in many extruders, different zones at the extruder's barrel can be set at different temperatures. Several reaction types have been conducted by REX including coupling reactions (Tzoganakis, 1989). In coupling reactions, a functional coupling agent, or chain extender, is used to link separated polymer chains by reacting with end-groups in polymer chains. This linkage produces longer polymer chain with higher MW and, therefore, increases the polymer's viscosity. Various coupling agents have been used in REX with R-PET and many good results were reported as will be discussed in the literature review chapter.

Therefore, the objective of this project is to investigate the possibility of producing a 3D-printing filament made from R-PET after enhancing its melt flow characteristics by increasing its molecular weight. Increasing the molecular weight will be done by reactive extrusion with a chain extender additive and the resulting effect will be sensed by measuring the Melt Flow Index (MFI) of the product. Additionally, other aspects will be studied including the effect of the extruder's

type on the rheology of the final product. Two types of extruders, single-screw and twin-screw, will be used for the reactive extrusion processing.

Chapter 2

Literature review

2.1- Additive manufacturing:

Additive Manufacturing (AM) is the formal terminology that is being used to refer to 3D-printing (Gibson, Rosen, & Stucker, 2015). This term has been increasingly replacing other terminologies, such as rapid prototyping and Solid freeform, mainly because of the growing range of applications that the technology is serving today. Precisely, the term “rapid prototyping” was used initially to refer to the process of building a concept non-commercial model, hence the word “prototype”. However, as the technology developed over the years this builder became a manufacturing machine that can build products to be used directly by the end user and, therefore, became a manufacturer rather than a prototype producer.

The concept of 3D printing is to convert a computer aided 3D drawing to a physical object via an automated building machine. In most cases, building this physical object is done by the successive depositing of thin cross-sectional layers on top of each other which ultimately makes the object body as illustrated in Figure 2-1. As one can imagine, the built object would be an approximation of the software design and the thinner the layers the closer the approximation to the software design.



Figure 2-1: CAD image of an object at the design stage (Gibson, Rosen, & Stucker, 2015)

It is believed that the great potential of this building technique lays in our ability of using different kind of building materials and, therefore, increasing the industries that the technology can contribute to.

The development of additive manufacturing, however, is dependant on several technologies that when integrated can make 3D printing more efficient. Since 3D printing converts software drawings to objects, development in drawing tools significantly benefits the industry. The conventional method for developing 3D models is to develop the drawing manually on a 3D Computer-Aided Design (3D CAD) tool. This is a powerful resource since users can alter the final product based on their needs. Another method that is being used in developing 3D models is Reversed Engineering (RE) where a device is used to capture the design of an existing object and project the collected data on a computer in a 3D model form. This method saves the customer's, as well as the designer's, time when it is desired to copy an existing model. Furthermore, development in 3D printing machinery is also crucial in expanding the applications of 3D printing. The specifications and technologies that are adopted in a 3D printer determines several aspects in the printed object such as: the resolution of the object, the speed of building objects, materials of construction that can be used etc. Additionally, developing engineered raw materials that can be used in 3D printing is also an important area at which researchers are working to make the industry more capable. Customizing the material of construction can be from the chemical or physical nature of the material. For example, changing the chemical composition of the material is often performed to enhance the performance of that material when 3D printed. This process usually starts with selecting a candidate material that has the potential to be desired by 3D printing users and alter it chemically to perform better. Alteration of the chemical nature of the material allows for customizing properties like heat resistant, chemical resistance, crystallization rate, strength, toughness etc. Such properties determine the possible uses of a printed object as well as the quality of the product. Furthermore, 3D printing materials are sometimes physically modified to suit the application they meant to serve. For example, 3D printing polymers can be done using a polymer in the form of filament, resin or powder. The difference in the physical nature of the material decides the technology that can be used to 3D print it and, therefore, the quality of the final product and the 3D printing experience. Today,

wide range of materials are being used in 3D printing including metals, polymers, cement, chocolate and biological tissues.

This section will cover a brief background on the development of the additive manufacturing industry over the past two decades as well as other related technical topics including the technologies used in 3D printing. Moreover, since this thesis is about the use of R-PET in additive manufacturing, a thorough discussion on the use of thermoplastic polymers in 3D printing will follow.

2.2- History and development

3D-printing might sound like a new disruptive technology although it was first invented in 1981. A Japanese scientist, Hideo Kodama, was the first to report a fabrication of a tangible object via a three-dimensional additive manufacturing machine (Kodama, 1981). In his experiment, Kodama was able to construct a plastic model using a photo-hardening polymer that solidifies when exposed to UV light. This achievement had lay out the main concept and technical approach toward what a lot of people believe to be a new revolution in manufacturing. Later in 1984, an American scientist and entrepreneur Chuck Hull founded a company called (3D System Inc.) and filed a patent for a 3D printing technology known as “Stereolithography”, or (SL). This technology introduced the concept of converting a digital data, essentially 3D models, to an object using 3D building machines. Eight years later, in 1992, a Stereolithography Apparatus (SLA) was invented by Hull which was seen to be the first efficient 3D printer that can build relatively complex objects in relatively short time (Goldberg, 2014). The SLA used a liquid photo-polymer that hardens when subjected to a UV beam. Therefore, a UV light source was used to direct a beam on spots on the liquid polymer surface so that it hardens and construct the bottom layer of the object and other layers are then built on top of it sequentially. During the same year, similar machine was invented, known as selective laser sintering (SLS) machine, which uses the same concept as SLA except that it uses powder as a material of construction for building objects (more on these technologies will follow in next section). Figure 2-2 shows the typical setup of laser-based 3D-printers.

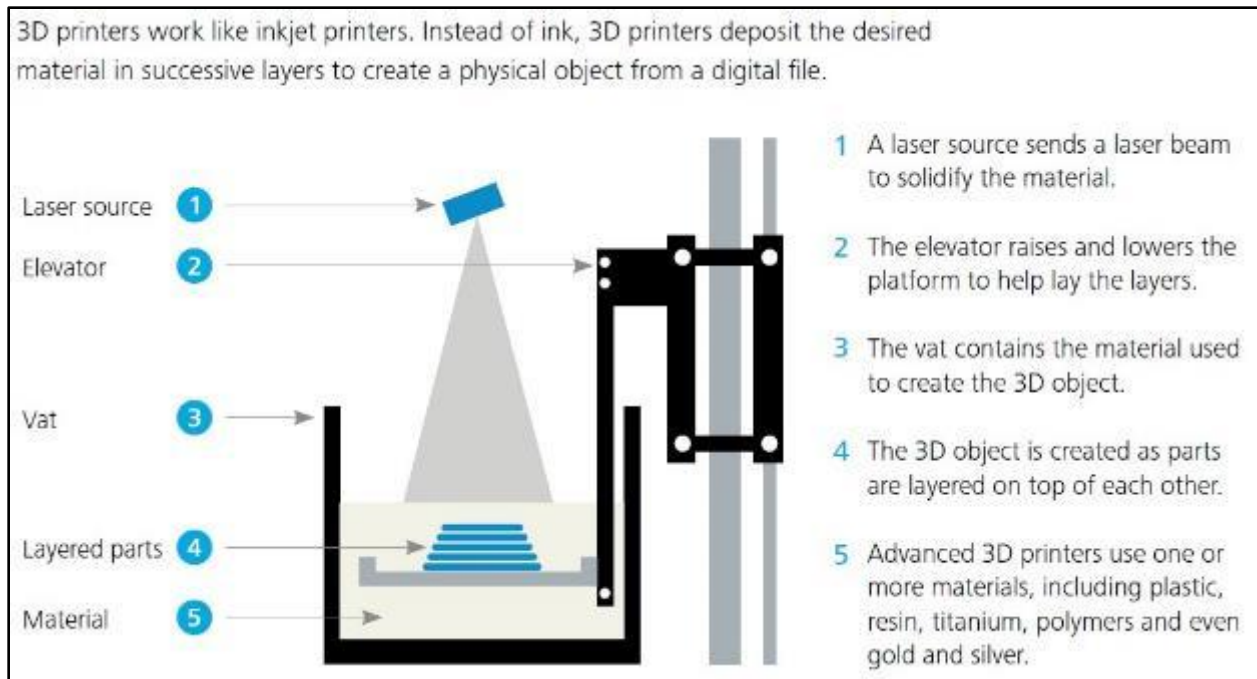


Figure 2-2: General setup of a laser-based 3D-printer (Grymol, 2013)

In 1999, a major breakthrough in the 3D printing history took place when the first 3D printed organ was implanted in human. Scientists at Wake Forest Institute successfully developed this technology when they 3D printed a bladder synthetic scaffold and coated it with a lab grown cells that were taken originally from the patient. This coating was applied in order to prevent rejecting the organ by the patient's immune system. This achievement opened the door for scientists in the medical field to realize the revolution that 3D printing can bring about to their field.

In the last 15 years, 3D-printing became increasingly popular as people realize the diversity of applications that 3D-printing can contribute to. Therefore, more researchers and entrepreneurs dedicated time and effort to develop new technologies as well as enhancing existing once. As a result, the additive manufacturing industry thrived in an unprecedented way with the invention of various of robust and commercially viable machineries.

2.3- Additive manufacturing technologies:

Classifying technologies of additive manufacturing processes can be done in many different ways based on the specific aspect that the consumer is looking for in the process. For example, it is common to classify 3D-printers based on the technology baseline of the device whether it uses a laser-source to construct the object or an extrusion-based technology as the case in Fused

Deposition Modelling (FDM) processes. But this classification does not take into account the type of the raw material (i.e. liquid photo-polymer, powder, solid polymer...etc.) which is an important piece of information to end-users. Therefore, a more inclusive classification was developed that specify two important dimensions in any additive manufacturing process: the method of constructing layers and type of raw material (Pham & Gault, 1998). First, the methods of constructing layers was divided into two main subcategories; 1-dimensional source of construction, such as a nozzle, and 2-dimensional source which is essentially an array of 1-dimensional sources of construction such as the once used in Polyjet technologies. The second dimension in Pham’s classification recognizes 4 types of raw materials used in additive manufacturing: liquid polymers, discrete particles, molten materials and solid sheets. Figure 2-3 provides a matrix that shows several 3D-printing methodologies with classifying them based on Pham’s classification.

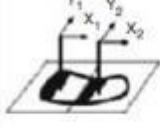
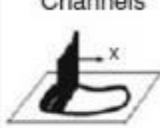
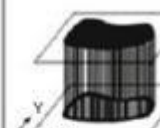
	1D Channel 	2x1D Channels 	Array of 1D Channels 	2D Channel 
Liquid Polymer	SLA (3D Sys)	Dual beam SLA (3D Sys)	Objet	Envisiontech MicroTEC
Discrete Particles	SLS (3D Sys), LST (EOS), LENS Phenix, SDM	LST (EOS)	3D Printing	DPS
Molten Mat.	FDM, Solidscape		ThermoJet	
Solid Sheets	Solido PLT (KIRA)			

Figure 2-3: Classification of 3D-printing technologies (Pham & Gault, 1998)

In this research, I will not be going through describing each technology since this does not serve the objective of the research. However, it is beneficial to briefly discuss the most popular 3 technologies with highlighting major differences between them. This should prepare the reader for the next section which will go deeply into kinds of raw materials used in FDM printing.

2.3.1- Fusion Deposition Modelling (FDM):

This technology is by far the most popular 3D-printing technology due to its relatively low cost and simplicity. It was first developed by the American company Stratasys but competition from many other entities led to lowering the cost of this technology which made it feasible for home uses. In this type of 3D-printing, raw materials are supplied in the form of rounded filament of a thermoplastic or sometimes a metal wire. In this technology, the 3D-printing device is equipped with a small nozzle, or in some case two nozzles, that is connected to a heating element which allows to setup the temperature of the nozzle at the melting point of the thermoplastic, or metal, raw material. The inlet I.D. of the nozzle comes in two different standard-sizes: 3.0 mm and 1.75 mm, whereas the printer's nozzle size is often found at 0.4 mm (although it can be modified). The principle of this technology is that the raw material is fed to the heated extrusion nozzle where it melts, while maintaining certain melt flow characteristics, and then it is ejected through the nozzle outlet on the printer's bed. This bed is movable by a motor and is often connected to a heating element in order to allow the melt to adhere to the heated bed. With the bed being movable in the Y-axis and the nozzle movable on the x-axis, the printer uses the digital code, the 3D-model, of the object to construct the first layer on the bed by continuous dispositioning of the melt on specific x and y coordinates. Once the first layer is constructed, the nozzle moves in the z-axis to start constructing the second layer on the top on the first one (which has already solidified). This move in the z-axis is as small as the thickness of the first layer (often is 0.1 mm) and the smaller the thickness of each layer the higher resolution the object will be. The nozzle moves to the third layer after completing the second and so on till the whole object is constructed. Figures 2-4 and 2-5 illustrate the typical setup and the operational concept in FDM 3D-printers.

FDM printing devices comes in a wide range of kinds, qualities and advanced features which is the reason why its cost ranges from around \$500 for small private printers to \$400,000 for advanced commercial devices.

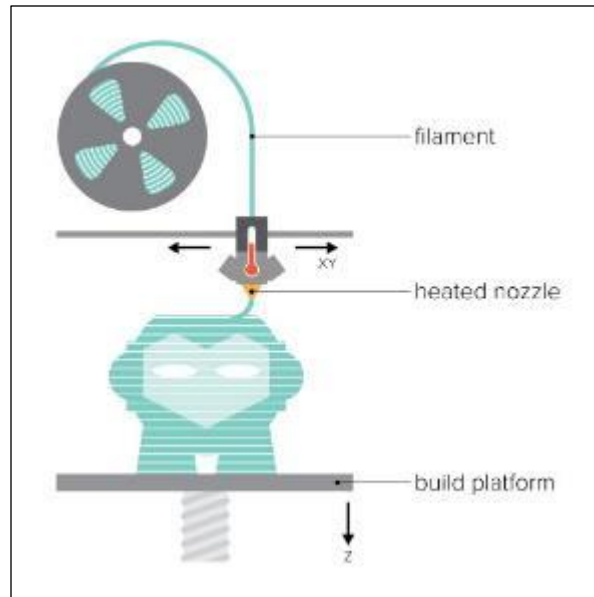


Figure 2-4: Illustration of FDM technology. (source: <http://og3dprinting.com>)

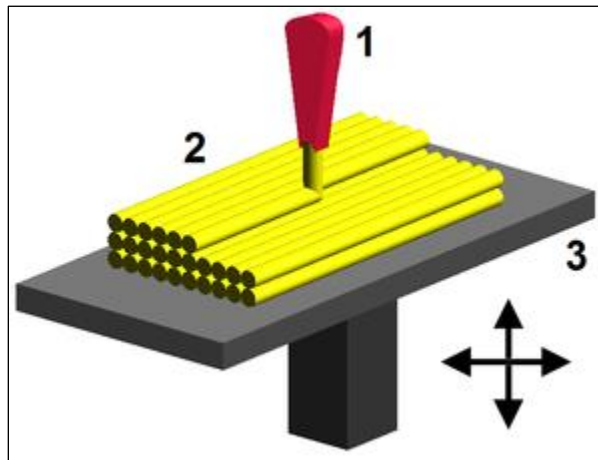


Figure 2-5: 3-Dimensional illustration of FDM technology

2.3.2- Liquid photopolymer-based machines

Generally, liquid photopolymer printers are used for commercial and prototyping purposes rather than private uses mainly due to their relatively higher cost which starts from around \$5000. The principle of these machines is basically curing liquid photopolymer raw material via exposing it to a light source. This will result in hardening the polymer which, therefore, constructs

a hard layer of the object and successive layers are constructed in the same way till the whole object is built. There are two kinds of liquid photopolymer machines which differ only when it comes to the light source projection technique: laser SLA and DLP.

In laser SLA machines, a UV light source direct a beam on two galvanometers (motorized mirrors) that move to reflect this beam on the surface of a resin tank to construct a layer of hard polymer. On the other hand, DLP machines use direct projection of light to the surface of the resin (a projection of a whole layer at a time). Clearly, this feature makes DLP devices have less moving parts compared to laser SLA and, as a result, less maintenance cost. Moreover, DLP is relatively faster in printing than SLA as one can image (because layers are projected instead of being drawn out). This fast printing, however, comes with a marginal tradeoff in the printing quality when compared with SLA technology. Having said that, both technologies are considered as an advanced form of 3D printing that produces models in much higher resolution than the FDM technology. Figures 2-6 and 2-7 show setups of SLA and DLP 3D-printers, respectively.

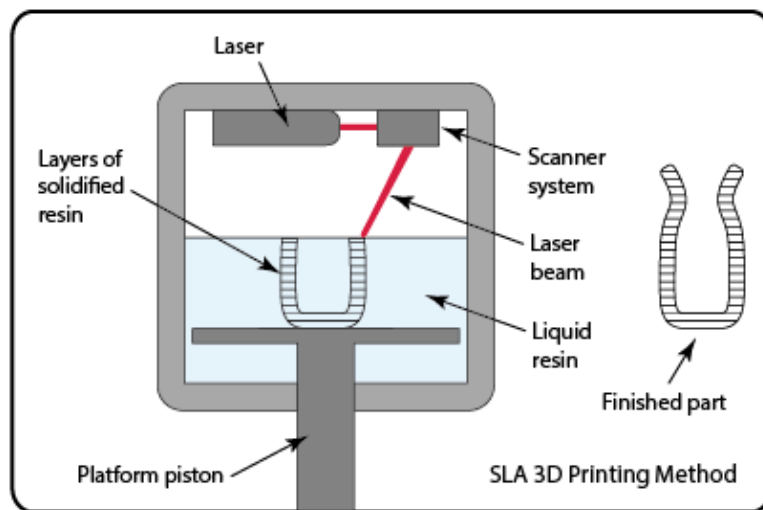


Figure 2-6: Illustration of SLA 3D-printer (source: <https://leedsunicareers.wordpress.com>)

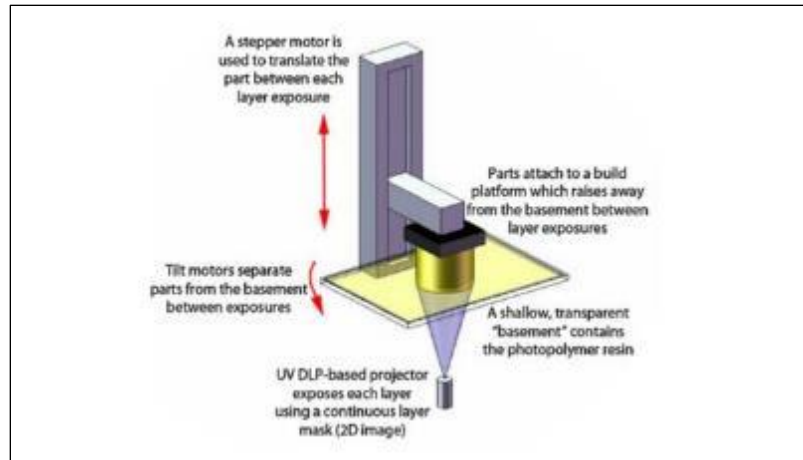


Figure 2-7: Illustration of DLP 3D-printer (Wallace et al., 2014)

2.3.3- Selective Laser Sintering (SLS)

SLS technology is very similar to SLA in terms of using laser beam for constructing cross sectional layers of an object. However, the main difference between the two is that SLS uses raw materials in the powder form, which can be metals or polymers, and the beam is used to fuse the powder particles together making a hard layer as shown in Figure 2-8. In SLS machines, once the first layer is made, a roller rolls a thin powder layer on top of the constructed layer. Then, the laser source draws out the second layer and so on until the object is built. This technique is often used in 3D-printing various types of metals including, but not limited to, carbon steel, aluminum and bronze.

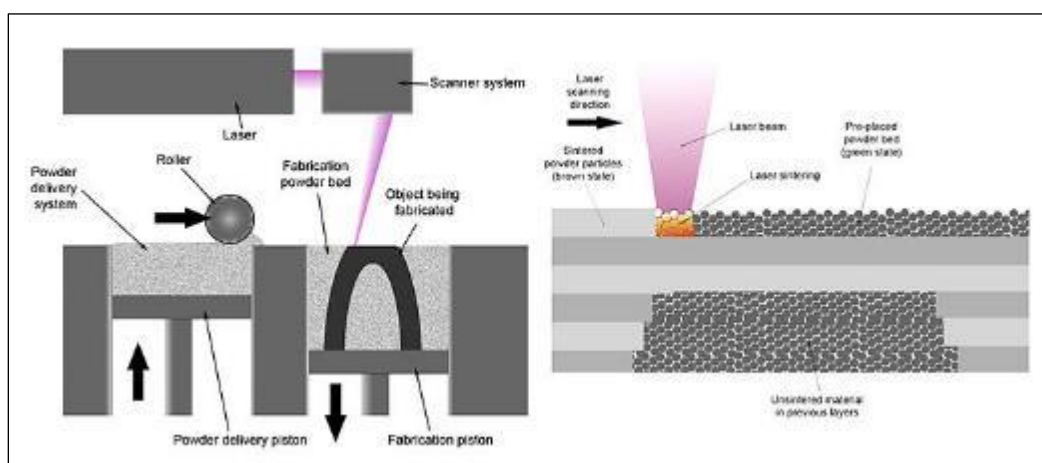


Figure 2-8: Illustration of SLS 3D-printer (source: <http://www.spilasers.com>)

Since this research concerning making a filament for FDM machines, the rest of this chapter will aspects related to FDM 3-D printing and thermoplastics that are used by this technology.

2.4- Thermoplastics in Additive Manufacturing

With FDM 3D-printing technology being the most affordable and popular, thermoplastics came about as the most suitable type of material for this extrusion-based technology. Because in FDM technology raw materials should experience a phase change, from solid to viscous paste-like, when heated in the extrusion chamber as well as being able to retain the mechanical properties when cooled down. Furthermore, melting and solidification has to be well studied with respect to temperature and time in order to evaluate suitability of a thermoplastic for additive manufacturing. It is suggested that amorphous thermoplastics are generally more suitable for FDM 3D-printing than crystalline polymers (Gibson, Rosen, & Stucker, 2015). This is because amorphous polymers do not have a specific melting point and, therefore, keeping them in the semisolid (paste-like) phase can be easily done by finding the right temperature to do so. Having said that, some semi-crystalline thermoplastics, such as PLA, has been proven very suitable, and popular, polymer for FDM printing. Some thermoplastics have been proven more suitable for 3D-printing than others and here is a brief list of most commonly used thermoplastics:

- Acrylonitrile Butadiene Styrene (ABS)

ABS is one of the two most popular thermoplastics used in FDM machines (along with PLA). It is known of being uniquely tough and ductile amorphous polymer that can withstand heavy uses. Moreover, ABS has a very good temperature resistance since it starts soften at relatively high temperature (around 230 °C). ABS is also cheaper than other thermoplastics used for 3D-printing.

On the other hand, ABS has few disadvantages from the environmental and health point of view. Since it is a petroleum-based polymer, it is a non-biodegradable plastic. Furthermore, while 3D-printing with ABS it is anticipated that a mild fume will be released that can be easily smelled. Therefore, it is often recommended to have some sort of ventilation in the room where ABS is being 3D-printed. ABS require a heated bed in the printing machine in order to avoid warping.

- Polylactic Acid (PLA)

Being a biodegradable polymer and relatively easy to use, PLA has become one of the most favorable materials for 3D-printing. When compared with ABS, PLA is considered as a healthier and safer material to work with since it is not toxic and it produces much safer fumes than ABS when 3D-printed. From the mechanical performance point of view, however, it is not as tough as ABS and it is definitely more brittle. Moreover, PLA starts to soften at relatively low temperatures (around 50 °C) which makes less heat resistant than ABS. 3D-printing with PLA is done at roughly 210 °C and it does not require heated bed (although having a heated bed at around 60 °C can enhance the product's quality depending on the object's size and shape).

Since it is derived from renewable resources, such as corn starch, PLA can be used in printing parts for the biomedical uses. For example, it can be used in a composite for making parts like screws and pins that ultimately degrade in human body over certain period of time (Russias et al., 2006) Moreover, PLA has been used in making scaffolds for organs that are to be implanted in human body (Scott, 2016). Scaffolds are synthesized structural supports on which living cells can be safely seeded, grow and regenerate.

- High Impact Polystyrene (HIPS)

HIPS is known of having similar properties as ABS but it is slightly more expensive. Because HIPS is soluble in Limonene, it is often used as a structural support for 3D-printing other objects. Then, it is easily dissolved and removed which results in a cleaner finishing for the object that was supported. This will save users the effort of sanding their built object which is relatively much more tedious job. HIPS is usually printed at 250 °C on heated bed and is likely to experience less warpage than ABS.

- Nylon

Nylon, or as often called PolyAmide, is an increasingly used material in FDM printing. It has several desirable properties such as strength, flexibility and durability. On the other hand, it is one of the most hygroscopic polymers among all kinds of thermoplastics. Meaning that it absorbs moisture significantly and, as a result, users might need to dry it in an oven before using it in order to obtain good printing quality as shown in Figure 2-9. Nylon is printed at around 250 °C and required a heated bed at around 65 °C.



Figure 2-9: An object 3D-printed with dried nylon (left) has better quality than non-dried (right)

- Thermoplastic Elastomers:

There are two kinds of thermoplastic elastomers that are available commercially for 3D-printing, TPE and TPU (Thermoplastic Elastomer and Thermoplastic Polyurethane). Although there are minor differences between the two, these differences are not noticeable for many users and, therefore, we will consider both products as one kind of thermoplastic.

Elastomer filaments are unique by being elastic as opposed to all other kinds of filaments. Some sources claim that objects printed with TPE can be stretched to as much as twice their original dimension and retain their original shape (Tyson, 2016). These unique filaments allow for further diversification in the applications that 3D-printing can serve. Although elastic, elastomer filaments are known for being durable and they do not wear easily. This might be a result of the excellent adhesion between the layers while 3D-printing objects. Printing elastomers is often done at a lower speed compared to other filaments and, as a result, printing an object with elastomer filament can take as much time as printing with PLA or ABS (but it is also dependent on the printer). Usually elastomer filaments are printed at a nozzle temperature of 230 °C on a heated bed at around 55 °C.

- Glycol-modified Poly(ethylene terephthalate) (PETG)

Glycol-modified PET has been proven as a competitive thermoplastic for FDM 3D-printing although not as popular as previously mentioned kinds. Unlike PET, PETG is an amorphous polymer and, therefore, it maintains its semi-solid phase when heated which makes it more suitable for 3D-printing. Moreover, it is known to be more durable and heat resistant than PET. Several sources claim that PETG filaments combine desirable properties from both ABS (by being strong and ductile) and PLA (by being “easy” to print with) [PETG Filament for 3D Printing: Explained & Compared, page]. On the other hand, the commercial availability of PETG filaments are significantly less than other filaments for several reasons. First, it is relatively new to the market and, therefore, many users prefer to go with more popular and well-reviewed options. Additionally, PETG required higher printing temperature (around 255 °C) than other conventional filaments like ABS and PLA. This is considered as a disadvantage since most 3D-printers’ manufacturers do not recommend printing at high temperatures (250 °C – 260 °C) for long time as some wiring insulators in the printer can soften and ultimately fail at 260 °C.

In addition to these well-known kinds of filaments, researchers devoted a lot of time prototyping engineered thermoplastics that can serve many different applications. This is usually done by selecting a candidate polymer and modifying it in order to enhance certain properties. This modification is often done by producing a copolymer that combines a blend for several polymers or by chemically modifying the polymer using additives. This has resulted in what is commonly known as “exotic filaments” which are engineered polymers with some unique features either from the mechanical point of view or from their finishing appearance.

When prototyping an engineered thermoplastic, it is often that the main objective is set to have a specific property at certain level in the final product. There is another important aspect, however, that scientists often come across during the prototyping process and that is: thermoplastic’s suitability for manufacturing. In other words, while it is important to have certain desirable mechanical and visual properties in the thermoplastic, it is also important to consider how easy, or difficult, the manufacturing process of a filament from that thermoplastic could be. In order to evaluate that, it is important to study the thermal and chemical nature of the candidate thermoplastic as well as the production line that the thermoplastic will be processed in. Therefore, the next section of this chapter will shed some light of the manufacturing process of 3D-printing

filaments in order to highlight certain important aspects that need to be taken into consideration for manufacturing a filament for FDM machines.

2.5- Manufacturing process of thermoplastic filaments

The manufacturing process of 3D-printing filaments is relatively a simple process that can be customized to wide range of capacities. Despite of the lack of formal literature that discusses the manufacturing processes of 3D-printing filaments, there is a decent informal electronic content available online that gives clear idea on how fused filaments are being manufactured commercially. There are several technology-providers who designed manufacturing processes for fused filament making, however, the difference between these technologies is often minor. Therefore, in this section I will go through the main process engineering concepts that are employed in manufacturing 3D-printing filaments. Understanding these concepts is crucial to my research since I am going to mimic the manufacturing process in laboratory scale to produce a prototype filament from recycled PET. The process can be divided into 4 main stages:

2.5.1- Mixing

Manufacturing fused filament for FDM machines starts with a mixing stage in which the thermoplastic is mixed with additives. This operation takes place in a blender that is suitable for mixing the specific type of additive that is used. Additives can be used for several purposes such as; enhancing the mechanical properties of the filament product or coloring the pellets, by coloring pigments, that ultimately make a colored filament.

2.5.2- Drying

Drying is a common step in general prior to polymer processing as it aims to remove moisture absorbed by the polymer. This is considered as a crucial step since the presence of water molecules in the polymer advocates for degradation reactions when polymers are exposed to high temperatures as the case in extrusion processes. This results in a dramatic decrease in the polymer's molecular weight which compromises the structural integrity of the polymer's melt. Therefore, the drying step should be done thoroughly to ensure a stable polymer melt quality.

It is important for any commercial filament-making process to identify the optimum drying conditions in order to achieve an economical feasible operation. Because although longer drying

time can slow down the output rate (or increase the capital cost by requiring more dryers), it can save a considerable operational down-time caused by product instability.

Although drying is necessary prior to extruding most thermoplastic, some thermoplastics, which have a high affinity to absorbing moisture, would need more intensive drying than others. Therefore, based on the hygroscopic nature of the thermoplastic a proper drying time and temperature has to be developed.

2.5.3- Extrusion

Once the thermoplastic along with additives are dried, this mixture is fed to an extruder for melting. In this step, several variables have to be setup properly in order to assure a stable operation such as; the operating temperature and the residence time of the material inside the extruder. At too high temperature or residence time can advocate for degradation reactions to occur in the extruder and, therefore, negatively impact the viscosity of the melt.

When extruding thermoplastic for making fused filaments, there are two output parameters that are continuously monitored in order to make sure the filament is in good shape which are; the filament diameter and ovality. The filament diameter size and tolerance is probably the most important specification that end-users are considering when buying a spool of filament. Because not only it has an impact on the printing quality but it is also important to keep the printer running smoothly without the filament getting jammed in the filament feeding section. From a production point of view, a filament diameter is controlled through the extruder die size as well as a proper winding system (or as often called in the industry a “tractor system”). What tractor systems do is that it pulls the melt that comes out of the extruder die at certain constant speed which is extremely important maintaining the filament diameter size with a very low tolerance. As one can imagine, a faster pulling speed will results in a filament with lower diameter size and vise versa. Although the extruder die size should be sized close to the desired final diameter, with the ability to manipulate the pulling speed of the tractor system it is possible to produce filaments with a diameter size significantly lower than the die diameter. Fused filaments are produced in two sizes as mentioned previously (1.75mm and 3.00mm) with a reported tolerance of 0.05mm. Ovality is another important parameter which concerns the roundness of the filament. Since filament ovality is strongly affected by the filament post-extrusion treatment, it is going to be discussed as part of the quenching step.

2.5.4- Quenching

When a filament melt exit the die of the extruder, it is mostly found is a transition phase between the solid and melt forms. While this transition phase is desirable since it allows for pulling the filament to a smaller diameter, it can also pose a challenge as the filament has not completely solidify and, hence, is susceptible for further shape change. As mentioned earlier, when the filament is extruded the product is pulled from the extruder discharge and that pulling is usually done using two rollers that the filament passes between then. Therefore, unless the filament solidifies before being fed between these two rollers it will be squeezed and, as a result, lose its roundness (or ovality). Due to this, filament extrudate is quenched right after exiting the extruder's die in a cooling water tank before it enters the tractor machine. This quenching allows the filament to completely solidify and takes its final shape and dimensions.

An important parameter to take into consideration when quenching the filament is the temperature of the cooling water. Most fused filaments manufacturing processes conduct quenching in 2 stages: warm or hot water quenching and cold water quenching. The reason behind this technique is that rapid quenching with cold water often results in rapid shrinkage of the thermoplastic which results in inconsistent filament diameter. Therefore, identifying an optimum temperature for the warm cooling water is crucial for a stable on-spec operation and this is temperature can be different for each thermoplastic.

2.6- Reactive extrusion, chain extension and degradation routs for reprocessed PET

2.6.1- Types of Extruders and their Suitability for Reactive Extrusion

Nowadays, extruders are being used for several purposes including polymer melting, shaping or modification. When an extruder is used to carry out a chemical reaction, it combines two different operational concepts: chemical reaction and melt processing and shaping (Tzoganakis, 1989). Thus, among the several design specifications that an extruder can have, it is important for a researcher to select the machine that suits the purpose and nature of the experiment.

Raw materials, or reactants, are first conveyed either manually or by automatic feeders to the feed hopper which is the feeding point in the extruder. Once it is fed to the extruder, reactants will be subjected to the pre-set temperature of the extruder barrel and simultaneously are transferred throughout the barrel via rotating screw(s). Furthermore, the barrel can have integrated ports

which can be used as injection or/and de-volatilization facilities (Figure 2-10). This enables introducing additives at a desired stage throughout the reaction.

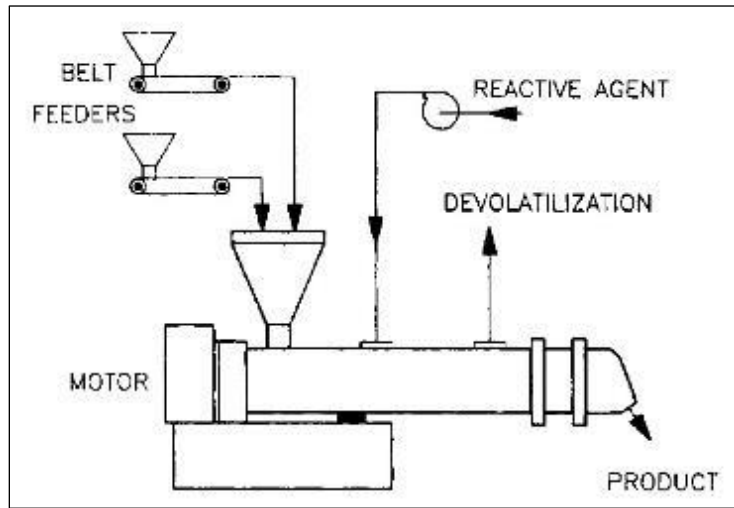


Figure 2-10: Scheme of reactive extrusion process (Tzoganakis, 1989)

In some extruders, the barrel is divided into zones with the possibility of controlling the temperature of each zone independently. This can be essential when the operation is thermally sensitive or when additives are introduced via an injection port and require higher temperature to react than the melting temperature. Processed materials are discharged from the extruder through a die at which it starts to solidify and then pelletized.

Extruders are commonly distinguished by the number of screws inside the barrel which can be either single-screw or twin-screw. Moreover, the arrangement and design shape of the screw(s) are often carefully selected based on the nature of the operation and the properties of the materials to be processed. The main difference between single and twin screw arrangement is the mechanism of which the melt is transported from the feed hopper to the die (Janssen, 2004). For instant, in single-screw extruders the movement of the melt in the barrel is caused by the friction force between the screw and the barrel wall. Hence, if the processed material happened to slips, the melt might rotate on the screw surface rather than being pushed forward. Therefore, the transport efficiency in single-screw extruders is strongly dependent on the materials properties. On the other hand, in twin-screw extruders it is common to arrange the screws in a way that the flights of one screw is inside the channels of the other (Janssen, 2004). As a result, better transport

efficiency throughout the barrel is usually expected when twin-screw extruders are used. Various kinds of screws arrangements are shown in Figure 2-11.

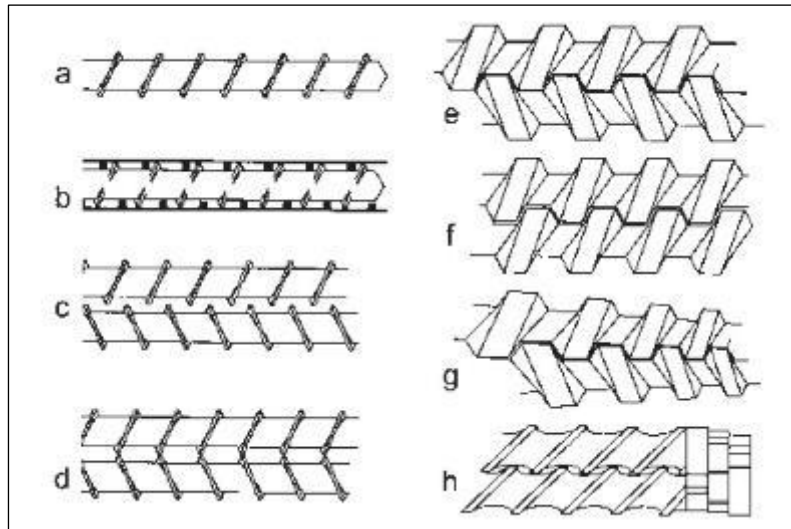


Figure 2-11: types of screw arrangements: (a) single-screw, (b) co-kneader, (c) nonintermeshing, mixing mode, (d) nonintermeshing, transport mode, (e) counterrotating, closely intermeshing, (f) corotating, closely intermeshing, (g) conical counterrotating, and (h) self-wiping, corotating (Xanthos, 1992)

Twin-screw extruders are also differentiated by the rotation direction of their screws. The rotation can be either co-rotating, when both screws rotate in the same direction, or counter-rotating when they rotate in opposite. Although both extruders, single and twin-screw, can be used for reactive extrusion, twin-screw extruders are generally preferred for several reasons. First, twin-screw extruders are known for their very well mixing capabilities. This is a crucial advantage since it allows for obtaining a homogenized product. Moreover, quality of mixing can also affect the residence time distribution (RTD) and, therefore, can impact the extent of reaction (Tzoganakis, 1989). Furthermore, corotating twin-screw extruders are considered to be more effective for reactive extrusion than counter-rotating screws (Tzoganakis, 1989). Because the co-rotating arrangement usually offers smaller gap between the screws in addition to the fact that corotating offers more efficient wiping of processed material from one screw by the other.

Reactive extrusion was first implemented by Dow Chemical back in 1948. They have used a single-screw extruder as a main polymerizer, downstream of a CSTR pre-polymerizer that was used to process low-viscosity polymer, for the production of polystyrene (Janssen, 2004). Later in 1968, Gouinlock conducted an experiment that produced a copolyester in a vented twin-screw

extruder (Gouinlock et al., 1968). Similar to Dow, pre-polymerization was conducted in a melt reactor and the product was successfully polymerized further in the extruder. A year later, Illing demonstrated the polymerization of nylon via reactive extrusion (Janssen, 2004). Gradually, engineers realized the potential in utilizing extruder in reactive processing. As a result, numerous studies were published in recent years that demonstrated successful attempts in carrying out wide range of chemical reaction kinetics via reactive extrusion. These chemical reactions can be divided into five main types:

- a. Bulk polymerization: In bulk polymerization process, a high MW polymer is prepared either from monomers or low MW polymers (Janssen, 2004).
- b. Grafting and functionalization reactions: In this type of reactions, a monomer or a short chain of polymer is chemically integrated to the backbone of the polymer chain. When only a single monomer is linked chemically to the polymer chain, the reaction is considered a functionalization reaction. Whereas when a short chain of polymeric material joins the backbone chain, the reaction in this case is a grafting reaction. Both reactions are known for changing the chemical and physical properties of the polymer and, therefore, are usually performed to introduce an industrial added value product. Grafting reactions usually produce a product with higher viscosity than when functionalization reactions are performed because larger molecules are bonded to the chain in grafting (Janssen, 2004).
- c. Degradation reactions: Controlled degradations reaction can also be performed in extruders. Such reactions usually performed when a polymer with lower MW is desired or for producing a grade of polymer with higher number of active sites that can be used in functionalization or grafting reactions (Tzoganakis, 1989).
- d. Interchain copolymerization: in this reaction, two or more polymers react together to produce a grafted copolymer. As oppose to grafting reactions, multiple reactive polymers are used in this type of reaction to make the final product.
- e. Coupling reactions: in this type of reaction, a polyfunctional coupling agent, or chain extender, is used to link separated polymeric chains. This link can result in a linear chain extension or branching which increases the MW or the polymer.

Examples of various kinds of polymerization reactions that were done in extruders are shown in Table 2-1.

Table 2-1: Various types of reactions were performed in extruders (Xanthos, 1992)

Type of polymerization	End product
Step polymerization (condensation reactions)	Polyetheramide
	Polyesters
	Polyethylterephthalate (PET)
	Polybutylterephthalate (PBT)
	Polyamide 6.6
	Polyarylate
	Polyurethanes
Chain polymerization (addition reactions)	Polyamide 6
	Polyoxymethylene
	Polymethyl methacrylate (PMMA)
	Acrylic polymers
	Polystyrene and styrene copolymers
Graft reactions and functionalization reactions	Water soluble polyamide
	Graft copolymer of polystyrene and maleic anhydride
	Graft copolymer of polyolefines and vinylsilanes
	Graft copolymers of polyolefines and (meth) acrylic monomers
	Graft copolymer of EVA with acrylic acid
Interchain copolymer formation	Graft copolymer of polyolefines and maleic anhydride
	Halogenation of polyolefines or EVA
	Copolymers of reactive polystyrene and polymers with amide, mercaptan, epoxy, hydroxy, anhydride or carboxylic acid groups
	Copolymer of polypropylene grafted with maleic anhydride and nylon 6
	Copolymer of polyolefines and polystyrene
Coupling reactions	Copolymer of EVA grafted with methacrylates and grafted polystyrene
	Coupling of PBT with diisocyanate and polyepoxide or polycarbodiimide
Degradation reactions	Coupling of PET with bis(2-oxalzone)
	Degradation of polypropylene by shear-heating
	Degradation of PET with ethylene glycol

2.6.2- Chain extension of PET via reactive extrusion

Chain extending additives has been increasingly used in increasing polymers' molecular weights. They are coupling agents that are capable of initiating addition reactions with functional groups in the polymers' chain (-OH and -COOH groups) which results in longer polymer chains. Furthermore, chain extenders are either bi or multi-functional chemicals which means that they

can react in a variety of mechanisms and, therefore, can provide a wide range of high IV. For example, bi-functional chain extenders are preferred when a linear chain extension is desired. On the other hand, multi-functional coupling agents can encourage branching and crosslinking reactions in the polymer chain. While solid-state polymerization is the conventional process for increasing polymers MW, chain extenders offer several advantages over SSP. First, they can be used in a reactive extrusion processes to react with polymers within minutes as oppose to SSP processes which could take up to 20 hours. Moreover, SSP operations require much larger capital and operational investment since it uses dryers with vacuum facility to maintain certain temperature for long time with continues gasses removal. That large cost is often difficult to be justified especially with the batch nature of the operation.

In theory, any chemical with bi- or multi-functional groups can be used as a chain extender. However, several chemicals can cause side reactions or produce by-products and, therefore, are not suitable for the application (Scheirs & Long, 2006). There are few chemical families that have been proven effective, safe and relatively stable chemicals to be used precisely for PET chain extension such as: bisanhydrides, bisoxazolines and bisepoxides.

Many experiments were conducted to evaluate the effectiveness of chain extenders in increasing IV of PET or R-PET. Moreover, variables that are thought to be important, such as CE's concentrations and reaction residence time, are often examined in order to obtain better understanding of the reaction between the polymer and the additive. Cardi have studied the effect of 2,2'-Bis(2-oxazoline) as a chain extender when added to R-PET and fiber-grade PET (Cardi et al., 1993). Drying, which is important prior to extrusion in order to remove contamination that can result in polymer degradation, was done at 120 °C over 16 hours. A twin-screw extruder was used in compounding the polyester with the chain extender at various ratios of carboxylic acid mol /CE mol content as well as at various residence time in the extruder. The results showed that the additive had successfully overcome the reduction in IV that commonly occurs when the thermoplastic is recycled but without achieving a PET grade with high IV. It was also observed that the increase in IV when additive-to-Carboxylic content ratio is 3:1 was less than when the ratio was 2:1. It was suggested that when high additive concentration is used, some unreacted additive acted as a lubricant which reduced IV. Another study had investigated the effectiveness of pyromellitic dianhydride (PMDA) as a chain extender for R-PET (Awaja, Daver, & Kosior, 2004). The researchers highlighted several advantages in using PMDA as a coupling

agent such as: low cost, availability and the fact that PMDA is a multi-functional chain extender which gives it a potential to increase IV significantly. In this experiment, researchers used an “intensive drying” technique on the polymer which involved blowing desiccated air at 170 °C over 4 hours. Moreover, they have studied the increase in IV versus residence time and PMDA concentration which was found to be strongly correlated. An increase of around 20% in IV was reported when PMDA was added at a relatively low level (0.3 wt%). Furthermore, an analysis was performed to measure the degree of crosslinking when a crosslinking reaction was anticipated. It was proven that crosslinking reaction took place when concentration of PMDA was around 0.35 wt% at extended residence time (around 112 seconds). The paper also shed a light on a widely-ignored operational parameter which is the extruder’s die pressure. As the polymer experienced heavy crosslinking and gel formation, it is anticipated that an increase in the extruder’s die pressure will occur. Awaja have recorded this increase in the die pressure versus residence time and the chain extender concentration. Throughout his experiment, he interpreted the die’s pressure reading to indicate thermal or chemical instabilities in the operation.

Multi-functional epoxy-based chain extenders were also tested and proven effective in increasing PET’s IV. Japon was interested in improving the melt strength on PET in order to perform better in foaming applications (Japon et al., 2000). In his work, he emphasizes on the fact that there are important factors in producing a polymer suitable for foaming; the average MW, MWD and the degree of branching and, therefore, he tried three epoxy-based chain extenders and tested their effectiveness in reacting with PET. These chain extenders are 4-glycidyoxy-N,N0-diglycidaniline (Araldite MY 0510, Ciba SC) tri-functional resin, Tetraglycidyl diamino diphenyl methane (TGDDM) (Araldite MY 721, Ciba SC) a tetra-functional resin and a glycidyl ether of bisphenol A Novolac resin (Epon resin SU-8, Shell Chemical Company) which has a high epoxy functionality of 8 functional sites.

Effectiveness of each additive was tested by mixing each of them with PET in a twin-screw extruder and observing the increase in torque, higher torque was interpreted to higher melt viscosity and, hence, higher reactivity between the additive and the polymer. PET was dried in a vacuum oven at 150 °C over 6 hours and the additives were dried at around 40-50 °C over 24 hours prior to extrusion. Then, PET/additive mixtures were fed to a twin-screw extruder that had been set to have the following temperature profile: 220 °C at the feeder, 270 °C at the center

and 250 °C at the die and 50 rpm rotation speed which allowed for a residence time of 40 ± 5 seconds. This effectiveness test showed that while the tetra-functional additive showed higher reactivity than the tri-functional one, there was almost no effect when glycidyl ether-additive was used. Then, different concentrations of the tetra-functional additive (TGDDM) were tested and it was revealed that secondary-undesired reactions can occur when 0.5 wt% additive is mixed with PET at long residence time (17 minutes). Thus, an optimum stable additive-concentration of 0.4% was tried and the product was analyzed for IV which showed that a maximum value of 1.13 dL/g, at a residence time of around 5 minutes, was achieved up from 0.81 dL/g for unmodified PET. It worth noting that this result was achieved via extruding the mixture twice. In another study, 2,2'-(1,4-phenylene)bis(2-oxazoline) (1,4 PBO) was used as a chain extender to increase IV of recycled PET (Karayannidis & Psalida, 2000). This additive, as well as 1,3 PBO, is a bi-functional chain extender that is known for its reactivity toward carboxylic acid groups in R-PET but not hydroxyl groups. Despite of that, there are several advantages in using PBO such as its very low-cost. Although chain extension reaction was conducted in flask, the required reaction time is believed to be around 3-5 minutes (can be done in an extruder).

The addition reaction was performed in a three-neck round-bottom flask with continuous stirring and in argon atmosphere. First, R-PET sample was dried at 120 °C inside the flask in oil bath and under argon atmosphere for around 30 min. Then, the polymer was melted at 290 °C and the chain extender additive was added with continuous stirring at 200 rpm. Continuous sampling from the flask was conducted at 5, 7.5, 10, 12.5, 15, 20, and 25 minutes in order to study how the reaction develops versus time. Furthermore, researchers investigated the addition of Phthalic Anhydride (PA) to the mixture assuming it will react with hydroxyl terminals in PET and, hence, produce carboxylic terminals that react with PBO. The first part of the experiment, which involved using 1,4 PBO solely, revealed that the additive successfully enhanced the IV of R-PET when added at a stoichiometry of 2:1 additive-to-carboxylic molar content. The maximum IV of 0.8 dL/g was obtained at a relatively long reaction time (25 minutes) and it accounts for around 16% higher than when the polymer was melted in same conditions but without additives. This result was enhanced further when PA was added prior to melting it with R-PET and adding 1,4 PBO after that. The results for this second part showed that higher IV was reached (0.85 dL/g) at shorter reaction time of around 15 min and remained constant through at the 25-minutes experiment.

2.6.3- Degradation routes of PET

When processing PET melt in an extruder or mold injection machine at high temperatures, it is anticipated that degradation is likely to take place. Although there are many possible degradation scenarios that can occur in these process, the most commonly encountered are Three: hydrolytic degradation, thermal degradation and thermo-oxidative degradation (Mrozinski, 2010; Venkatachalam et al., 2012). These degradation routes will be briefly discussed in order to realize how their occurrence can be minimized.

- a- Hydrolytic degradation: when water is present in PET, hydrolytic degradation is very likely to occur. In this case, the resulting polymer will have an increase in the hydroxyl end-group as well as carboxyl end-group content (Mrozinski, 2010; Venkatachalam et al., 2012). This degradation is self-catalyzed by the resulting carboxyl end-group and it occurs at much faster rate than other degradation routes (Venkatachalam et al., 2012). Since proper drying of the polymer can help avoiding the occurrence of this reaction, it is a standard that PET should be dried prior to processing. Drying PET is particularly important given the hygroscopic nature of the polymer that makes it a moisture-absorbing material.
- b- Thermal degradation: This degradation route is associated with the high temperature at which the polymer is processed. High temperature processing can initiate a scission in the ester linkage in PET followed by several reactions that result in reduction in the polymer's molecular weight (Venkatachalam et al., 2012). The resulting product from this degradation scenario usually shows an increase in the carboxylic end-group content (Venkatachalam et al., 2012). Limiting the polymer's exposure to high temperature is obvious way to avoid thermal degradation. This can be done either by operating at temperatures just above the melting temperature or by reducing the residence time of the polymer in the process (Mrozinski, 2010).
- c- Thermo-oxidative degradation: Thermo-oxidative degradation of PET is not yet fully understood reaction although suggested mechanisms for the reaction were reported (Venkatachalam et al., 2012). In this route, PET degrades when exposed to high temperature with presence to oxygen. Hence, avoiding this reaction would require operating the extruder under vacuum or nitrogen purging (Mrozinski, 2010).

Chapter 3

Methodology, Materials and Equipment

3.1- Experiment, Equipment and materials

In this project, we have used the MFI value of modified and unmodified R-PET as the main indicator for the suitability of the material for 3D-printing application. This approach is commonly used in the polymer industry in order to evaluate suitability of a grade of polymer for a specific process as going to be explained in this section. Moreover, the MFI test should show the effect of the additive on increasing the molecular weight by showing lower MFI value for modified product. Since it is known that any recycled polymers are susceptible to degradation reactions when reprocessed in an extruder, I have used the chain extender PMDA as an additive to overcome this degradation reactions and increase the molecular weight. PMDA was selected among many other options due to its efficiency, being a chain extender that has 4 active sites, its low cost and availability. Furthermore, PMDA has been proven effective when used on R-PET as as been shown the literature review chapter. Figure 3-1 shows suggested reaction mechanisms of R-PET with PMDA.

Moreover, another additive was selected to study its effect(s) on the modified R-PET which is SEBS-g-MA. The styrene-ethylene-butylene-styrene elastomer was reported to enhance thermal stability of PET in addition to its nucleation effect which helps accelerating crystallization (Jamaludin et al., 2015; Ganguly & Bhowmick, 2007; Ishak et al., 2008; Zhang et al., 2010). Both properties can be useful in our task since thermal stability might limit the thermal degradation of our recycled polymer and increasing the crystallization rate can allow the melt to hold its structure when it is discharged from the extruder die. SEBS-g-MA has been used for other purposes as well such as enhancing ductility and toughness when blended with other polymers (Ishak et al., 2008; Tanrattanakul et al., 1997). This additive, however, will not be the primary modifier in our project but rather few experiments were done to study the effect it makes on the melt flow when presented along with PMDA. Although PMDA should enhance the viscosity of

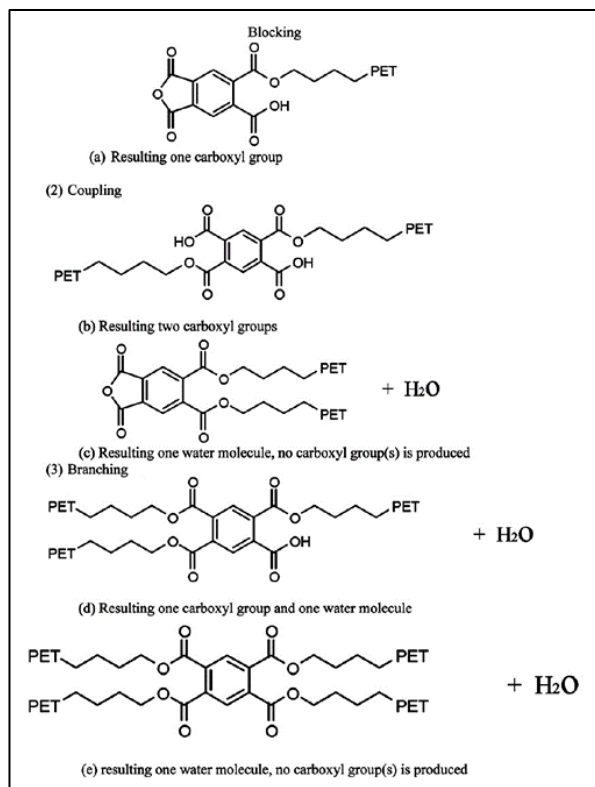


Figure 3-1: PMDA reactions with PET (Awaja et al, 2004)

R-PET to make it 3D-printable, another challenge was obvious which is the production of the polymer in the standard filament shape. I have put together a set-up that almost mimicked the production process and indeed provided good results as will be discussed in the results chapter. All main resources that were used in the project are listed in Table 3-1 and 3-2.

Table 3-1: Materials and Chemicals

Chemical	Application	Supplier	Product number
R-PET	Raw material	Post Plastics Inc.	Black R-PET FDA approved
PMDA	Additive	Sigma-Aldrich	412287
SEBS-g-MA	Copolymer	Kraton Polymers LLC	FG1901GT
KBr	FT-IR analysis	Sigma-Aldrich	221864
Filaments	Comparative study	N/A	N/A

Table 3-2: Equipment and apparatus

Equipment	Use	Supplier	Product number
Single-screw extruder	Compounding	Filabot	Wee extruder
Twin-screw extruder	Compounding	ThermoFisher	HAAKE 2 mini compounder
Melt Flow Index tester	MFI test	Dynisco	FG1901GT
FT-IR device	FT-IR analysis	Bruker	VERTEX 70/70v
Mill	Additive mixing	IKA	M20
Grinder	Grinding extrudate	Thomas-Wiley	Model 4
3D-printer	Trying filament product	Wanhao	Duplicator i3
Press machine	Making FT-IR samples	Craver	3853-0
Vacuum oven	Drying	VWR	1400E
Spooler	Tractor	Filabot	FB00073
Microscope	Verify ovality	Leica	MZ6
Cooling water bath	Melt-quenching	3D-printed	N/A

3.2- Methodology

- Melt Flow Index test

In this project, we have used the MFI value of modified and unmodified R-PET as the main indicator for the suitability of the material for 3D-printing application. MFI is one of the most common tests performed to investigate the melt-processability of various types and grades of polymers. Although it is considered as a simple and slightly old technique of determining polymer rheology, many polymer end users still use MFI value to determine the suitability of a polymer grade to their processes (Shenoy & Saini, 1986). Furthermore, an MFI value of a polymer

can give an idea about several mechanical and physical properties of the polymer such as: weight-average molecular weight, MWD and branching in the polymer chain (Shenoy & Saini, 1986).

The MFI test is very often conducted by following the ASTM D 1238- 04 standard titled “Standard Test Method for Melt Flow Rates of Thermoplastics by Extrusion Plastometer”. In an MFI test, the polymer sample is charged into heated barrel that is mounted vertically with a specific die size at the bottom and open whole at the top. As per the standard, after the material is charged it should be kept in the barrel for a standard time to allow the polymer to melt inside the barrel. Then, a piston and a weight attached to it are used to exert a gravitational pressure on the melt through the top whole till it come through the die at the bottom of the barrel. Finally, the amount of polymer that left the die is measured (grams) against time (seconds) and expressed in the standard unit (g/10 min) which is the MFI value.

It has been noted in the literature that the MFI test is very sensitive and requires a very careful conducting of the experiment in order to provide accurate results. The reason for that is being the number of variables involved that can sometimes be difficult to control through out the experiment and, as a result, become sources of error. These variables include; packing the sample in the barrel, the cleanness of the barrel, blockages in the die, delay between charging the packing the sample, worn piston and several other factors (Shenoy & Saini, 1986). Additionally, special care must be taken with moisture-sensitive materials are to be tested in MFI instrument because of the higher chances of degradation to occur while melting the sample which will have a significant effect on the test results (Shenoy & Saini, 1986). Since we will be testing R-PET in this project, which is indeed a moisture-sensitive material, all samples were dried in an oven before charged to the MFI instrument to avoid degradation. Despite the fact that MFI tests are sensitive to many variables, it remains to be a favorable test in the polymer industry for obtaining an indication about the polymer rheology due to its simplicity and very low cost. Other instruments that can be used to study melt flow are often expensive and require higher level of training (Shenoy, Saini, & Nadkarni, 1983).

- Investigating the chemical composition by FT-IR

While MFI results show enhanced mechanical properties of the modified R-PET, FT-IR analysis can provide very useful information about our modified material at the molecular level to confirm

our observations. Since a chain extender was used to couple the polymer's chains through functional hydroxyl and carboxyl end-groups, it might be possible to detect a change in the IR spectrum as a result of this reaction. Moreover, FT-IR will be used to seek an evidence of incorporating SEBS-g-MA into R-PET. Note that FT-IR is not very often used in quantifying end-groups of a chain extended R-PET as Pohl's method is the most commonly used (Pohl, 1954). Pohl's method, on the other hand, requires various resources as well as working with hazardous chemicals. In our FT-IR test, the spectrum was from 400 cm^{-1} to 4000 cm^{-1} , the resolution was at 4 cm^{-1} and 64 scans per test.

- Additives mixing and samples preparation

Whenever additives are compounded with polymers, a careful selection of mixing method is needed in order to achieve a uniformed mixture. This selection takes into consideration several factors including: the material's phases, forms, shapes and volumetric concentration. The most efficient way to uniformly feed two or more materials to an extruder is done using a gravimetric feeder to feed each material at certain rate directly to the extruder's hopper (Wagner, Mount, & Giles, 2014). However, those feeders might not be always available due to their cost or space limitation. Therefore, methods of mixing additives prior to processing them in an extruder are often applied.

In this project, the two materials that were mainly present in all samples are R-PET polymer, which is in flakes form, and the additive PMDA which is in the form of fine powder. Furthermore, the additive weight- concentration in the mixture ranges from 0.25% to 0.75% and the volumetric concentration of this additive is negligible in the mixture. Given these conditions, a high-intensity mixer was used for mixing the two components. High-intensity mixers are recommended when all materials to be mixed are in powder form or when a material is required to be added at very small proportion to the other (Wagner, Mount, & Giles, 2014). One important feature associated with using high-intensity mixers is the fact that they generate heat as a result of the high rotational speed of the blades. It was noticed that this heat sometimes made PMDA adhesive to the blender's walls which resulted in losing some amount of the additive to the blender's wall. As a result, a standard was set for mixing the samples by operating the blender in a pulse style to avoid heat generation in the mixing chamber. For each sample of R-PET and PMDA, the mixture was added to the mixing chamber of the blender and the blender was turned on for 1 second only and this

was repeated for two more times. This method was found to be very suitable for the kind of materials being used since the product mixture showed a uniform distribution of PMDA on the surface of the R-PET flakes. Eight samples were prepared as shown in Table 3-3.

Table 3-3: Prepared samples

Sample number	PMDA wt%	SEBS-g-MA wt%	Extruder's type
1	0.00	0	Single-screw
2	0.25	0	Single-screw
3	0.50	0	Single-screw
4	0.75	0	Single-screw
5	0.25	0	Twin-screw
6	0.50	0	Twin-screw
7	0.75	0	Twin-screw
8	0.25	5%	Single-screw

- Drying

Drying PET is an essential step prior to extrusion to avoid polymer degradation especially with the fact that PET is moisture sensitive. For the purpose of purely studying the additive's effect on the melt flow behavior, it was important to dry the sample completely in order to avoid any noise in the results caused by moisture presence. This was done by allowing the sample mixture to dry in a vacuum oven for overnight at 100 °C. Each sample was placed in a beaker and the beaker was covered by aluminum foil. Then, few pokes were made on the cover to ease degassing evaporated gasses.

As previously mentioned, the effect of drying duration on the polymer's MFI value was studied as part of this project. But it is worth noting that the experiment was done on pure unprocessed R-PET rather than a mixture of R-PET and the additive PMDA.

- Extrusion

Extruding compounded samples was done using two types of extruders: single-screw and twin-screw for comparison purpose. The single-screw mini-extruder is manufactured by Filabot and it is meant for private home-use where 3D-printing enthusiasts are expected to use this extruder to recycle their 3D-printed object and produce a filament (Figure 3-2).



Figure 3-2: Filabot wee single-screw extruder

This extruder has a fixed screw-rotational speed of 35 rpm whereas the temperature can be varied up to 400 °C. One unique feature in this extruder is the ability to replace the extruder's die with various die sizes that can be purchased from Filabot. Samples are fed to this extruder simply by pouring the sample the extruder hopper and the screw will draw the material into the barrel till the hopper is empty. Design sheets for the extruder's barrel and screw were obtained for reference (Figure A-4 and A-5). The other extruder is a co-current self-wiping twin-screw mini-extruder manufactured by ThermoFisher Scientific (shown in Figure 3-3). This extruder is a more advanced equipment than the first one and, therefore, provides many additional features such as: the ability to manipulate the rotation speed, displaying the value of the die pressure, the torque and the pressure difference across the barrel. These features are useful as they can indicate the melt behavior inside the barrel. For example, higher torque reading can be attributed to higher melt viscosity which also can be observed by an increase in the die pressure.



Figure 3-3: HAAKE 2 mini compounder (twin-screw extruder by ThermoFisher Scientific)

On the other hand, the die size of this extruder cannot be changed as oppose to the single screw. Additionally, feeding the material to the extruder has to be done manually by pouring small amount of the sample and forcing it into the barrel using a metal rod. Once the first portion was pushed, then another pour is supplied and pushed again and so forth. As one can see, this mechanism of feeding can result in inconsistence feeding rate and maybe inconsistent residence time of the material in the barrel throughout the run although no clear effect of this feeding method on the final product was observed. Table 3-4 summarizes the main advantages and disadvantages of both extruders used in the experiment.

Table 3-4: Comparison between the two types of extruders used in this project

Extruder's Type	Manufacturer	Advantaged	Disadvantages
Single-screw	Filabot	<ul style="list-style-type: none"> - Economical - Auto-feeding - Portable 	<ul style="list-style-type: none"> - Fixed rotational speed - No indications for operational parameters
Twin-screw	ThermoFisher Scientific	<ul style="list-style-type: none"> - Manipulation of rotational speed - Provides operational parameters (e.g. torque, die pressure) 	<ul style="list-style-type: none"> - Manual feeding - Not portable

As per the literature review, reaction of PMDA and PET takes place at a temperature of around 280 °C and, therefore, this temperature was selected as the extrusion temperature for all runs in both types of extruders. For the rotational speed, since one of the extruders had a pre-set speed of 35 rpm it was decided that this speed will be selected as the rotation speed for both extruders.

- Lab-scale filament production process

Although the manufacturing process of FDM filaments is relatively simple in terms of the number of equipment needed, the final product has to meet very precise specifications that might require very precise manufacturing tools. As mentioned earlier, FDM filaments are produced commercially with a filament diameter of 1.75mm and 3.00mm with a tolerance of $\pm 0.05\text{mm}$. With this very tight margin of tolerance, it is anticipated that only high-end manufacturing technologies would be able to provide an on-spec product in a continuous operation. Although some sources have estimated an acceptable tolerance of the 1.75mm filament to be $\pm 0.1\text{mm}$ (Dubashi, Grau, & McKernan, 2015), it was observed that this margin of tolerance is too large and it caused jamming of the filament in the filament-feeder section of the printer. Therefore, this project will consider the commercial standard ($1.75\text{mm} \pm 0.05\text{mm}$) as the reference for determining an on-spec product.

The filament production process in this project will consist of 3 main equipment: extruder, cooling water bath and spooler which is the equivalent of the tractor system in the conventional manufacturing processes. Although commercial processes use two cooling water baths (warm followed by cold) it was decided to eliminate the cold cooling bath, due to resources limitation and to simplify the process, unless we discover during the experiment that it is necessary which was not the case.

Filabot single-screw extruder was selected to be the extruder that is going to be used for the filament manufacturing for two reasons. First, being a desk-top extruder it has the advantage of being moved around and placed conveniently aligned with the other equipment. Second, drawing the sample from the hopper to the barrel is done without any interference as oppose to the other twin-screw extruder. This feature was considered important because when an interference is required by pushing the material to the extruder's barrel it is expected that this might result in inconsistent discharge of the melt which results in inconsistency in the product's dimensions. In other words, if an excessive pushing was applied at some point throughout the

experiment then the melt is expected to be discharged in faster rate which will create a variation in product spec.

A 3D-printed cooling water bath was used for the quenching stage. Although the designer of the bath is unknown, it was decided to try it and evaluate whether it provides sufficient cooling for our melt product. It is worth noting that for such small-scale filament manufacturing processes, it is common that designs of the cooling bath are obtained online and then 3D-printed since there are no commercial suppliers for them yet. Therefore, most designed cooling water baths are made by unknown enthusiasts, who found it to be suitable, and uploaded online for the public use.

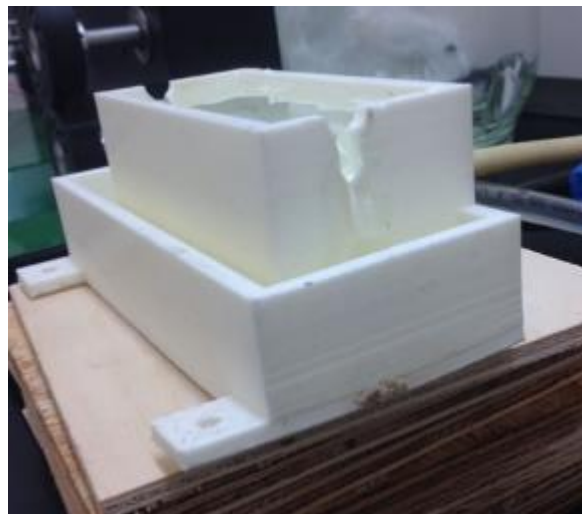


Figure 3-4: 3D-printed cooling water bath used in our project

A sufficient cooling here will be considered as the cooling that solidify the filament gradually and completely so that it should maintain its shape when it leaves the bath. The cooling water bath that was used in the project was 3D-printed with ABS material and is provided with inlet and outlet provisions for water circulation. It contains two chambers where water flows to the first, at which the filament will pass for cooling (Figure 3-4), and excess water overflows to the second chamber and drained through the outlet. The cooling water is supplied first to a container that is placed on a heating block and then it is supplied to the bath by a small water pump.

Winding, or pulling, the filament melt when leaves the extruder's nozzle was done using the Filabot Spooler instrument (Figure 3-5). This device is manufactured by the same vendor who manufactured the single-screw extruder and it is made precisely for the purpose of reducing the tolerance in the filament's diameter when making filaments at home. Filabot Spooler has two

circular rollers that are made of rubber, mounted vertically and rotate at a speed that can be controlled by the user. This device is the only small-scale device that was found online for filament-winding purpose which provides features similar to the tractor systems that are used in commercial filament making processes. Other spooling devices simply offer spooling the filament on a spooler for the sake of organizing the filament product without using rollers for precise pulling speed.



Figure 3-5: Filabot spooler

Chapter 4

Results and Discussion

4.1- Identifying melting point and crystallinity of R-PET by DSC analysis

PET is known to have a melting point at around 250 °C - 260 °C and this was confirmed through DSC analysis for our R-PET raw material. Identifying the melting point is precisely needed in this project because it will help setting up suitable extrusion temperature of the filament in the 3D printer as well as deciding the temperature for the MFI test. Figure 4-1 shows the DSC diagram for R-PET which indicates that the melting offset temperature is at around 255 °C.

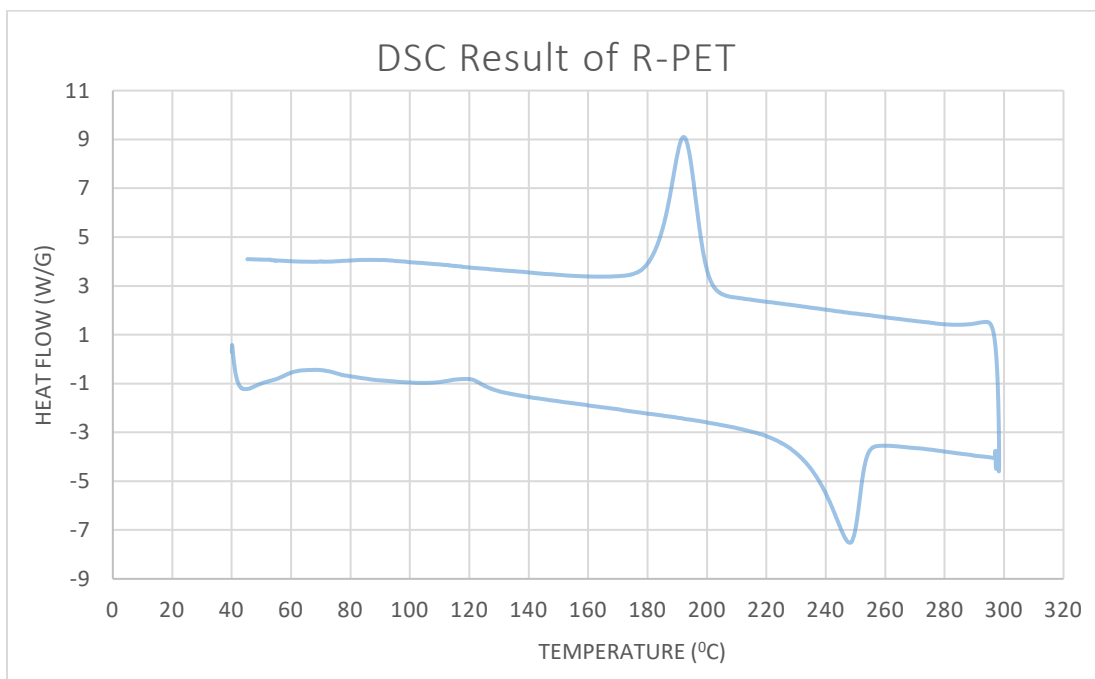


Figure 4-1: DSC results of unmodified R-PET

Hence, the minimum temperature for the MFI test was chosen to be 260 °C since below this temperature the polymer might not get completely melted which effects the MFI results.

4.2- Quantifying moisture in R-PET and its effect on the MFI value

Since PET is a hygroscopic polymer, the first step was to investigate the quantity of moisture that R-PET absorbs and how that affects the MFI test results. First, the weight fraction of moisture in R-PET was determined as a function of drying time. Drying the R-PET sample was done at 100 °C over 6 hours and weight measurement was taken every hour. The results are summarized in Table 4-1 and Figure 4-2.

Table 4-1: weight loss in R-PET due to drying

Drying time (h)	R-PET weight (g)	Weight loss percentage
0	44.811	0.00 %
1	44.7369	0.16 %
2	44.7184	0.206 %
3	44.7281	0.18 %
4	44.7218	0.199 %
5	44.7208	0.201 %
6	44.7192	0.205 %

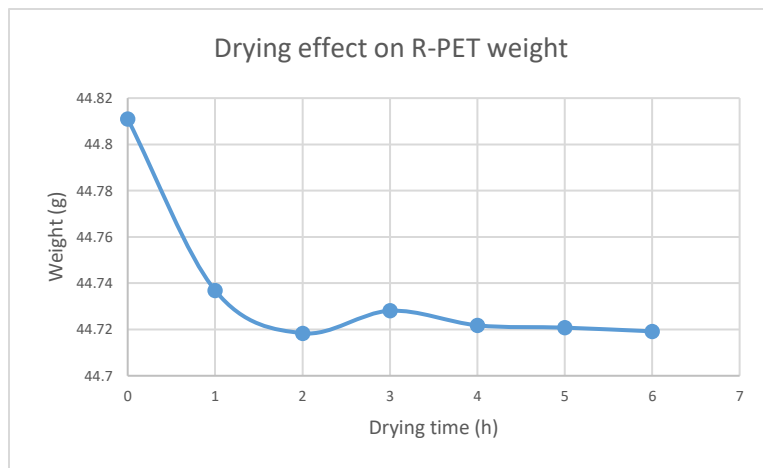


Figure 4-2: Weight loss as a function of drying time in R-PET sample

Results show that the R-PET sample had around 0.2% of its overall weight as moisture and possibly other volatiles. While this amount of moisture was measurable, it is significantly lower than contents that were reported for other moisture-sensitive thermoplastics such as Nylon. Furthermore, the figure shows that the weight loss occurred during the first two hours of drying.

This shows that in order to eliminate most of the moisture content, the minimum drying time that would be recommended is 2 hours (assuming drying at 100 °C). This drying time, however, is less than the commonly applied for recycled PET prior to extrusion which is often reported to be at least 6 hours (Cardi et al, 1993; Japon et al, 2000; Raffa et al, 2012). It is possible that drying for more than 2 hours is needed for the removal of some contaminations that are presented in the ppm level and, therefore, are non-measurable. Hence, further study was conducted to evaluate the effect of the drying time on the MFI value which should provide more accurate information on the drying requirements for R-PET that prevents material degradation.

R-PET was dried at various time intervals, ranging from 15 minutes to 4 hours, and MFI values were obtained for each dried sample. Figure 4-3 summarizes the results and it shows that the MFI value of R-PET is strongly affected by moisture presence as an increase of almost 4-fold in the MFI value was measured when R-PET was not dried. Furthermore, the data shows that the MFI value stays almost constant after half an hour of drying at 100 °C. These results helped in developing a standard practice when measuring the MFI value of R-PET that takes into consideration the importance of drying and the drying requirements prior to the test.

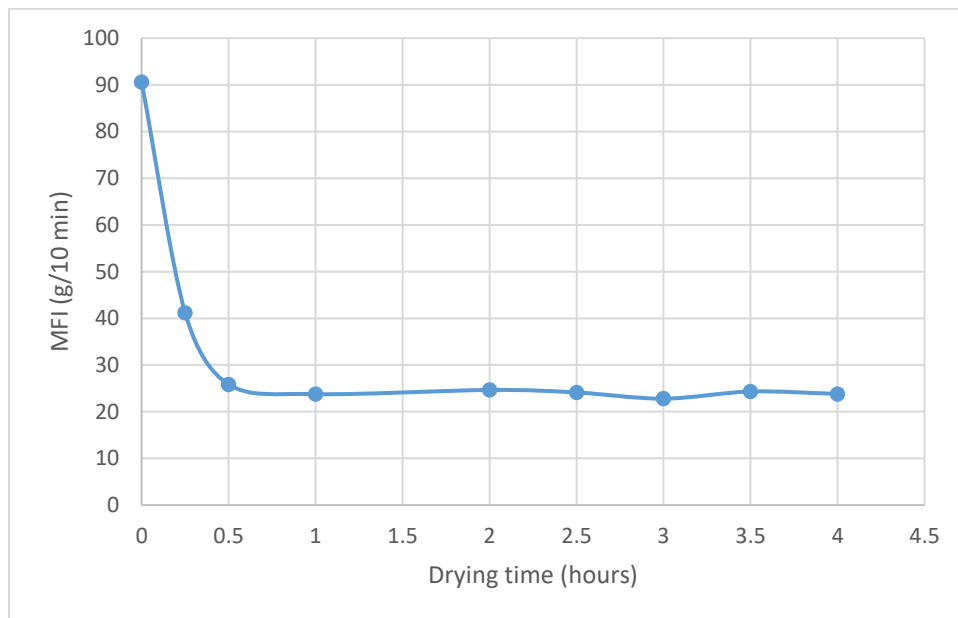


Figure 4-3: Drying effect on MFI result of unprocessed R-PET

4.3- Comparison between MFI values of commercial filaments and unmodified R-PET

The MFI value of several commercial filaments were measured and compared to reprocessed R-PET. The temperature at which the MFI test was conducted for each filament is the recommended printing temperature by the manufacturer since this will allow us to investigate the melt flow that takes place when printing with the filament. Further, the weight used to force the melt flow was kept constant for all tests (2.15 kg). Because when 3D-printing with various materials, the printer's motor forces the filament to the extruder at a specific force regardless of the kind of plastic being fed. The results are shown in Table 4-2 and Figure 4-4.

Table 4-2: Summary of MFI results of various filaments

Sample	Material (Manufacturer)	MFI T (°C)	Test 1 (g/10min)	Test 2 (g/10min)	Mean	SD
1	PLA (Dremel)	215.0	24.64	21.11	22.87	2.50
2	PLA (Wanhao)	215.0	25.49	31.71	28.60	4.40
3	R-PET (reprocessed)	260.0	100.51	80.6	90.56	15.04
4	ABS (HATCHBOX)	245.0	5.18	5.60	5.39	0.29
5	Nylon (Taulman)	240.0	4.19	4.68	4.44	0.34
6	TPE elastomer (Filaments.ca)	240.0	17.31	19.10	18.21	1.26
7	PETG (MG Chemicals)	260.0	5.37	5.26	5.32	0.08

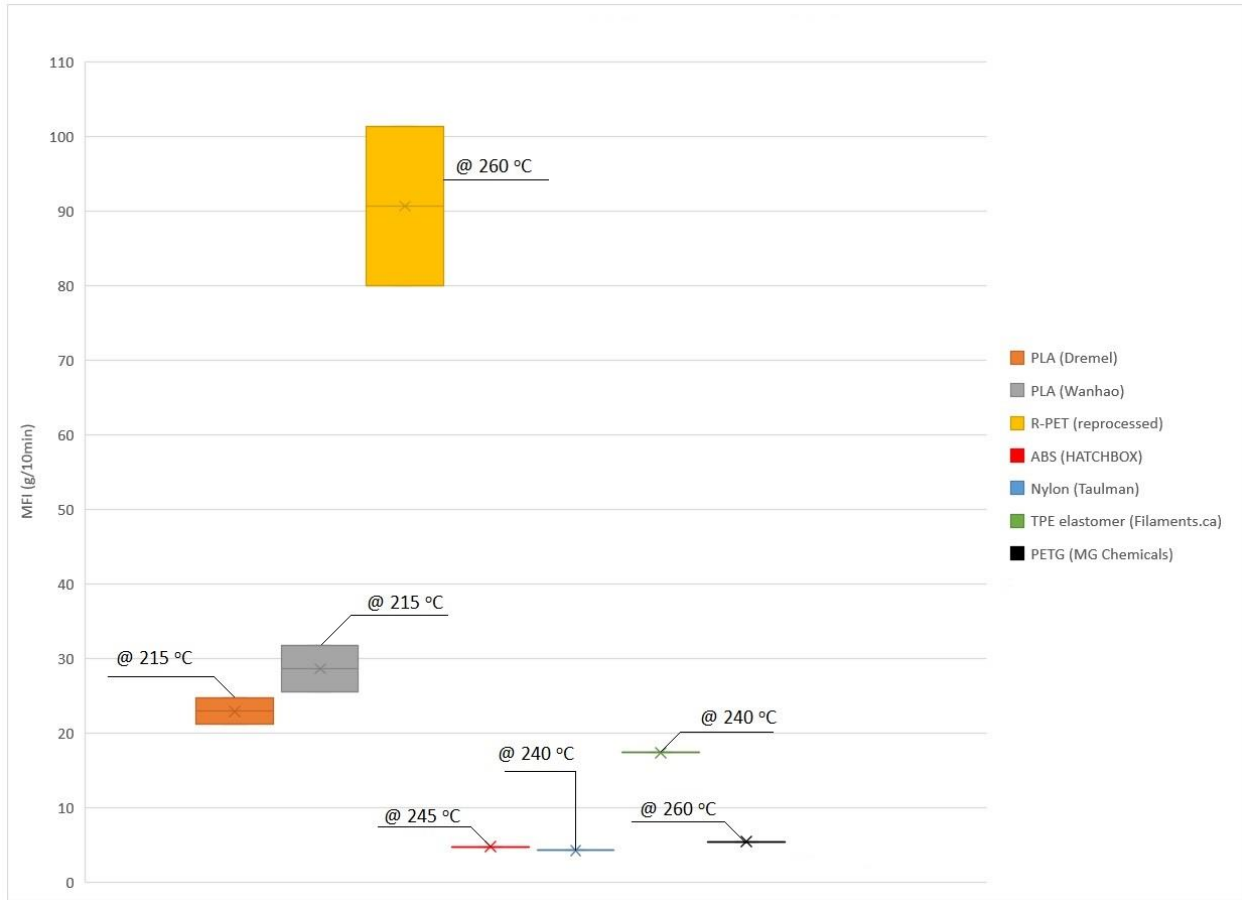


Figure 4-4: MFI results of various filaments

As shown in Figure 4-4, MFI results of all commercial filaments fall within a relatively narrow range (from 5 to 30 g/10min) whereas R-PET (reprocessed in a single-screw extruder) has a significantly higher value. Moreover, it was noticed that the MFI value of R-PET has steeply increased (viscosity reduced) when the polymer was reprocessed (re-extruded) compared to unprocessed material which is attributed to the degradation occurred while processing (Figure 4-5). Additionally, with R-PET getting degraded and becoming less viscous, the results became more vulnerable to sources of error which is observed by the higher variance value of the R-PET test result compared to the other filaments.

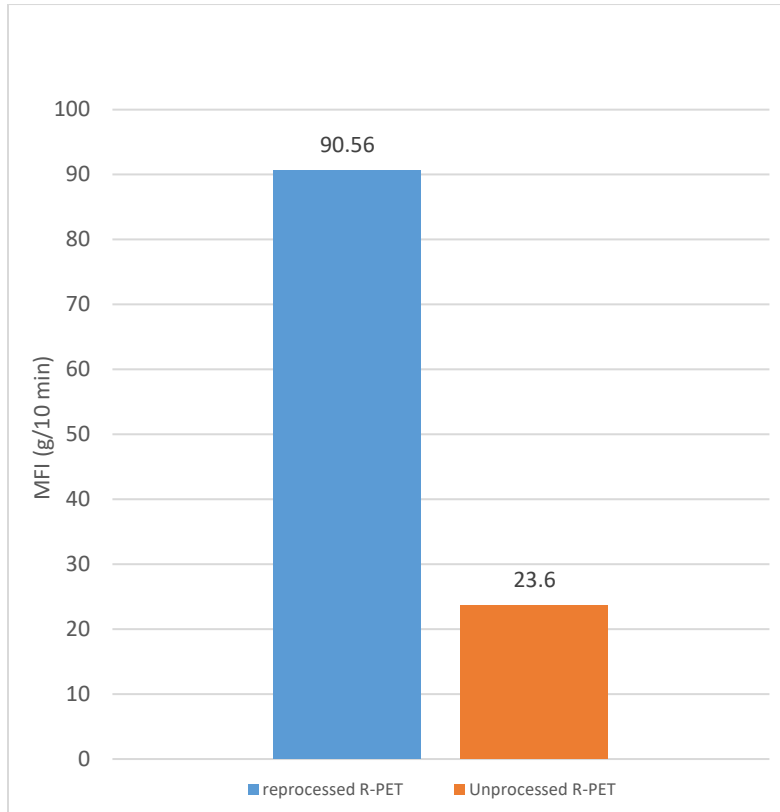


Figure 4-5: MFI values of reprocessed and unprocessed R-PET (both unmodified)

4.4 Effect of chain extender concentration and extruder's type on decreasing MFI of R-PET

The effect of PMDA chain extender on enhancing the melt viscosity of R-PET was studied by measuring the MFI values of modified R-PET. The additive concentration was varied at 3 levels which are 0.25, 0.5 and 0.75 wt% in order to obtain broad understanding on the effectiveness of the chain extender on the R-PET. Additionally, two types of extruders, single-screw and twin-screw, were used in compounding the additive with R-PET to study the difference that the extruder type can make especially in such experiments where mixing inside the extruder barrel can have an effect on the extent of reaction. MFI values were taken for all samples at 3 different temperatures 260, 275 and 290 °C in order to obtain more information about the melt behavior at various temperatures. These temperatures were precisely selected since they are expected to be at the suitable region for 3D-printing with R- PET. At 260 °C R-PET starts melting, 275 °C is the maximum temperature that can be achieved by our 3D-printer and 290 °C is the temperature that

provides gap margin between the melting and 3D-printing temperature that is close to the gap applied when 3D-printing with some commercial filaments. Since this project is about enhancing the properties of processed R-PET, we are going to use the processed unmodified R-PET as the baseline for the comparison against modified R-PET. Table 4-3 summarizes the MFI test results for modified R-PET.

Table 4-3: MFI results of modified R-PET

Sample	MFI at 260 °C (g/10min)				MFI at 275 °C (g/10min)				MFI at 290 °C (g/10min)			
	Test 1	Test 2	μ_{260}	SD_{260}	Test 1	Test 2	μ_{275}	SD_{275}	Test 1	Test 2	μ_{290}	σ_{290}
1	100.51	80.6	90.56	14.08	> 200	> 200			> 200	> 200		
2	4.33	4.12	4.22	0.15	5.46	5.10	5.28	0.26	15.55	16.27	15.91	0.51
3	1.43	1.51	1.47	0.06	3.13	3.38	3.25	0.18	9.79	9.14	9.47	0.46
4	1.26	1.17	1.21	0.06	2.80	2.83	2.81	0.02	6.33	6.49	6.41	0.11
5	7.55	7.03	7.29	0.37	13.01	13.80	13.41	0.56	29.30	30.55	29.93	0.88
6	5.53	5.31	5.42	0.16	10.72	10.66	10.69	0.04	18.18	18.42	18.30	0.17
7	1.19	1.21	1.20	0.01	1.80	1.84	1.82	0.03	4.88	4.79	4.83	0.06
8	15.11	16.10	15.61	0.70	29.14	28.11	28.63	0.73	49.77	51.36	50.57	1.12

Figure 4-6 Compares MFI values at 260 °C of unmodified and modified R-PET that were processed in both extruders. Results confirm that we have successfully increased the viscosity of the polymer via reactive extrusion with the PMDA chain extender. The figure shows a significant decrease in the MFI value, around 21-fold, even at low PMDA concentration level 0.25 wt%. Furthermore, the results show a milder decrease in the MFI value when PMDA concentration was elevated to 0.5 wt% and 0.75 wt%. The lowest MFI value that was reached, at 260 °C, using the single screw extruder was at PMDA 0.75 wt% with 72-fold reduction in MFI compared to unmodified R-PET. Moreover, results show that very minor change in MFI was recorded when PMDA concentration was increased from 0.5 wt% to 0.75 wt% when samples were tested at 260 °C. The difference, however, became clearer when samples were tested at 290 °C as going to be shown. Figures 4-7,4-8 and 4-9 show the MFI values obtained by single-screw versus twin-screw extruders as a function of the concentration of chain extender at various testing temperatures.

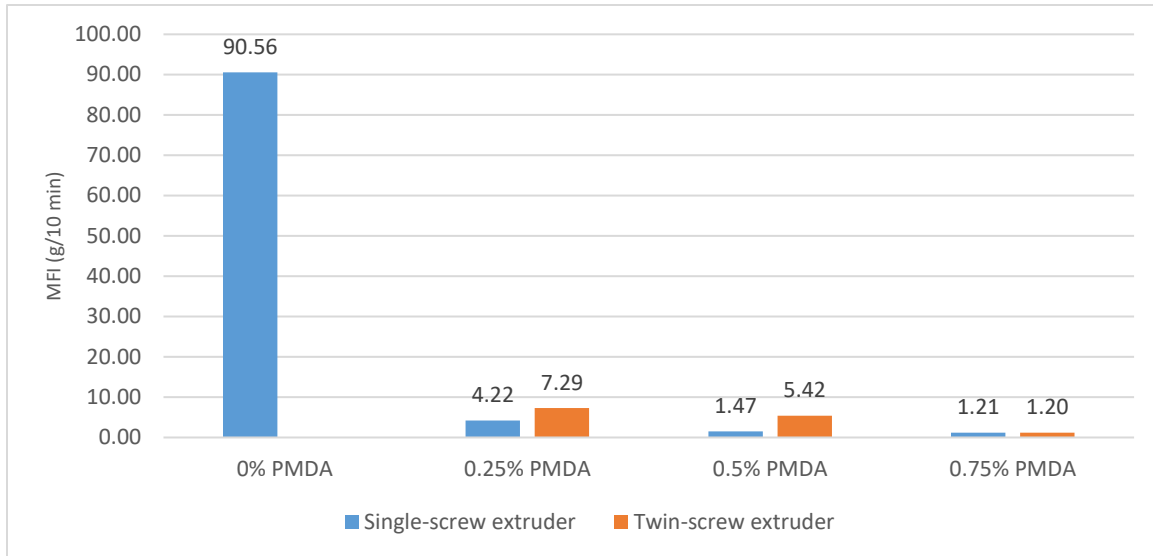


Figure 4-6: MFI values of modified and unmodified R-PET at 260 °C

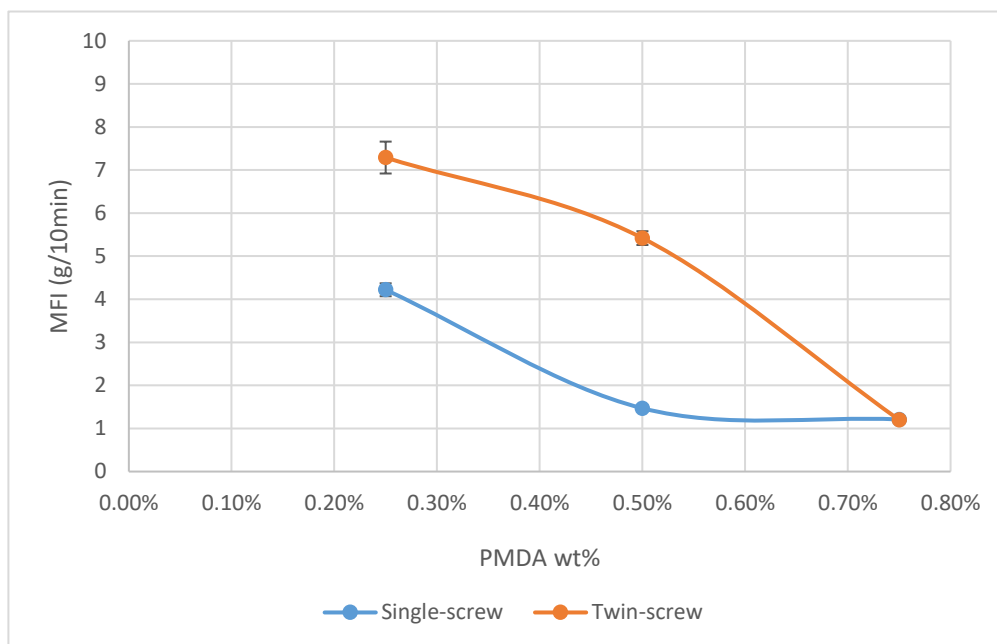


Figure 4-7: MFI values obtained by single-screw vs. twin-screw extruders (MFI at 260 °C)

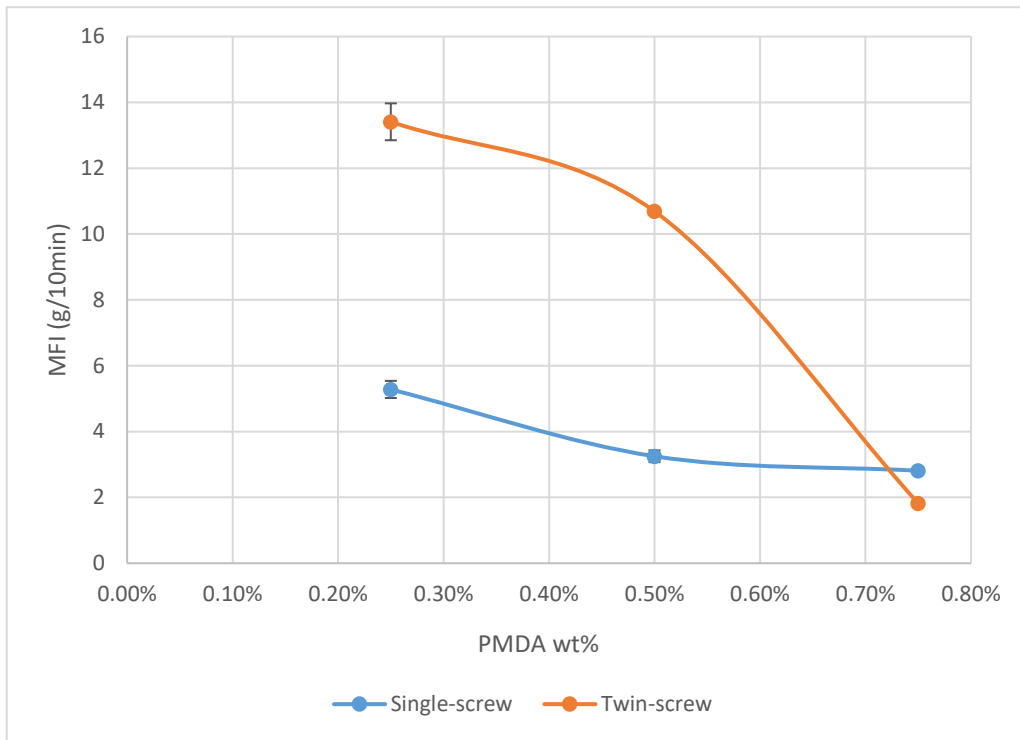


Figure 4-8: MFI values obtained by single-screw vs. twin-screw extruders (MFI at 275 °C)

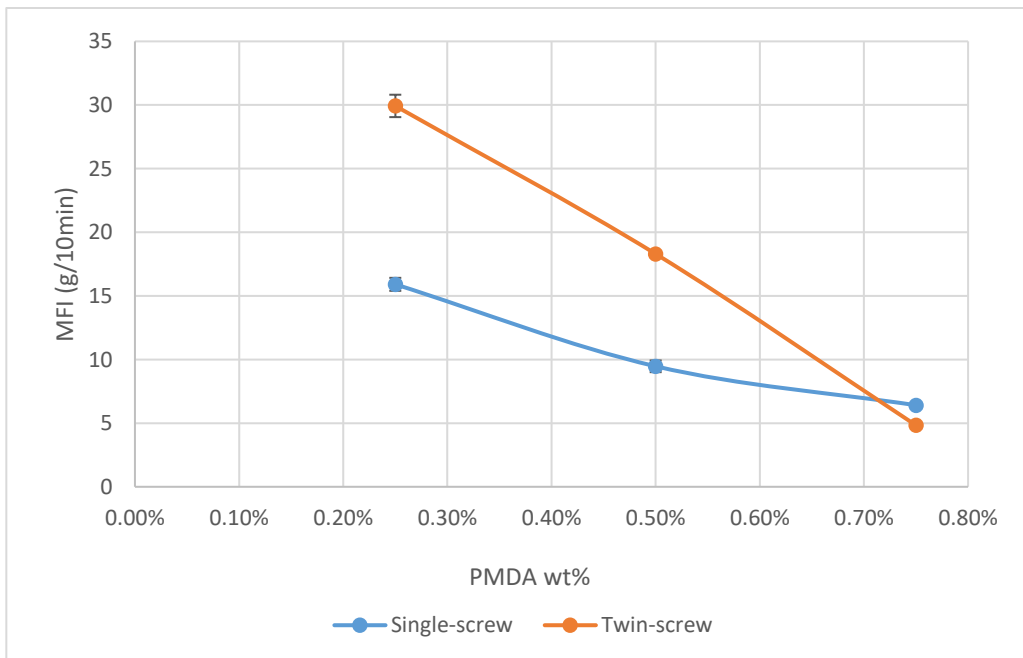


Figure 4-9: MFI values obtained by single-screw vs. twin-screw extruders (MFI at 290 °C)

Figures show that at PMDA levels of 0.25 wt% and 0.5 wt%, the product of single-screw extruder have lower MFI values than those processed in the twin-screw extruder. At 0.75 wt% PMDA, however, the product of the twin-screw extruder had lower MFI. It is possible that mechanical degradation has occurred in the twin-screw extruder since this type of extruder exerts higher shear on the melt which can degrade the polymer and, hence, the higher MFI when twin-screw extruder was used with 0.25 wt% and 0.5 wt%. However, this degradation, which caused by the extruder's type, probably had less significant effect when PMDA concentration was at 0.75 wt% because the higher additive concentration might have helped to overcome this degradation and, therefore, lower MFI was obtained compared to single-screw extruder. Because in the twin-screw extruder, the transportation mechanism that takes place in the barrel exposes more melt contact-surface to air that exist inside the barrel and, therefore, makes it more susceptible to thermo-oxidative degradation. As mentioned, these degradation scenarios, which are associated more with the twin-screw extruder, might have been less important when excess PMDA was available at 0.75 wt% concentration.

Moreover, the MFI data of 0.5 wt% and 0.75 wt% PMDA shows different pattern between samples processed in single-screw and twin-screw extruders. When twin-screw extruder was used, the MFI was reduced significantly as the additive concentration was increased from 0.5 wt% to 0.75 wt%. On the other hand, the MFI was reduced at much lower rate (MFI vs. additive concentration) in the same region for samples processed in the single-screw extruder. This is true when MFI test was conducted at 260 °C and 275 °C as shown in Figure 4-7 and 4-8. Although the mild change in the MFI reading for single-screw processed samples with 0.5% and 0.75% could falsely suggest that the reaction did not progress much further when the additive concentration was elevated, the fact that we captured the difference in MFI at 290 °C allowed us to rule out this theory. Another observation was that all MFI readings were increased more drastically when melting temperature changed from 275 °C to 290 °C. Figures 4-10 and 4-11 uses the same data of previous figures but plotted differently for each extruder (MFI vs. Temperature).

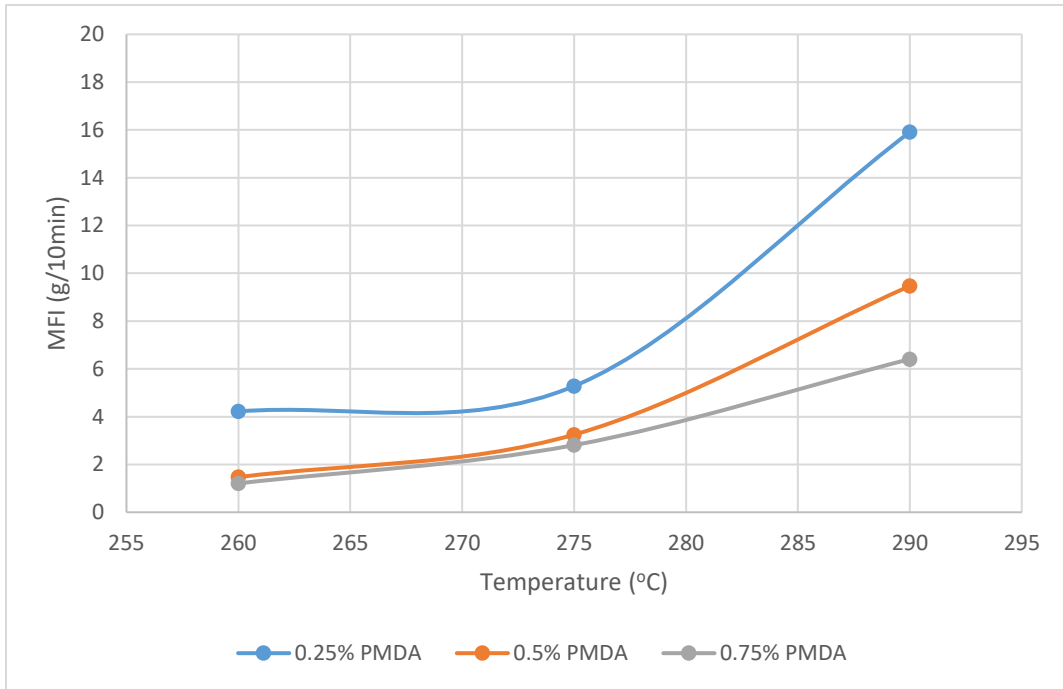


Figure 4-10: MFI as a function of temperature (Single-Screw)

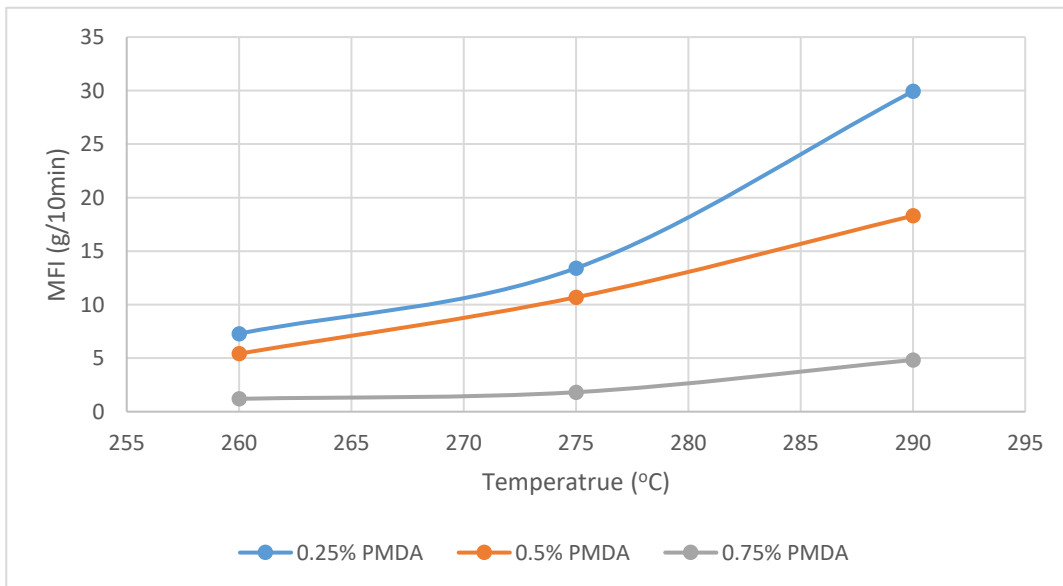


Figure 4-11: MFI as a function of temperature (Twin-Screw)

Moreover, a comparison was performed between the rheology of R-PET modified with 0.25 wt% PMDA versus modified with 0.25 wt% PMDA and 5 wt% SEBS-g-MA. It was decided to investigate the effect of the presence of the copolymer in the blend on the melt flow. The comparison in Figure 4-12 shows that SEBS-g-MA has negatively impacted the MFI value when added along with PMDA to R-PET. The difference between the MFI values of the two samples ranges from 2 to 5-fold which is significant. As we tested the MFI values at 260, 275 and 290 °C, the difference between the MFI of R-PET and SEBS-g-MA became even more significant. SEBS-g-MA copolymer has a lower melting point (230 °C) than R-PET and, hence, it may have experienced a drastic increase in MFI value when tested at 260 °C and above. Another possible scenario that might have occurred is that the functional groups in SEBS-g-MA have competed with PMDA on functional sites in R-PET end groups. In this case, the resulted product will be a less branched polymer, since SEBS-g-MA has only two active sites which only promotes linear coupling reactions, and that can have different effect on enhancing the viscosity.

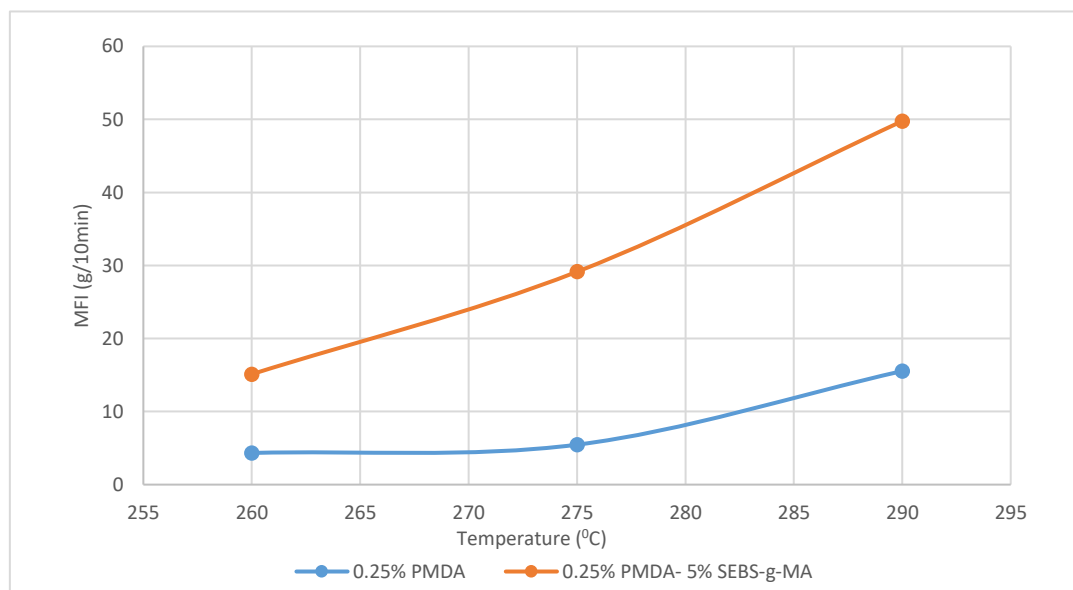


Figure 4-12: MFI values of R-PET modified with PMDA and PMDA / SEBS-g-MA

It was decided to eliminate the use of SEBS-g-MA in modifying the R-PET since it significantly impacted the MFI value and there was no clear benefit from using it from the mechanical properties point of view. However, in the next section we will verify that we have successfully dispersed SEBS copolymer into the backbone of R-PET by capturing the relevant peaks using FT-IR test.

Finally, the modified product had an MFI value that is comparable to those of commercial 3D-printing filament as shown in Figure 4-13. While this was a milestone in our project, it was observed that the modified product has developed other useful characteristics that should help in making the product a good candidate for 3D-printing. For example, it was clearly observed during the MFI test that modified R-PET melt had a structural integrity that allows the polymer to maintain its shape while still in the melt phase compared to unmodified R-PET. This was expected since increasing the polymer viscosity also increases the melt strength which is an important property when melt is to be blown or pulled as the case in the next phase of our project. Melt strength of a polymer is the maximum tension that can be applied to the polymer's melt before it breaks and, therefore, it is needed in the filament extrusion process.

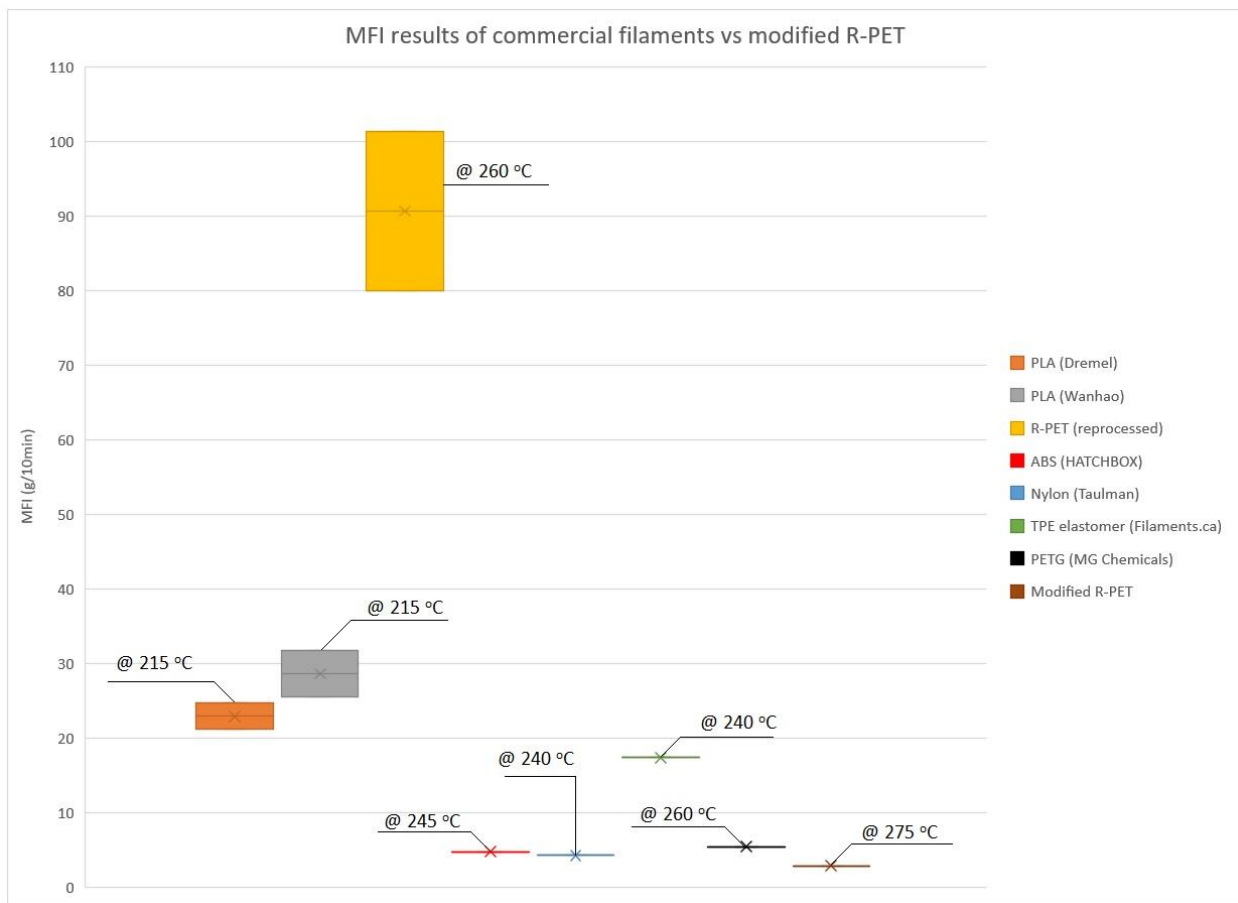


Figure 4-13: MFI values of various filaments and modified R-PET

In all, we have successfully modified R-PET by the chain extender PMDA via reactive extrusion in a single-screw and twin-screw extruders. We were able to reduce the MFI value of R-PET

significantly, around 72-fold, compared to reprocessed R-PET with no additives. Furthermore, our modified product showed better structural integrity and higher melt strength which was needed in order to be able to shape the melt to a filament shape. Considering the MFI results and all observations, we decided that our filament product will have 0.75 wt% PMDA and processed in the single-screw extruder. The single-screw extruder was preferred since it does not require interference while feeding the raw material. Moreover, at 0.75 wt% PMDA the polymer seemed to have reached the sufficient requirements for the filament manufacturing process.

4.5 FT-IR test

Investigating the change in the chemical composition of the modified R-PET was done by FT-IR analysis. In this analysis, all polymers samples were tested in a thin film form that was made using a hot-press machine. This includes R-PET, modified R-PET and SEBS-g-MA copolymer. When one of these polymers is tested, the background signal was the air signal. For powder PMDA, the tested sample contained a mixture of PMDA and KBr that was made in a flake form using cold-press and pure KBr was the background signal.

First, we investigated the effect of drying prior to extrusion on the chemical composition of product extrudate. Figure 4-14 shows the IR spectrum of reprocessed R-PET with and without drying. In theory, the difference between the two IR spectrums should be at the region where hydroxyl end-groups are to be seen. Because reprocessing R-PET without drying makes is susceptible to hydrolytic degradation, due to water presence, and hydroxyl end-groups are expected to be produced in this degradation rout. Other degradation routs, such as thermal and oxidative degradation are expected to take place regardless of drying since the polymer is processed at high temperature with presence of oxygen. Hence, difference in hydroxyl end-groups content should be seen in the spectrum at around 3560 cm^{-1} (Liang & Krimm, 1959). Figure 4-14 and 4-15 shows higher signal intensity at that region when R-PET was processed without drying which confirms that hydrolytic degradation has happened. Hence, the effect of hydrolytic degradation was seen in previous section from the rheology point of view (MFI value) and we verified this observation by investigating the chemical composition by FT-IR. Note that the signal of O-H group in the spectrum is generally weak and, as a result, thicker film sample was required to show stronger signal which explains the low transmittance of our sample.

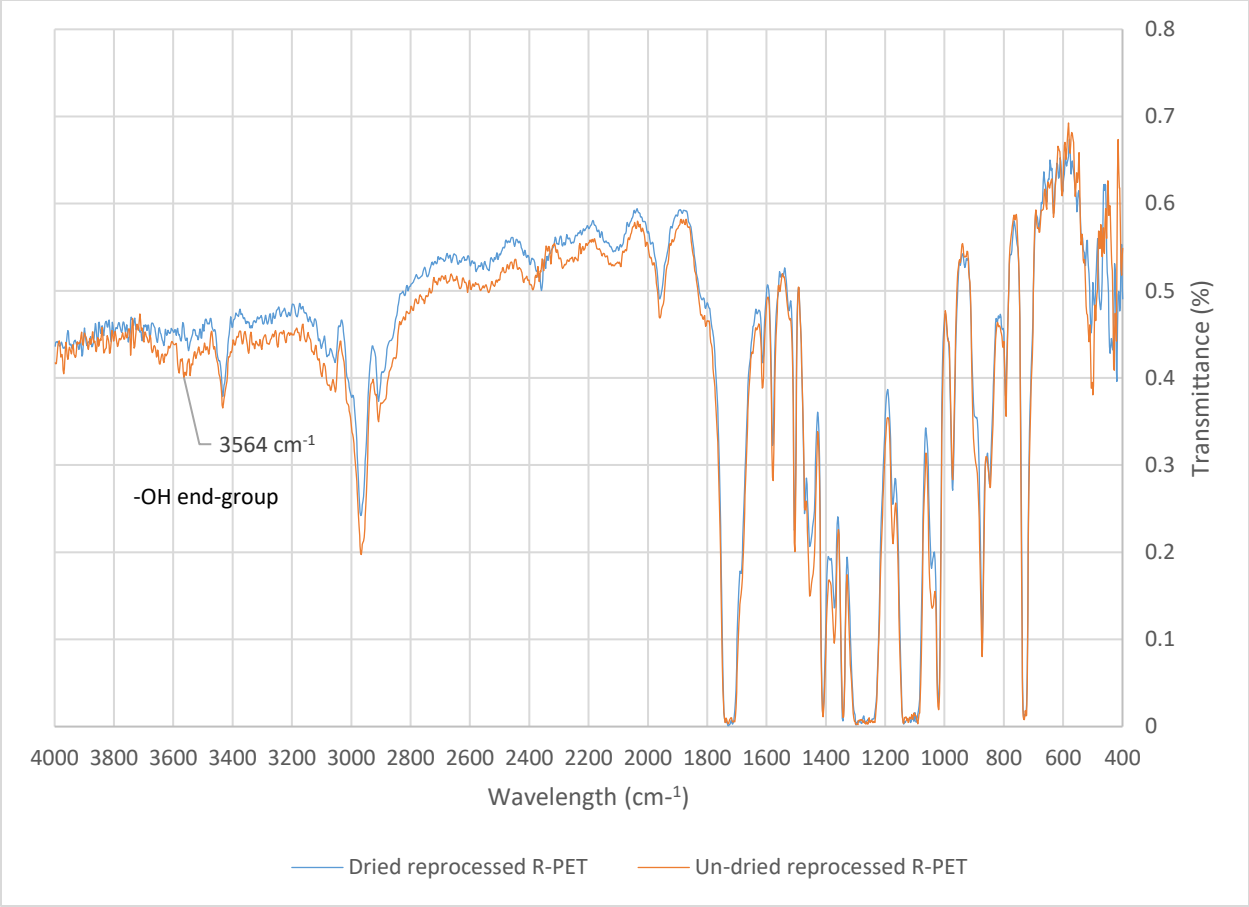


Figure 4-14: FT-IR spectrum of reprocessed R-PET dried and undried prior to extrusion

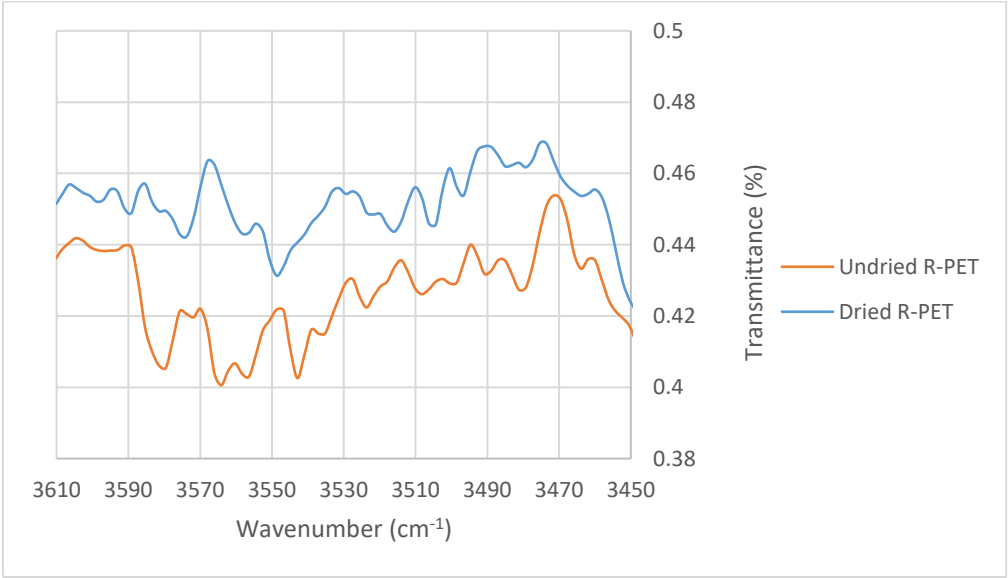


Figure 4-15: Hydroxyl end-group region shows different intensities between dried and undried R-PET

Moreover, Figure 4-16 shows FT-IR spectrums of modified R-PET at different levels of PMDA concentrations by the single-screw extruder as well as the IR spectrum of the PMDA additive. In this figure, we see a mild difference in transmittance between the samples at the region around 3250 cm^{-1} to 3280 cm^{-1} . This region is important for characterizing PET in general since it is the carboxyl end-group absorption region (Chalmers & Robert, 2008; Al-Abdulrazzak, Lofgren, & Jabarin, 2002). Figure 4-16 and 4-17 show that when PMDA concentration was at the highest level (0.75 wt%), lower signal intensity was captured at around 3270 cm^{-1} which indicates lower -COOH end-group presence (higher polymerization). The difference between the other two samples (0.25% and 0.50%), however, was not clear. On the other hand, Figure 4-18 shows the carbonyl group region for the modified R-PET. The detected signals do not provide a consistent pattern that can be correlated with the additive concentration.

In the PMDA spectrum, the strong signals at around 1770 cm^{-1} and 1859 cm^{-1} are assigned to the C=O stretching in the $\text{O}=\text{C}-\text{O}-\text{C}=\text{O}$ that exists in the PMDA molecule (Hase, Kawai, & Sala, 1975). The absence of these signals in the modified R-PET spectrum might suggest that they all have reacted and generated functional sites as anticipated.

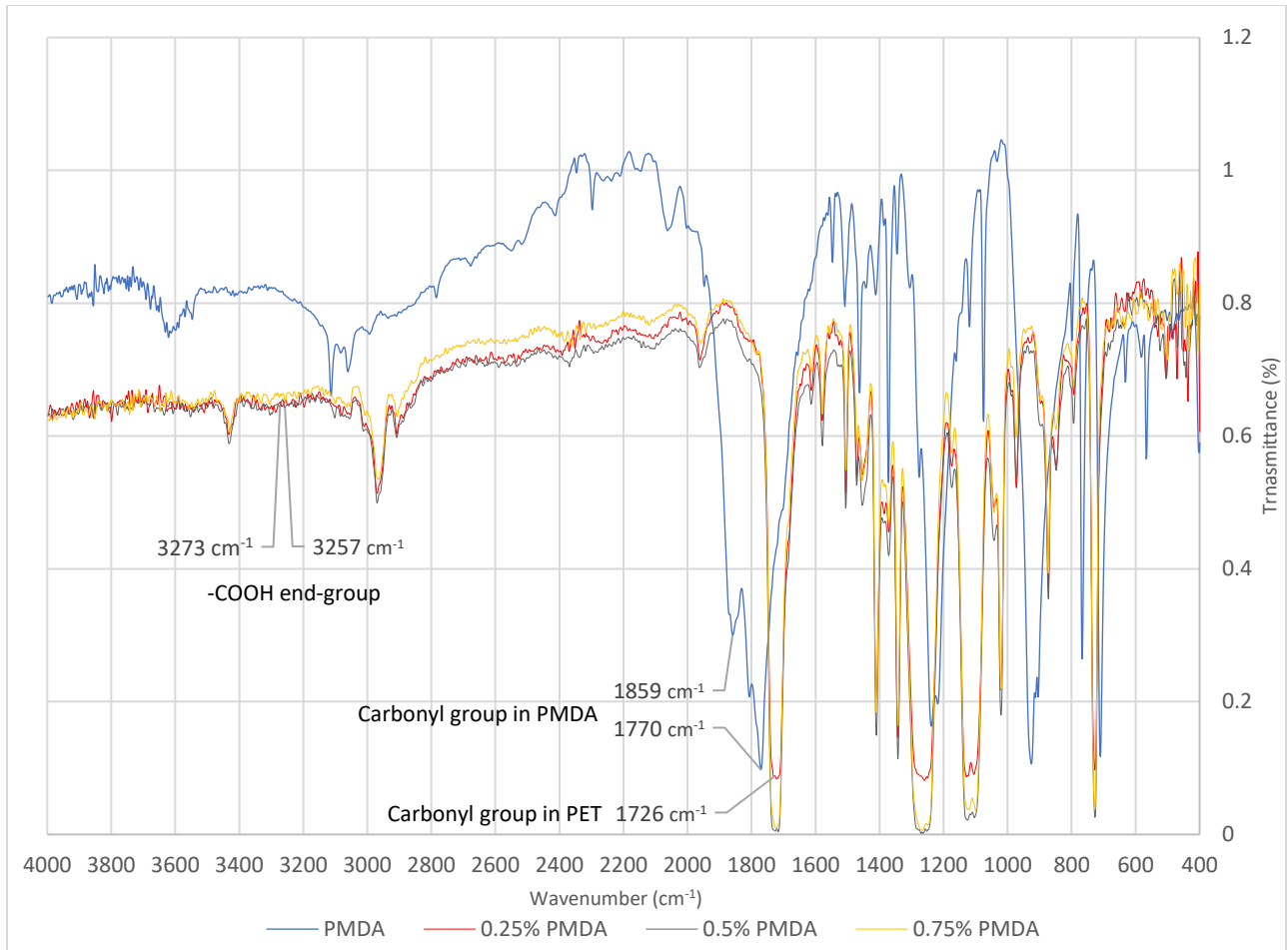


Figure 4-16: FT-IR results of modified R-PET (single-screw) and PMDA

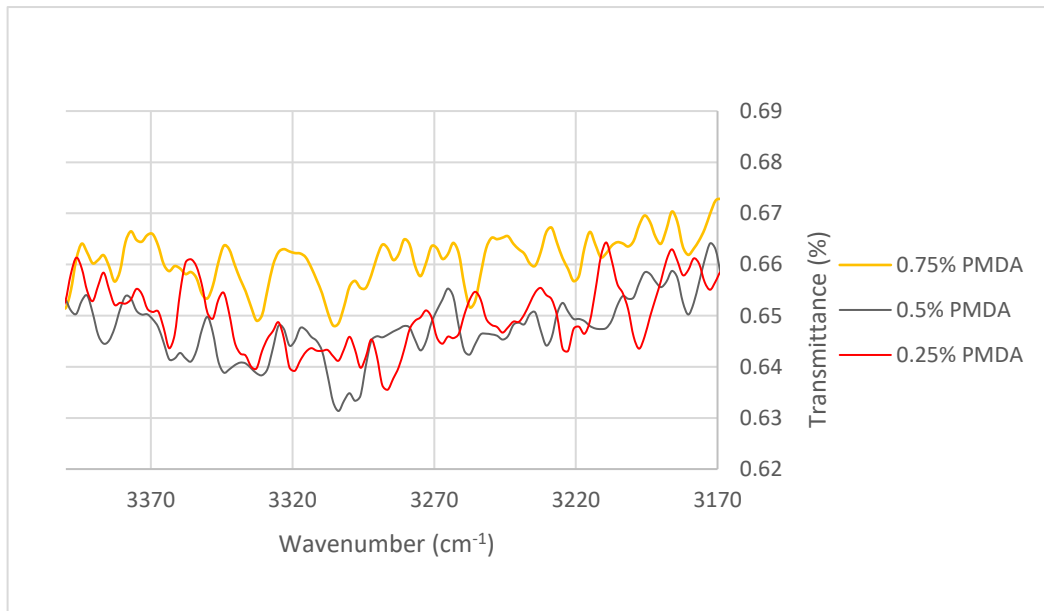


Figure 4-17: Carboxyl end-group region for modified R-PET

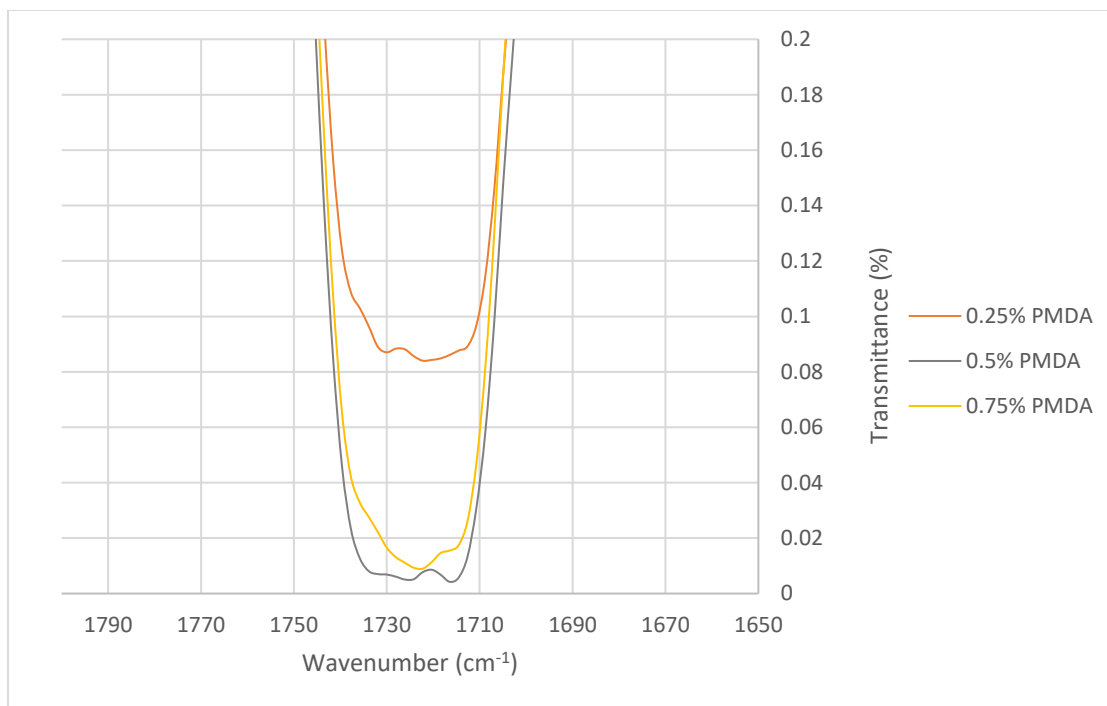


Figure 4-18: Carbonyl group region for modified R-PET

Furthermore, a comparison was made between R-PET/PMDA-99.75%/0.25% and R-PET/PMDA/SEBS-g-MA - 94.75%/0.25%/5% in order to identify the change in the chemical composition when SEBS-g-MA was added. Figure 4-19 shows 3 clear consecutive dips at around 2852 cm⁻¹, 2923 cm⁻¹ and 2959 cm⁻¹ which are typically seen in SEBS-g-MA spectrum and assigned to the C-H stretching (Jamaludin et al., 2015; Tanrattanakul et al., 1997). This strongly suggests that the copolymer was successfully dispersed in the modified product.

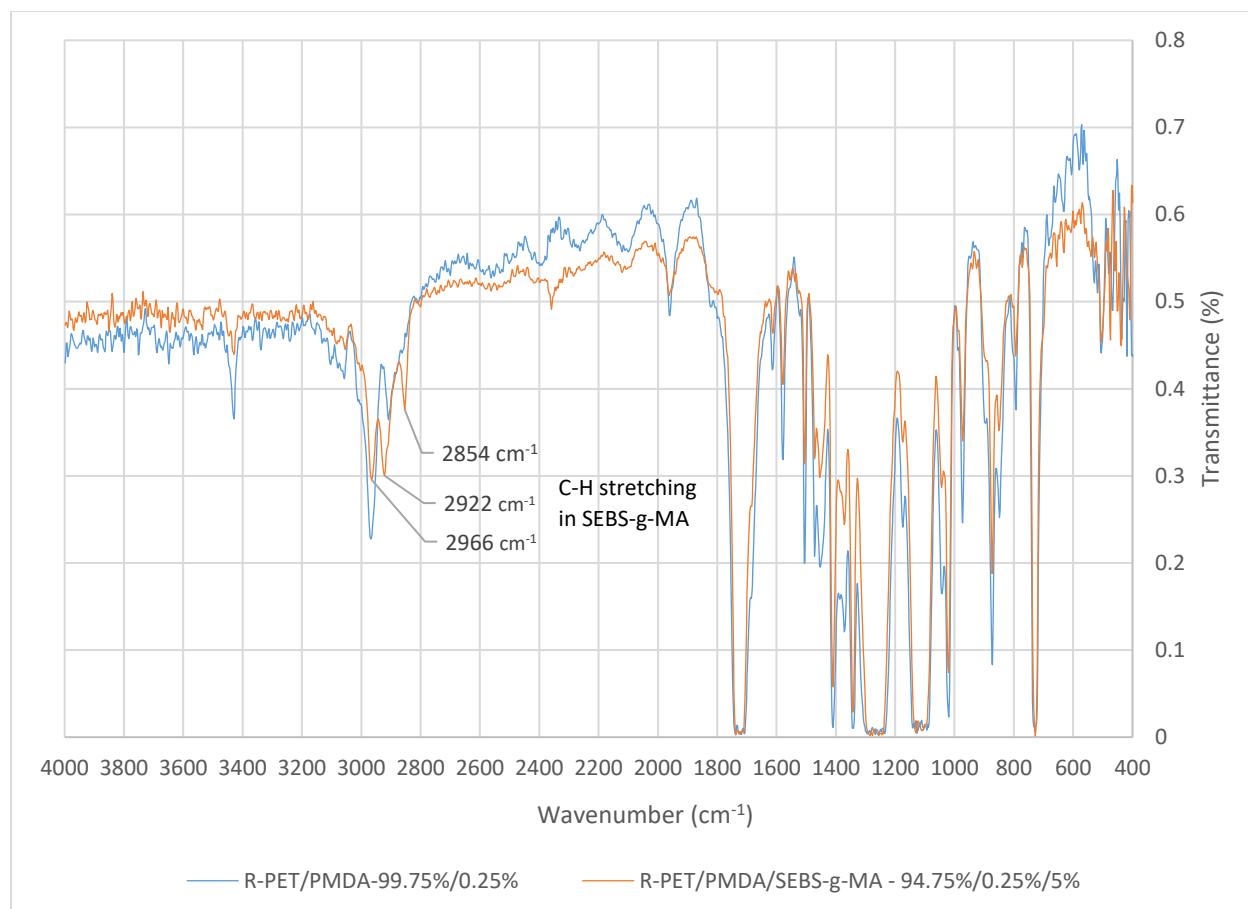


Figure 4-19: FT-IR results of R-PET modified R-PET with PMDA and PMDA/SEBS-g-MA

In conclusion, FT-IR analysis showed that hydroxyl end-group content has increased when R-PET was reprocessed without prior drying. This is explained by the occurrence of hydrolytic degradation which increases hydroxyl and carboxyl end-groups in R-PET. Moreover, our analysis showed that SEBS-g-MA was incorporated into R-PET as clear signals that were associated with the copolymer were observed on modified R-PET. Finally, R-PET modified with PMDA had a very similar spectrum as unmodified R-PET. The reason for this; either because the additive was added at low concentrations that did not allow it to be seen clearly in the modified product or because it was completely consumed in the reaction. Table 4-4 summarizes the relevant absorption regions in PET, PMDA and SEBS-g-MA IR spectrums.

Table 4-4: Relevant IR assignments in PET, PMDA and SEBS-g-MA

PET			
Wavenumber (cm ⁻¹)	R.I.	Assignment	Sources
1724	very strong	C=O (Carbonyl group)	(Liang & Krimm, 1959)
3256, 3271	broad, weak	O-H in carboxyl end-group	(Chalmers & Robert, 2008), (Al-Abdulrazzak, Lofgren, & Jabarin, 2002)
3560	weak	O-H in hydroxyl end-group	(Liang & Krimm, 1959)
PMDA			
1775	very strong	C=O (Carbonyl group)	(Hase, Kawai, & Sala, 1975)
1854	very strong	C=O (Carbonyl group)	
SEBS-g-MA			
2852		C-H stretching	
2923	medium (as observed)	C-H stretching	(Tanrattanakul et. al, 1997)
2959		C-H stretching	

4.6 Manufacturing a lab-made 3D-printing filament

Making a 3D-printing filament from modified R-PET seemed to be possible considering the enhanced properties that we have seen while testing the melt flow characteristic of the product. Since the MFI results showed that the MFI value was acceptable at 0.75 wt% PMDA and given that higher PMDA should yield higher melt strength which is desirable, it was decided that this concentration will be applied first when attempting making the filament. There are 3 main components that we used in making the filament which are: the single-screw extruder, the water cooling bath and the spooler device. Samples were prepared and dried by following the same procedures that were performed when compounding the additives.

The first step in the experiment was to establish a steady flow of warm water into/out of the cooling water bath. Since the available water supply was cold water, an arrangement was made to rout this cold water to water container placed on a heating. Heated water from the container is

then pumped to the water cooling bath inlet by a small water pump. Maintaining a constant water flow from the water source to the container was challenging since the supply was fluctuating and no flow regulator was used. This have resulted in fluctuation in the temperature of the water supplied to the bath although the impact of this fluctuation was not observed. The temperature of the cooling water in the bath was in the range of 40 ~ 47 °C throughout the experiment.

Once the flow to the cooling water bath was stabilized, extrusion was started at around 280 °C and 35 rpm. As a standard, we waited around a minute to let the extruder's operation stabilized in order to have a consistent residence time of our polymer inside the extruder. Because when the extruder's barrel is empty, the material get delivered from the hopper to the die discharge at faster time compared to when the barrel is filled. Then, the melt was pulled manually, immersed in the water bath and fed to the spooler. The spooling speed was adjusted to have the filament at the desirable diameter and also to maintain a tension on the melt being pulled from the extruder's die. The filament diameter was measured manually every 30 seconds using a digital dial caliper tool and the spooler's rotational speed was adjusted accordingly. The measuring point was chosen to be at the downstream of the spooler's rollers in order to avoid disturbance of the pulling process. Figures 4-20 and 4-21 show the laboratory filament extrusion setup that was used.

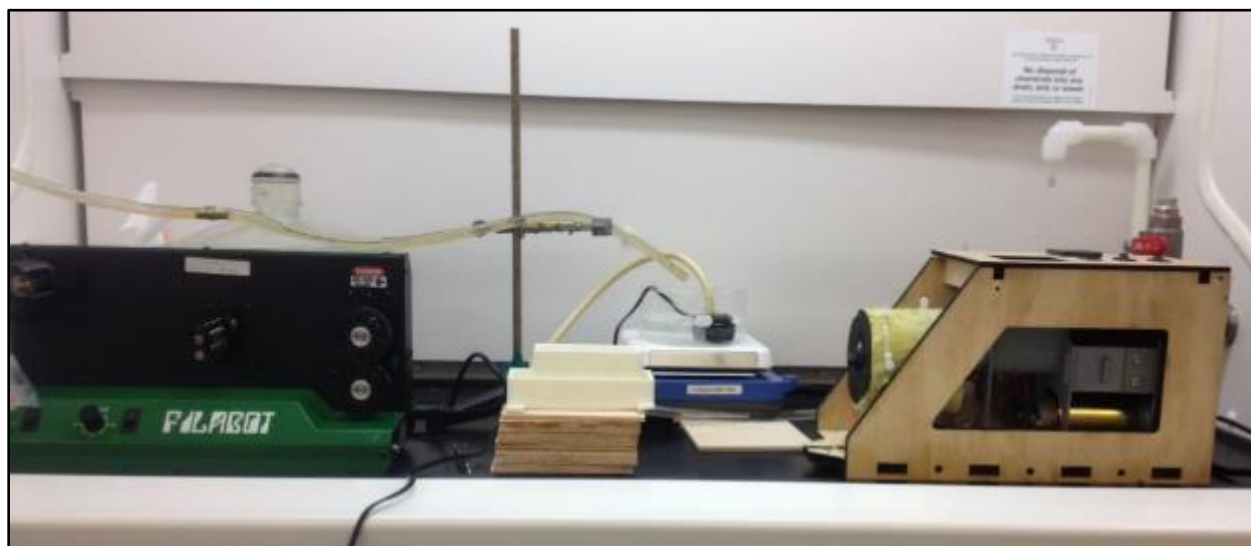


Figure 4-20: Laboratory filament-making setup

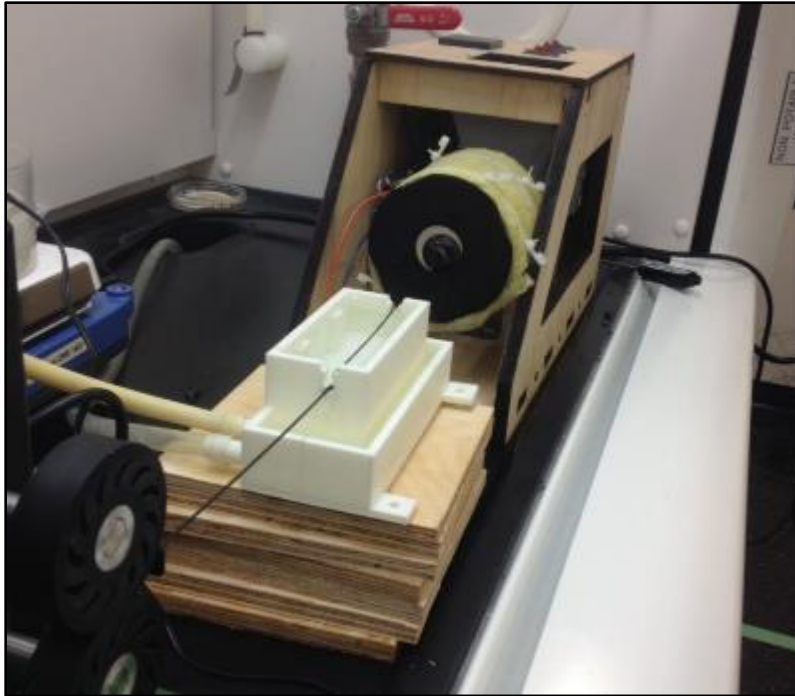


Figure 4-21: Modified R-PET filament being pulled from the extruder

We were able to produce few short-segments of modified R-PET that have an on-spec filament dimensions when PMDA concentrations was at around 0.75 wt%. Moreover, the ovality, although was inspected visually, seemed to be very good and has no clear deficiency which suggest that quenching the cooling water bath was done properly from the temperature and residence time point of view.

In order to investigate the effect of the water temperature on the ovality, similar experiment was conducted but with using cold water in the cooling water bath (at around 15 °C). It was very clear that the melt was losing its dimension and creates kind of twists as soon as it enters the water bath. These twists were created frequently that it did not allow producing segments that meet the standards. Figure 4-22 shows a cross-sectional view for the filament and Figure 4-23 shows a magnified image that validates the good ovality that was achieved. Measurements of the filament diameters at 4 different angles are reported in Table 4-5. Additionally, a magnified image of ABS commercial filament was also obtained (Figure A-3).



Figure 4-22: Cross-sectional view of the filament shows good ovality

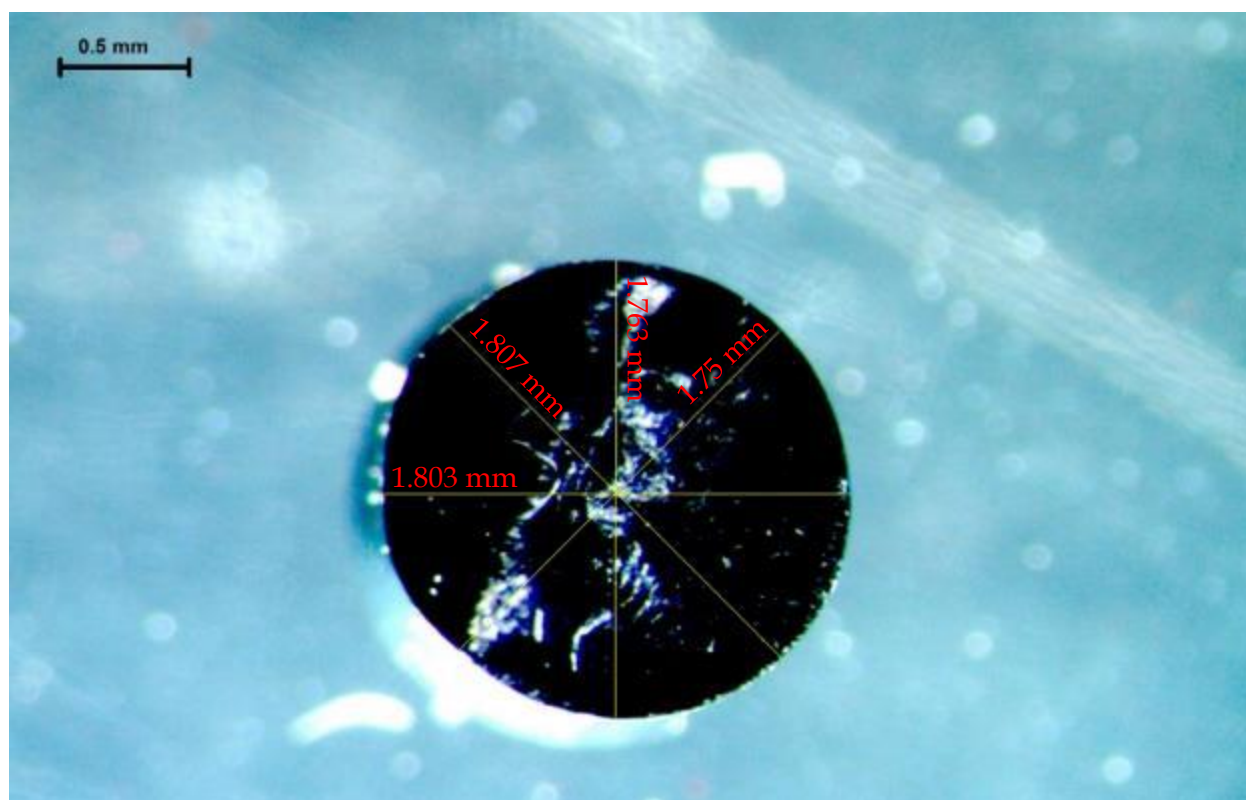


Figure 4-23: Magnified image of cross-sectional area of lab-made filament from modified R-PET shows good ovality (magnification: X12.6)

Table 4-5: Measurements of the diameter of the lab-made filament from modified R-PET

Line #	Angle	Length (mm)
1	0	1.803
4	45	1.807
2	90	1.763
3	135	1.75
Mean		1.78
Variance		0.0008

In order to investigate the effect of the water temperature on the ovality, similar experiment was conducted but with using cold water in the cooling water bath (at around 15 °C). It was very clear that the melt was losing its dimension and creates kind of twists as soon as it enters the water bath. These twists were created frequently that it did not allow producing segments that meet the standards.

Additionally, we made two other attempts to pull a filament of R-PET modified with PMDA concentrations of 0.5 wt% and 0.35 wt%. At 0.5 wt% PMDA it was possible to make few segments that have an on-spec shape although the yield of these segments was much lower than processing with 0.75 wt% PMDA concentration. In other word, fewer segments with shorter lengths of on-spec filament were made when the additive concentration was reduced to 0.5 wt%. Furthermore, pulling a filament was not possible when PMDA concentration was lowered further to 0.35 wt% due to low melt strength. The melt broke in every attempt of pulling it even when it was done manually. Hence, this experiment has demonstrated that melt strength is an important property to have in order to be able to have a control over the filament's diameter as well as being able to pull a filament at all. Although our previous results showed that the MFI value of modified R-PET/PMDA-99.75%/0.25% was significantly reduced compared to unmodified R-PET and was relatively close to the MFI value of R-PET/PMDA- 99.50%/0.5%, the difference in the melt strength between samples that contained 0.35% and 0.5 wt% PMDA was clearly noticed during the filament making process.

In conclusion, we have mimicked the manufacturing process of 3D-printing filament in lab-scale. Despite the fact that we used equipment that were less advanced technologically than commercial

machines, we were able to make few segments that can be used in a 3D-printer. Therefore, the next step was to try printing with it.

4.7 3D-printing with lab-made R-PET filament

Testing the lab-made filament was the final phase of the project and it was considered as the test that is going to reveal validity of many assumptions that were made throughout the project. For instant, it was assumed that once the MFI value of our modified R-PET is changed so that it is close to MFI values of other commercial filaments then the product can be 3D-printed with. Moreover, it was expected that when 3D-printing with modified R-PET there will be no issue in getting each extruded layer intact to adjacent layers. Because it was very clear as we worked with R-PET that the material does not solidify rapidly nor that it builds a “skin” quickly when extruded which suggests that when a layer is extruded it will remain in its melt form for a reasonable period of time so that adjacent layer can be printed meanwhile. Note that the printing speed can be controlled when 3D-printing but increasing it is not preferred as it impacts the print’s resolution.

It was very important to verify suitability of our filament’s diameter size to the 3D-printer. After selecting segments of our filaments that meets the diameter standards for the printer ($1.75\text{mm} \pm 0.05\text{mm}$) we decided to verify that our filament is on-spec by pushing the filament through the feeding barrel in order to see how smoothly the filament will pass this region while printing. This practice should reveal regions that have diameter sizes bigger than on-spec size which are susceptible for filament jamming in the barrel. Hence, we had higher confidence that jamming should not occur with segments that have passed this test.

Deciding the printing conditions is a crucial step when evaluating the performance of a thermoplastic filament for 3D-printing and so was the case for our modified R-PET. There are Three major variables that should be finely tuned in order to produce the best possible print quality and those are: the hot-end (nozzle) temperature, the heated-bed temperature and the printing speed. The hot-end temperature is often selected to be considerably higher than the melting point of the thermoplastic because the residence time of the filament in the hot zone while printing is usually not very long (around 2~2.5 minutes for 1 gram filament at typical printing speed of 90 mm/s). This margin between the melting point and the printing temperature should help in preventing nozzle-clogging which can occur due to un-melted filament. For example, although PLA has a melting offset temperature of 172 °C (according to the DSC analysis), the

thermoplastic is conventionally printed, as manufacturers recommend, at around 215 °C (Figure 4-24). Similar DSC graphs of Nylon and TPE filaments were also obtained for reference (Figure

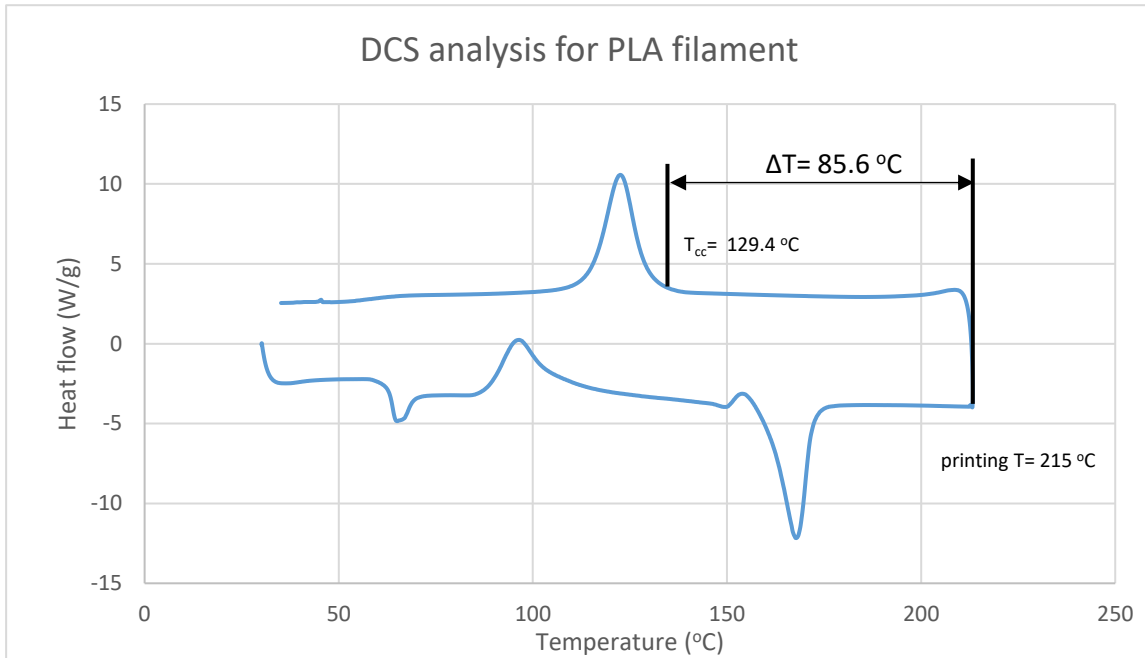


Figure 4-24: DSC result of commercial PLA filament

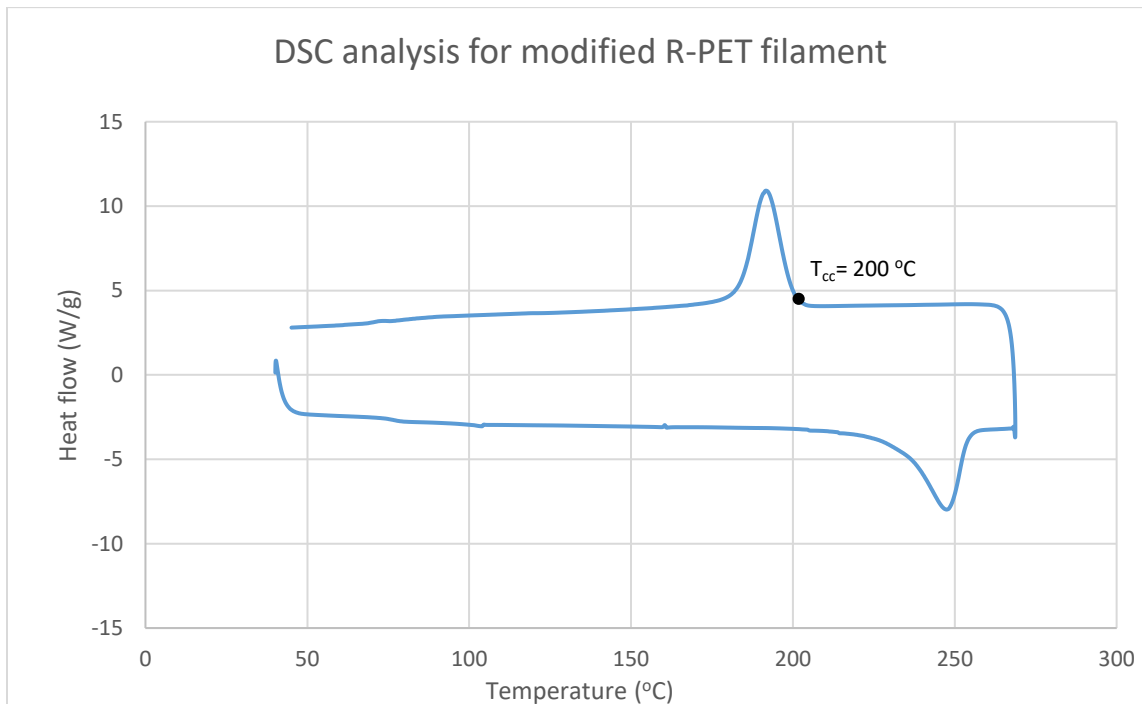


Figure 4-25: DSC results of Modified R-PET

A-1 and A-2, respectively). This margin of around 43 °C is meant to ensure smooth printing but without causing significant change of the melt integrity which is also important. Also, the net difference between the printing temperature in PLA and the onset T_{cc} is around 85 °C. For modified R-PET, as shown in Figure 4-25, the melting offset temperature of around 255 °C and assuming a margin of say 40 °C for printing means that printing should be done at 295 °C which poses a challenge since it is a very high 3D-printing temperature. But when T_{cc} onset temperature is considered, printing at 285 °C gives similar margin as in PLA. For some printers, as the case for our Wanhao Duplicator i3 that is being used in this project, the maximum recommended printing temperature by the manufacturer is 260 °C because some insulations that are used in the printer, mainly Teflon insulations, cannot withstand higher temperatures for long time. Subsequently, some temperature controllers were designed for the same maximum limit and, therefore, they lose precision as operation temperature deviate from design specifications. Although this maximum recommended printing temperature does not provide a comfortable margin for our prototype filament, it was decided that a trail will be performed at a lower printing speed of 50 mm/s to take preliminary observations. Lowering the printing speed allows for higher residence time of the filament in the melting zone which can help avoiding clogs. Before this trail was attempted, a small upgrade on the printer was done by replacing the manufacturer's hot-end set-up by a Micro-Swiss all metal hot-end. This kind of upgrade is often recommended when printing at higher temperatures because it includes replacing a Teflon tube in the printer's feed section, which is susceptible for failure, as well as providing an enhanced heat transfer in that section. The heated bed temperature was set at 120 °C (maximum recommended by the manufacturer) based on our understanding of R-PET and the fact that it is a good heat resistant material and, therefore, high bed temperature should help passing heat through between vertical layers (Z-axis).

After setting up the printing conditions, the first 3D-printing attempt was started by feeding the filament to the printer's feed section in order to see whether the printer will extrude the filament at all. The filament got extruded indeed but it was clear that extrusion was not going smoothly since extrudate came out at inconsistent rate and shapes (Figure 4-26).

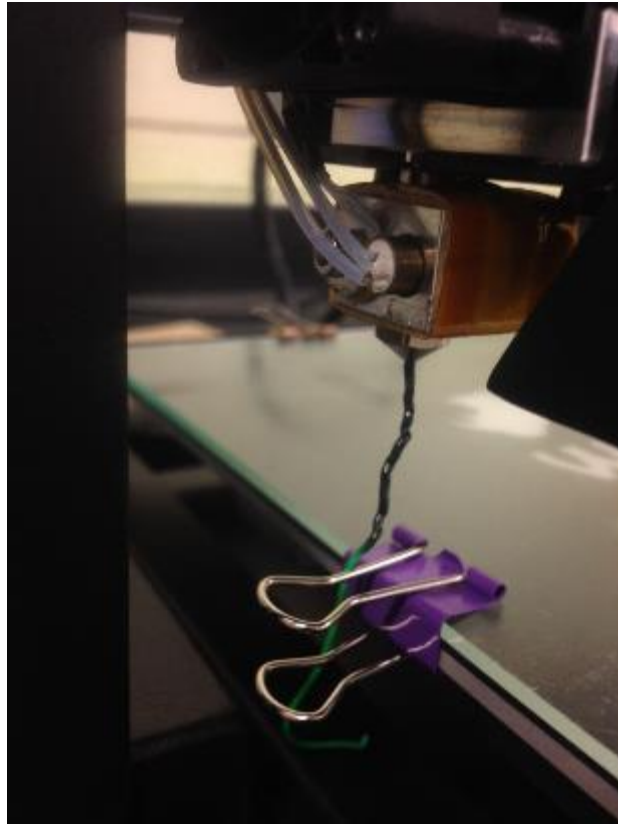


Figure 4-26: Modified R-PET filament being extruded in 3D-printer

By observing the kind of deficiency in the extrusion process, one can suspect that the extrusion temperature was the issue as the extrudate seems to be in a semi-solid state. Given this observation, the attempt was aborted without proceeding to printing an object.

Further adjustment was needed to be done on the printer to allow for an increase in the printing temperature. Although the user interface of our printer limits the maximum printing temperature at 260 °C, it was found that with the aid of a software this limit can be increased to 275 °C. Before going into details about our second printing attempt, I believe that it is useful to briefly discuss the concept of the maximum allowable temperatures in 3D-printers and how users can manipulate them since this was a key that allowed us to 3D-print with our prototype filament.

There are multiple temperature limits that are set for open-source 3D-printers and users can break these limits using software or, sometimes, hardware. For instant, our 3D-printer had a first maximum temperature limit at 260 °C known as the “user interface maximum temperature”. Meaning that users cannot set higher temperature using the printer’s settings screen. But there is often a higher limit that can be reached using an external software that can be installed on a

computer and controls the printer through a USB connection. In our case, the software “Repetier-Host” was used to break the 260 °C first limit to the 275 °C second limit. Technically, the second limit of 275 °C can also be waived by a method called “firmware flashing” which essentially allows for overriding any constrain that was pre-set by the manufacturer. This method involves sending a user-modified operation code to the printer replacing the original manufacturer files. In our project, an attempt was made to use this technique to exceed the 275 °C but it was not successful due to an unclear error that occurs while sending the modified operation code to the printer.

The second attempt was done at an extrusion temperature of 275 °C and with keeping other settings unchanged from our first attempt. Furthermore, another minor modification was done on the printer by replacing the 0.4mm nozzle with 0.8mm as bigger nozzle size should reduce required stress to push the extrudate through the nozzle. This modification was suggested since while 275 °C is a higher temperature than the melting offset temperature of our polymer, it still does not provide a comfortable margin from melting the polymer (compared to printing conditions of PLA filaments for instant) and, hence, this increase in the nozzle size could help the overall conditions. At 275 °C, it was clear that extrusion was going much smoother than previous attempt although not quite as smooth as when other conventional thermoplastics are used. This might indicate that a higher printing temperature might offers even better extrusion for our modified R-PET. Despite of that, a first layer of a small object was successfully 3D-printed as shown in Figure 4-27.

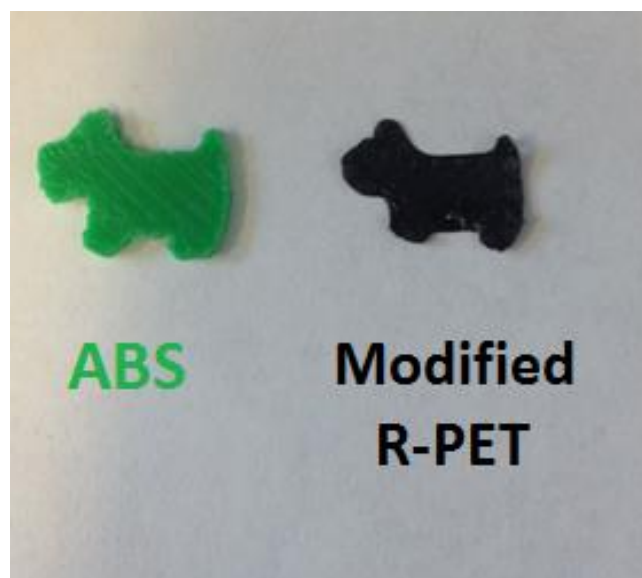


Figure 4-27: Small dog-shape 3D-printed with modified R-PET (right)

Few observations were noted during the second attempt and we believe that tackling these observations can help enhancing the printing experience with our modified R-PET. First, as mentioned earlier that increasing the extrusion temperature to 290 °C, for instant, can possibly bring on a greater success for two reasons. First, higher printing temperature should provide a smoother melt which can enhance the resolution of printed parts. It should also help in maintaining stable printing tasks especially when printing large objects. Second, this adjustment can also allow building layers on top of each other in the z-axis which was not achieved when printing at 275 °C. Note that there are many printers that can be modified to reach temperatures up to 300 °C which is often done when printing in thermoplastics like polycarbonate. Additionally, increasing bed temperature can also be useful, when possible, for a successful print with our filament. Having said that, many printers struggles to maintain stable temperature higher than 120 °C.

Chapter 5

Conclusions and Recommendation

In this work, we have studied the suitability of R-PET for 3D-printing applications by studying the melt flow characteristics of the polymer. When compared with commercial 3D-printing filaments, R-PET showed significantly higher melt flow rate, and therefore lower viscosity, which is a well-known deficiency associated with recycled polymers in general. This low polymer viscosity would hinder R-PET from being 3D-printable from two aspects. First, due to this low viscosity the melt would have a low melt strength not sufficient for the filament-making process which involves pulling the melt at certain force to achieve the desired filament diameter. Second, the polymer would have a significantly higher melt flow when extruded in the 3D-printer and that is likely to result in a very poor printing quality if not a failure for the printing task.

Our hypothesis was that R-PET can be modified with a reasonable effort and resources to overcome the low viscosity problem which should enhance both the melt strength and the melt flow of the polymer. Since the filament-making process involves extrusion, it was decided that reactive extrusion is the most suitable modification method to be followed. This method is known for its economical effectiveness and has been growing more popular than conventional modification methods. Moreover, the melt flow index test was chosen to be an indicator of suitability of a thermoplastic for 3D-printing applications. In other words, it was argued that thermoplastics that are used in 3D-printing have MFI values that fall within a certain range and modifying R-PET to have an MFI in that range would make it a good candidate for 3D-printing.

First, the effect of moisture presence on the melt flow of unprocessed R-PET was studied. Because PET is hygroscopic, we measured the weight fraction of moisture in R-PET as a function of drying time. Drying was done in an oven at 100 °C with no vacuum. The results showed a mild reduction in the overall weight of our sample after drying equivalent to 0.2%. Further, we studied the effect of drying the sample prior to the MFI test to study the effect of moisture presence as a source of error for the test. This was an important piece of information to obtain since the ASTM D 1238 standard mentioned that a special care should be taken when measuring MFI values of moisture sensitive material due to the effect that moisture can make. Results showed that for unprocessed

R-PET, the MFI value was 400% higher when the polymer was not dried compared to the value obtained after 1 hour of drying.

Second, the melt flow index of unmodified reprocessed R-PET was measured and compared with commercial filaments. The results showed a vast difference in the MFI value of reprocessed R-PET and all other kinds of filaments that are commonly used in 3D-printing. The MFI values of 6 commercial filaments, that include 5 different kinds of thermoplastics, were all found to be within the range of 5 ~ 38 g/10min when the MFI test for each filament was performed at the recommended 3D-printing temperature. R-PET, on the other hand, had an MFI value of around 90.56 g/10min (mean value) when tested at 260 °C. This proved that there is a significant difference in the melt flow characteristics between R-PET and 3D-printable thermoplastics.

Modifying R-PET for the purpose of enhancing its melt flow characteristics was done by reactive extrusion with the chain extender PMDA. In general, twin-screw extruders are believed to be more effective than single-screw extruder when it comes to reactive extrusion. The reason being that mixing takes place more aggressively in twin-screw extruders which allows for the coupling reaction to occur at higher rate. In this project, both types of extruders were used for compounding and the MFI results of final products were compared. Moreover, PMDA concentration were varied at 3 levels 0.25, 0.5 and 0.75 wt% to study the concentration effect on the MFI. Moreover, MFI test was conducted for all samples at 3 different temperatures, 260, 275 and 290 °C, to have a broad knowledge on the melt behavior at various temperature. These temperatures were selected for the test since we were likely to attempt 3D-printing R-PET at. The MFI test of our products revealed that PMDA has successfully increased the viscosity of our polymer when used as chain extender. A decrease of around 72-fold in the MFI was recorded when PMDA was added at 0.75 wt% which made the MFI of our modified R-PET very close to MFI values of commercial 3D-printing filaments. Moreover, the comparison between the products processed by single-screw and twin-screw extruders showed that lower MFI was achieved when the single-screw extruder was used at PMDA concentrations of 0.25 wt% and 0.5 wt%. At 0.75 wt%, however, the product of the twin-screw extruder had slightly lower MFI. It was proposed that when 0.75 wt% PMDA was added, an excess PMDA has helped in recovering the molecular weight loss caused by several degradation routes that are anticipated to take place. Having said that, it worth noting that the difference between MFI obtained by single-screw and twin screw extruders at 0.75 wt% is not vary large. Moreover, effect of SEBS-g-MA copolymer on

melt rheology when added along with PMDA has been studied. SEBS-g-MA has been used as a toughening agent but it was also reported that it can act as thermal stabilizer in addition to its nucleation effect. Our results showed that MFI was higher when the copolymer was added. Two possible reasons can explain this result: since the copolymer has a lower melting point than R-PET, testing at 260 °C and above has significantly lowered its viscosity. Second, it is possible that the copolymer has competed with PMDA to react with R-PET end groups which has produced a less branched polymer since SEBS-g-MA has only two active sites compared to 4 sites in PMDA. Due to this negative effect on the MFI results, the copolymer was eliminated as an additive from our final product.

Furthermore, FT-IR analysis was performed to investigate the chemical composition of our product and compare it with unmodified R-PET. Three cases were investigated which are: the composition change resulted from not drying the polymer prior extrusion, the change in the chemical composition resulted from PMDA addition and the change resulted from addition of SEBS-g-MA. First, when the polymer was not dried prior to extrusion it is expected that hydrolytic degradation will occur and, as a result, an increase in the hydroxyl end-group content should be seen. FT-IR analysis have confirmed that as stronger signals were detected associated with hydroxyl end-group in undried reprocessed R-PET. Additionally, FT-IR results showed a mild indication of lower carboxyl end-group content for the sample that had PMDA at 0.75 wt% concentration. For the other two samples (0.25 wt% and 0.50 wt%), however, no clear difference was seen. Moreover, sample that contained SEBS-g-MA in the blend showed clear signals that are associated with SEBS-g-MA presence. This indicates that SEBS copolymer was successfully dispersed in the modified R-PET.

The next milestone in this project was to be able to make a 3D-printing filament from our modified R-PET. Since an improvement in the polymer's rheology was seen clearly through the MFI test, it was decided to move on to the filament manufacturing task. Main processing stations that exist in the filament making process were mimicked in lab which included: extrusion stage, water bath cooling stage and spooling stage. R-PET was processed with 0.75% PMDA since a desirable MFI was obtained at this temperature in addition to the fact that higher PMDA should help increasing the melt strength which is also desirable. With selecting certain important operational parameters, including extrusion temperature and cooling water bath temperature, we were able to obtain segments of on-spec filament shape. This result was much harder to be achieved when

PMDA concentration was lowered to 0.5 wt% and it was impossible to be done with PMDA concentration of 0.35 wt%. At 0.75 wt% PMDA, the melt strength was satisfactory for pulling the filament by the spooler to control the filament's diameter. Produced filaments were then tried in a 3D-printer.

Before printing with modified R-PET, certain modifications were advised to be made on our printer to increase the chances of a successful print. These modifications were in the printer's hot-end where filament is fed and extruded and this included upgrading the nozzle, the feeding tube and the cooling block. That was necessary since most printers, including ours, are designed to print at temperature lower than 260 °C and some parts will be impacted by this high temperature. The first attempt of printing with R-PET was performed at 260 °C and it was not very successful as it was noticed that the polymer was not being melted completely. This was attributed to the fact that 260 °C was not high enough for the polymer to get completely and smoothly melted in the printer's extruder. The second attempt was done after a software modification on the printer that allowed us to reach printing temperature of 275 °C after overriding a programmed constrain. At this temperature, the polymer was melted smoother and a small shape was printed with our modified R-PET. This was a breakthrough in the project since we proved our concept that R-PET can be made into 3D-printable filament. It was noticed, however, that the quality of the print would require some improvements that can possibly be made by adjusting the printer's settings and operational conditions. For example, it was believed that increasing the heated-bed temperature to 150 °C should make it easier to print more layers in the Z-axis (building upward). Our printer, however, had limitations that did not allow maintaining stable high heated-bed temperature. Some 3D-printers which have an enclosed chamber in which prints are built would offer much better environment for printing due to efficient heat preservation. In these conditions, it is believed that even better results can be obtained. Furthermore, increasing the printing temperature (which could not be done in our printer specifically) to 285 °C ~290 °C might also enhance the printing quality since smoother melt gives higher printing resolution.

Bibliography

- 2014 Postconsumer Plastics Recycling in Canada (Rep.). (2016, June). Retrieved November 22, 2016, from Canadian Plastics Industry Association website.
- 3D printing scales up. (2013, September 7). *The Economist*. Retrieved February 15, 2017, from <http://www.economist.com/news/technology-quarterly/21584447-digital-manufacturing-there-lot-hype-around-3d-printing-it-fast>
- 5 Most Popular 3D Printing Thermoplastics. (2017). Retrieved 2016, from <http://3dinsider.com/5-most-popular-3d-printing-thermoplastics/>
- Al-Abdulrazzak, S., Lofgren, E. A., & Jabarin, S. A. (2002). End-group determination in poly(ethylene terephthalate) by infrared spectroscopy. *Polymer International*, 51(2), 174-182. doi:10.1002/pi.814
- Awaja, F., Daver, F., & Kosior, E. (2004). Recycled poly(ethylene terephthalate) chain extension by a reactive extrusion process. *Polymer Engineering and Science*, 44(8), 1579-1587. doi:10.1002/pen.20155
- Cardi, N., Po, R., Giannotta, G., Occhiello, E., Garbassi, F., & Messina, G. (1993). Chain extension of recycled poly(ethylene terephthalate) with 2,2'-(1,4-phenylene)bis(2-oxazoline). *Journal of Applied Polymer Science*, 50(9), 1501-1509. doi:10.1002/app.1993.070500903
- Chalmers, J. M., & Meier, R. J. (2008). Chapter 5. In *Molecular characterization and analysis of polymers*. Amsterdam: Elsevier.
- Columbus, L. (2015). 2015 Roundup Of 3D Printing Market Forecasts And Estimates. *Frobes*. Retrieved February 28, 2017, from <https://www.forbes.com/sites/louiscolombus/2015/03/31/2015-roundup-of-3d-printing-market-forecasts-and-estimates/#76edc4fd1b30>.
- Dubashi, J., Grau, B., & McKernan, A. (2015). *AkaBot 2.0: Pet 3D printing filament from waste plastic* (Unpublished thesis). Santa Clara University. Retrieved from http://scholarcommons.scu.edu/cgi/viewcontent.cgi?article=1043&context=mech_senior

- Ganguly, A., & Bhowmick, A. K. (2007). Sulfonated Styrene-(ethylene-co-butylene)-styrene/Montmorillonite Clay Nanocomposites: Synthesis, Morphology, and Properties. *Nanoscale Research Letters*, 3(1), 36-44. doi:10.1007/s11671-007-9111-3
- Gibson, I., Rosen, D., & Stucker, B. (2015). Extrusion-Based Systems. In *Additive Manufacturing Technologies 3D Printing, Rapid Prototyping, and Direct Digital Manufacturing* (2nd ed.). doi:10.1007/978-1-4939-2113-3
- Goldberg, D. (2014, September 5). History of 3D Printing: It's Older Than You Are (That Is, If You're Under 30). Retrieved November, 2016, from <https://redshift.autodesk.com/history-of-3d-printing/>
- Gouinlock, E. V., Marciniak, H. W., Shatz, M. H., Quinn, E. J., & Hindersinn, R. R. (1968). Preparation and properties of copolyesters polymerized in a vented extruder. *Journal of Applied Polymer Science*, 12(11), 2403-2413. doi:10.1002/app.1968.070121103
- Grymol, B. (2013). Disruptive manufacturing : The effects of 3D printing (Rep.). Retrieved 2016, from Canadian Electronic Library website: <https://www2.deloitte.com/content/dam/Deloitte/ca/Documents/insights-and-issues/ca-en-insights-issues-disruptive-manufacturing.pdf>
- Hase, Y., Kawai, K., & Sala, O. (1975). The Infrared and Raman Spectra of Pyromellitic Dianhydride. *Journal of Molecular Structure*, 26(2), 297-302. doi:10.1016/0022-2860(75)80013-5
- Jamaludin, N. A., Inuwa, I. M., Hassan, A., Othman, N., & Jawaid, M. (2015). Mechanical and thermal properties of SEBS- g -MA compatibilized halloysite nanotubes reinforced polyethylene terephthalate/polycarbonate/nanocomposites. *Journal of Applied Polymer Science*, 132(39). doi:10.1002/app.42608
- Janssen, L. P. (2004). Introduction. In *Reactive extrusion systems*. New York: Marcel Dekker.
- Japon, S., Boogh, L., Leterrier, Y., & Manson, J. (2000). Reactive processing of poly(ethylene terephthalate) modified with multifunctional epoxy-based additives. *Polymer*, 41(15), 5809-5818. doi:10.1016/s0032-3861(99)00768-5

- K., Ishak, Z. M., Chow, W., Takeichi, T., & R. (2008). Influence of SEBS-g-MA on morphology, mechanical, and thermal properties of PA6/PP/organoclay nanocomposites. *European Polymer Journal*, 44(4), 1023-1039. doi:10.1016/j.eurpolymj.2008.01.019
- Karayannidis, G. P., & Psalida, E. A. (2000). Chain extension of recycled poly(ethylene terephthalate) with 2,2'-(1,4-phenylene)bis(2-oxazoline). *Journal of Applied Polymer Science*, 77(10), 2206-2211. doi:10.1002/1097-4628(20000906)77:103.3.co;2-4
- Kodama, H. (1981). Automatic method for fabricating a three-dimensional plastic model with photo-hardening polymer. *Review of Scientific Instruments*, 52(11), 1770-1773. doi:10.1063/1.1136492
- Lianc, C. Y., & Krimm, S. (1959). Infrared Spectra of High Polymers: Part IX. Polyethylene Terephthalate. *Journal of Molecular Spectroscopy*, 3, 554-574. Retrieved from <http://www.sciencedirect.com/science/article/pii/0022285259900487?via%3Dihub>
- McCue, T. (2016, April 25). Wohlers Report 2016: 3D Printing Industry Surpassed \$5.1 Billion. *Forbes*. Retrieved January 11, 2017, from <https://www.forbes.com/sites/tjmccue/2016/04/25/wohlers-report-2016-3d-printer-industry-surpassed-5-1-billion/#32e4161319a0>.
- Mrozinski, B. A. (2010). Acetaldehyde scavengers for poly(ethylene terephthalate): Chemistry of reactions, capacity, and modeling of interactions (Unpublished doctoral dissertation).
- Palermo, E. (2013, September 19). Fused Deposition Modeling: Most Common 3D Printing Method. Retrieved March 2, 2017, from <http://www.livescience.com/39810-fused-deposition-modeling.html>
- Pham, D., & Gault, R. (1998). A comparison of rapid prototyping technologies. *International Journal of Machine Tools & Manufacture*, 38, 1257-1287. Retrieved from <http://www.sciencedirect.com.proxy.lib.uwaterloo.ca/science/article/pii/S0890695597001375>
- Pohl, H. A. (1954). Determination of Carboxyl End Groups in Polyester, Polyethylene Terephthalate. *Analytical Chemistry*, 26(10), 1614-1616. doi:10.1021/ac60094a024

- Raffa, P., Coltelli, M., Savi, S., Bianchi, S., & Castelvetro, V. (2012). Chain extension and branching of poly(ethylene terephthalate) (PET) with di- and multifunctional epoxy or isocyanate additives: An experimental and modelling study. *Reactive and Functional Polymers*, 72(1), 50-60. doi:10.1016/j.reactfunctpolym.2011.10.007
- Russias, J., Saiz, E., Nalla, R., Gryn, K., Ritchie, R., & Tomsia, A. (2006). Fabrication and mechanical properties of PLA/HA composites: A study of in vitro degradation. *Materials Science and Engineering: C*, 26(8), 1289-1295. doi:10.1016/j.msec.2005.08.004
- Scheirs, J., & Long, T. E. (2006). Additives for the Modification of Poly(Ethylene Terephthalate) to Produce Engineering-Grade Polymers. In *Modern polyesters: Chemistry and technology of polyesters and copolyesters*. Retrieved from http://www.excelplas.com/admin/media/pages/43/PET_chapter.pdf
- Scott, C. (2016). Celprogen 3D Prints a Pancreas from PLA and Human Stem Cells. Retrieved 2016, from <https://3dprint.com/157430/3d-printed-pancreas-celprogen/>
- Shenoy, A., Saini, D., & Nadkarni, V. (1983). Estimation of the melt rheology of polymer waste from melt flow index. *Polymer*, 24(6), 722-728. doi:10.1016/0032-3861(83)90010-1
- Shenoy, A. V., & Saini, D. R. (1986). Melt flow index: More than just a quality control rheological parameter. Part I. *Advances in Polymer Technology*, 6(1), 1-58. doi:10.1002/adv.1986.060060101
- Tanrattanakul, V., Hiltner, A., Baer, E., Perkins, W., Massey, F., & Moet, A. (1997). Toughening PET by blending with a functionalized SEBS block copolymer. *Polymer*, 38(9), 2191-2200. doi:10.1016/s0032-3861(96)00774-4
- Tyson, E. (2016). What is the difference between TPE and TPU Flexible Filament? Retrieved 2016, from <https://rigid.ink/blogs/news/172062855-what-is-the-difference-between-tpe-and-tpu-flexible-filament>
- Tzoganakis, C. (1989). Reactive Extrusion of Polymers: A Review. *Advances in Polymer Technology*, 9(4), 321-330.

- Venkatachalam, S., Nayak, S. G., Labde, J. V., Gharal, P. R., Rao, K., & Kelkar, A. (2012). Degradation and Recyclability of Poly (Ethylene Terephthalate). In M. S. El-Din (Author), Polyester (pp. 75-98). Rijeka, Croatia: INTECH. doi:10.5772/2748
- Wagner, J. R., Mount, E. M., & Giles, H. F. (2014). Part 2: Twin Screw Extrusion. In Extrusion the definitive processing guide and handbook (pp. 83-89). Oxford: Andrew, Elsevier. Retrieved from <https://www.scribd.com/doc/282529324/Extrusion-The-Definitive-Processing-Guide-and-Handbook>.
- Wallace, J., Wang, M. O., Thompson, P., Busso, M., Belle, V., Mammoser, N., . . . Dean, D. (2014). Validating continuous digital light processing (cDLP) additive manufacturing accuracy and tissue engineering utility of a dye-initiator package. *Biofabrication*, 6(1), 1-14. Retrieved from CRKN Institute of Physics Journals Current.
- Xanthos, M. (1992). Reactive extrusion: Principles and practice. Munich: Hanser.
- Zhang, Y., Zhang, H., Ni, L., Zhou, Q., Guo, W., & Wu, C. (2010). Crystallization and Mechanical Properties of Recycled Poly(ethylene terephthalate) Toughened by Styrene-Ethylene/ Butylenes-Styrene Elastomer. *Journal of Polymers and the Environment*, 18(4), 647-653. doi:10.1007/s10924-010-0223-y

Appendix

1- DSC Data:

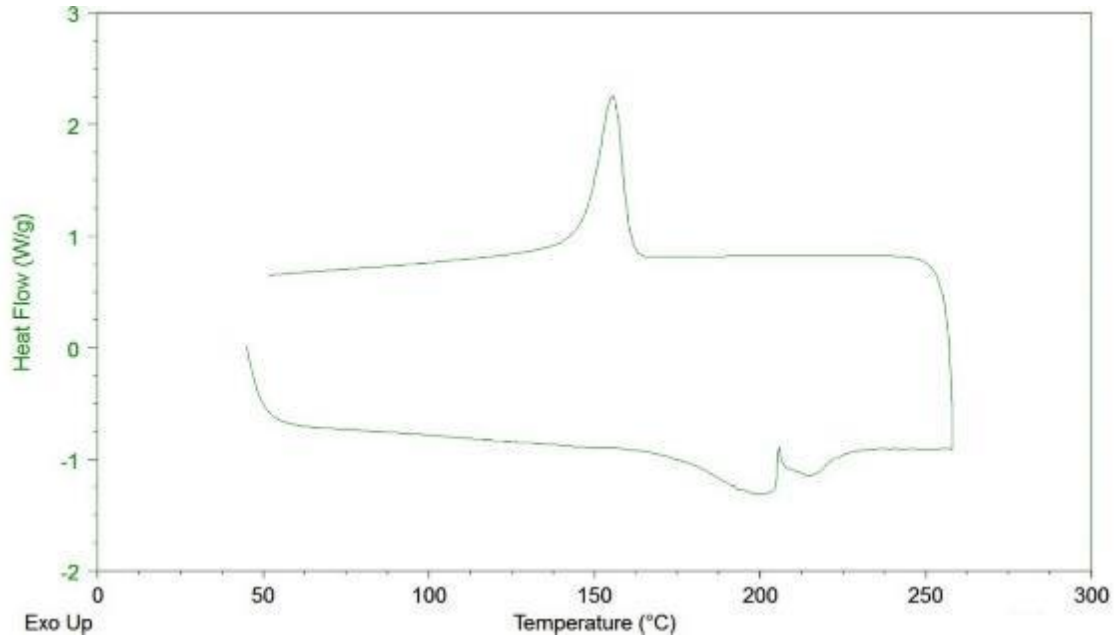


Figure A-1: DSC results of Nylon 3D-printing filament

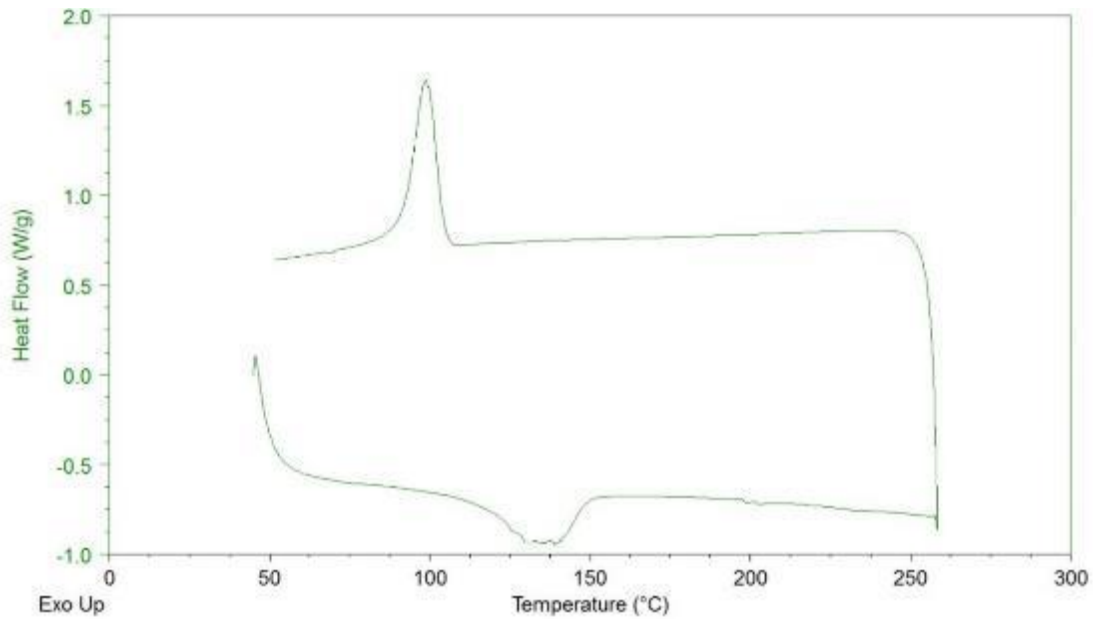


Figure A-2: DSC results of TPE 3D-printing filament

2- Microscopic pictures

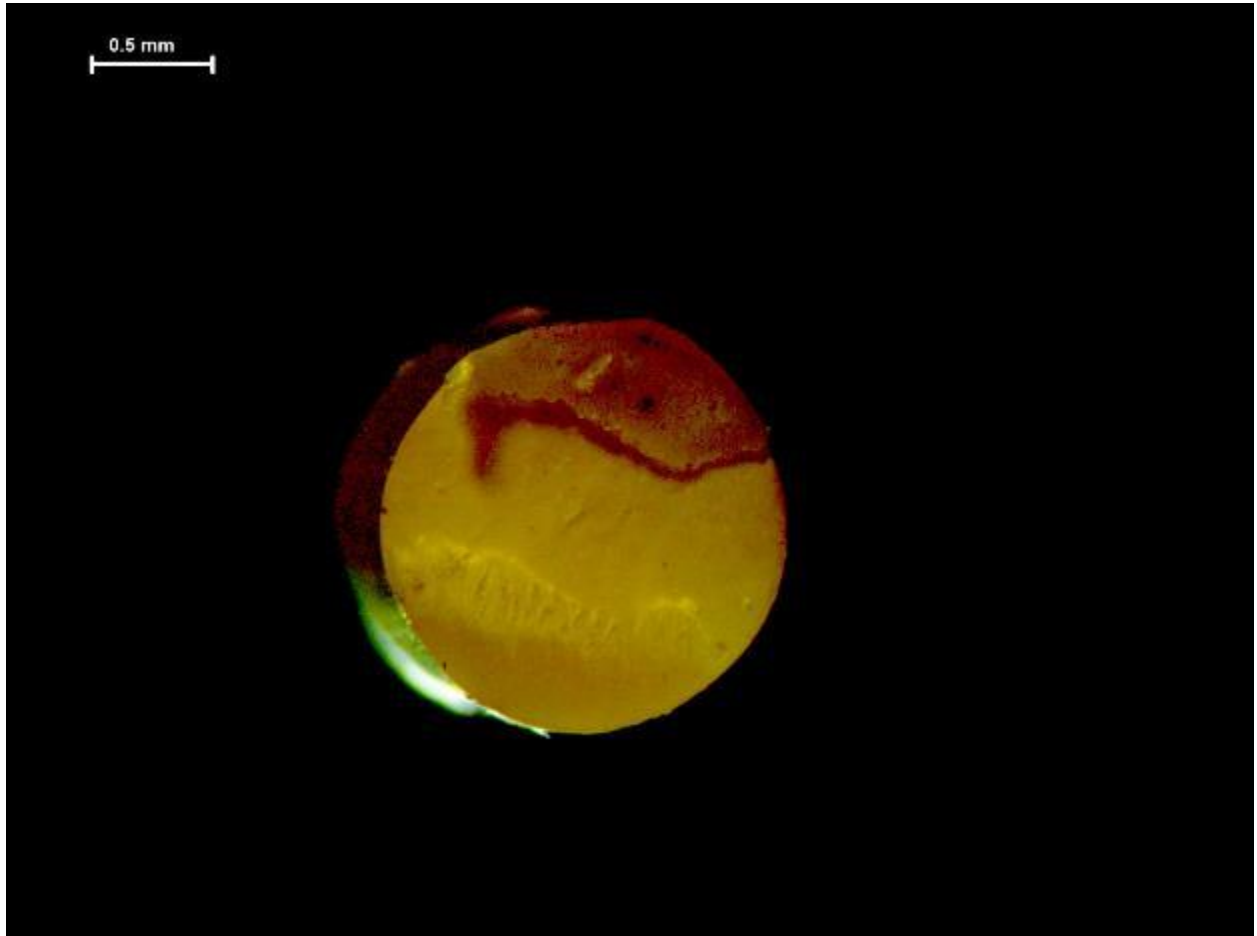


Figure A-3: Magnified image of the cross-sectional area of ABS commercial filament

3- Design sheets

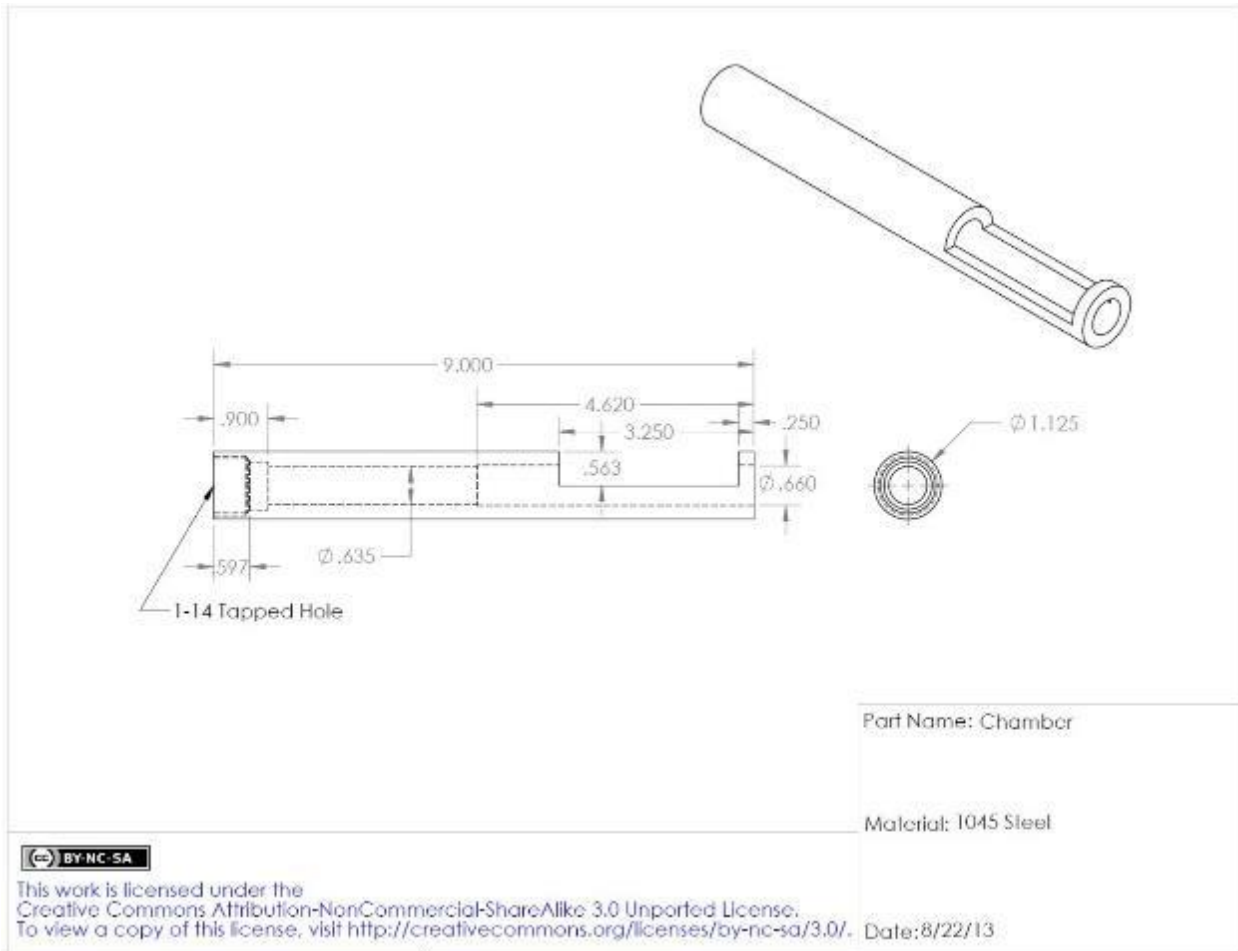


Figure A-4: The barrel design (dimensional) in Filabot Wee extruder

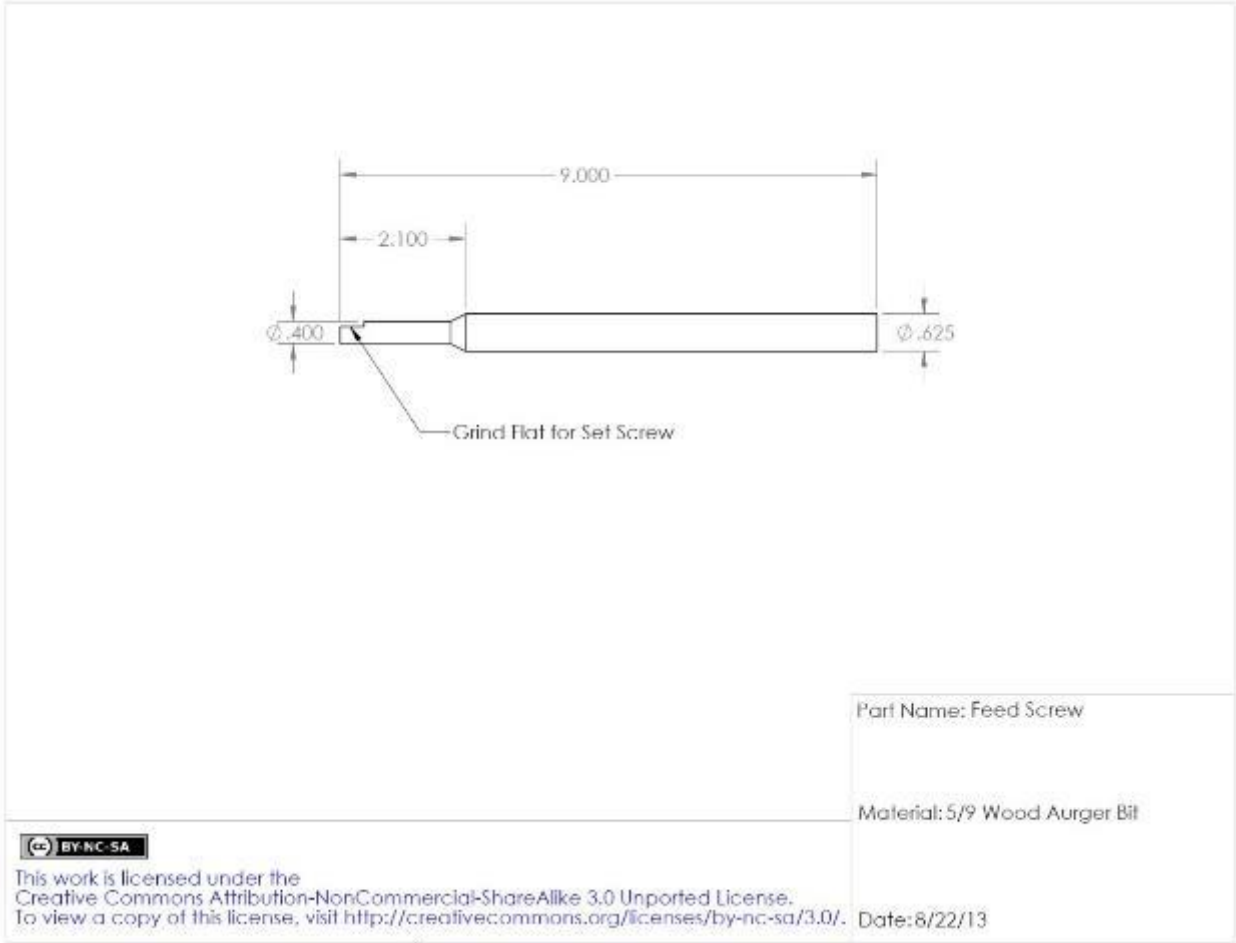


Figure A-5: The screw design (dimensional) in Filabot Wee extruder